Wire Explosion via Electromagnetic Induction

Ryan van Herel

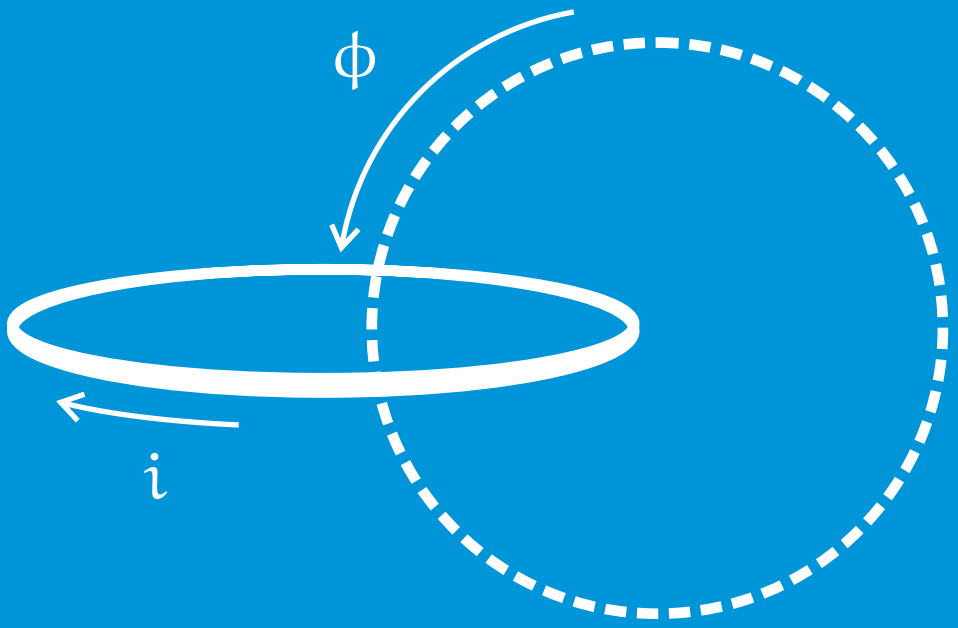

Wire Explosion via Electromagnetic Induction

M J W M R van Herel

A thesis submitted in partial fulfilment
of the requirements for the degree of
Master of Engineering
in
Electrical and Computer Engineering
at the
University of Canterbury,
Christchurch, New Zealand.

12 August 2011

List of Publications

JOURNAL PUBLICATIONS

van Herel, R., Sinton, R., Enright, W., Bodger, P., 'Wire Explosion by Electromagnetic Induction', *IEEE Transactions on Plasma Science*, volume 40, number 7, July 2012

Sinton, R., van Herel, R., Enright, W., Bodger, P., 'Observations of the long distance exploding wire restrike mechanism', *Journal of Applied Physics*, volume 108, number 5, 2010

Sinton, R., van Herel, R., Enright, W., Bodger, P., 'Investigating Long-Distance Exploding-Wire Restrike', *IEEE Transactions on Plasma Science*, volume 38, number 4, pp 1015 - 1018, April 2010

CONFERENCE PUBLICATIONS

Sinton, R., van Herel, R., Enright, W., Bodger, P., 'Design and construction of a triggered spark gap for long distance exploding wire experiments', *20th Australasian Universities Power Engineering Conference (AUPEC)*, 2010

van Herel, R., Sinton, R., Enright, W., Bodger, P., 'Formation of a Plasma Conductor by Induction', *Asia-Pacific Power and Energy Engineering Conference (APPEEC)*, 25 - 28 March, 2011

Sinton, R., van Herel, R., Enright, W., Bodger, P., 'A Marx Generator for Exploding Wire Experiments', *Asia-Pacific Power and Energy Engineering Conference (APPEEC)*, 25 - 28 March, 2011

MAGAZINE ARTICLES (not peer reviewed)

Sinton, R., van Herel, R., Enright, W., Bodger, P., 'Plasma conductors and windings', *Australian Transmission and Distribution* magazine, Vol. 5, pp 22-23, October/November, 2009

Sinton, R., van Herel, R., Enright, W., Bodger, P., 'Exploding Wire', *The Shed* magazine, pp 60-62, October/November, 2010

Sinton, R., van Herel, R., Enright, W., Bodger, P., 'Atmospheric Partial Discharge Experiments', *Australian Transmission and Distribution* magazine, Issue 1, pp 78-79, February/March, 2011

Abstract

This research is aimed at exploding a wire via electromagnetic induction, with a preference for obtaining restrike of the exploding wire in a ring shape or otherwise. Literature on both exploding wire and electromagnetic induction are introduced together. A mathematical framework to describe the wire explosion by induction is formulated from first principles using the idea of magnetic flux linkages. The environment in which the experiments took place is described, with reference to matters of laboratory safety and also measurement of transient electrical current and voltage in the wire explosion by induction. The results describe the approaches taken to explode a wire by induction to obtain a plasma conductor. Voltage and current data are displayed and described. Throughout this work, there are long-exposure digital photographic images of the experiments taking place. These contribute to determining the outcome of experiments, and support the conclusions. Wires were exploded by induction in an air-cored mutually coupled coils system, and restrike of those wires was procured. Electrical characteristics of wire explosion by electromagnetic induction are displayed and discussed based on what is known about straight exploding wires. Future works involving creation of plasma rings, electromagnetic thrust and exploding wires in vacuum are discussed.

Contents

Acknowledgements

With these words, my writing of this thesis is finally accomplished. To Dr Wade Enright, thank you for your generosity and those endless sunny days spent in spirited discussion of our seemingly hopeless endeavours, under the tree. I will always recall with warmth our travels to frozen picnic tables in foreign lands, and look forward to many such meetings to come. Whenua Tautahi left the biggest impression on me, as a way of taking up the whakawhanaungatanga that you opened my eyes to.

To my dear Rowan Sinton I offer my sincerest gratitude for our friendship over the years. I have spent a wonderfully rewarding time with you studying wire explosion, overcoming confusion and sharing together our fascination of all the strange phenomena we came across. That sixty metre lightning bolt you created last February is something I will never forget. It was all a dream come true.

To Professor Pat Bodger, your guidance and steady support was inspirational. Your educational philosophy is something that I will always aspire to pass on to others.

To Kerry Tunstall, your artistic endeavours drew me toward high voltage research, and I found your work communicated many significant physical ideas that were new to me when I began.

To Mr Evan Webb, thank you for your perpetual and welcome curiousity about my work, and also our warm friendship.

For my technical supporters, Dave Healy, Ken Smart and Jac Woudberg. Thank you for your exemplary patience and expertise in the workshop.

To my buddies Andrew, Shreejan, Mickey D., Irvin, Lance, Thahira, Kalyan, Ali, Michael, James and Parash; Sohrab, Yanosh and Bevan. Thank you for the sailing trips, the laughs and all the Chinese food.

Lastly to my mum and dad. I love you both. I dedicate this thesis to you, and to my sibilings, Aleida, Herman, Jan, Tracey, and Cornelia. Thank you for supporting me wherever I went, and thanks for all the bedtime stories.

Foreword

"Something is doing we don't know what" - Sir Arthur Eddington, 1927

. I collaborated with Ryan van Herel on a number of experiments, not only for art but for science as an observer. Together I feel we discovered that light acting in time and space is one of the most complex activities available to research. Everything that came before is from the past, everything happening now is for the future and from this we can learn.

As Ryan's writing covers the emergence of exploding wire activities and its relationship to current high voltage research being carried out at the department of Electrical and Computer Engineering of the University of Canterbury, these pages attest to the possibilities or usefulness of the research being carried out. The van Herel writing herein points out to the reader the electrical unknowns of our time and the stepping stones like manner needed to go forward.

Kerry Tunstall

New Brighton, Christchurch, New Zealand

2011

Notation

Symbol	Description	Unit
Mathematical Operators		
d	Differential operator	
Δ	Difference operator	
$\int$	Integration operator	
∇	Vector differential operator	
Electromagnetic Fields		
A	Magnetic vector potential	V s m^{-1}
B	Magnetic flux density	T (Wb m^{-1})
E	Electric field	V m^{-1}
H	Magnetic field	A m^{-1}
Functions		
$\mathrm{K}(\mathrm{k}) = \int_0^{\frac{\pi}{2}} \frac{1}{\sqrt{(1-\mathrm{k}^2\sin(\vartheta))}} \mathrm{d}\vartheta$	Complete Elliptic Integral of the First Kind	
$\mathrm{E}(\mathrm{k}) = \int_0^{\frac{\pi}{2}} \sqrt{(1-\mathrm{k}^2\sin(\vartheta))} \mathrm{d}\vartheta$	Complete Elliptic Integral of the Second Kind	
$\mathrm{R}_{\mathrm{ew}}(\mathrm{t})$	Exploding wire resistance in time	Ω
$\mathrm{Z}_{\mathrm{ew}}(\mathrm{t})$	Exploding wire impedance in time	Ω

Symbol	Description	Unit
Coordinates		
$\rho,\ \vartheta,\ z$	Cylindrical polars	m, rad, m
$\rho,\ \theta,\ \varphi$	Spherical polars	m, rad, rad
t	Time	s
Circuit Quantities		
a	Area	m^2
α	Exponential damping coefficient	s^{-1}
C	Capacitance	F
i	Current	A
κ	Coefficient of magnetic coupling	
L	Self inductance	H
M	Mutual inductance	H
μ	Magnetic permeability	H m^{-1}
μ_0	Vacuum permeability	H m^{-1}
P	Power	W
ϕ	Magnetic flux	Wb
R	Resistance	Ω
S	Enclosed area	m^2
v	Voltage	V
V	Volume	m^3
Y	Admittance	S
Z	Impedance	Ω
$\delta,\ \ell,\ R,\ r$	Length	m

List of Figures

List of Tables

Chapter 1

Introduction

1.1 Insight

Exploding wires can form plasma channels. The wire can be bent into different forms, and the resulting plasma channels maintain those forms. As such, in this work the plasma is regarded as a type of conductor, and the plasma conductors formed from a wire explosion can be used to create novel machinery. This thesis explores the possibility of applying energy to a wire via electromagnetic induction, to create an electrically isolated plasma. It is important that the electrical, and where possible physical, behaviour of wires exploded by induction is catalogued and described. It is important if there is to be any further opportunity to create novel machinery with plasma conductors.

1.2 Objective

This research is aimed at exploding a wire via electromagnetic induction, with a preference for creating a ring-shaped plasma, or otherwise.

1.3 Overview

No previous literature describes exploding wire by electromagnetic induction. Therefore literature on both exploding wire and electromagnetic induction are introduced in succession. A mathematical framework to describe the wire explosion by induction is introduced and developed from a first principles approach and from the idea of magnetic flux linkages in conjunction with Faraday's law. The environment in which the experiments took place is described, with particular attention being paid to issues of laboratory safety and also measurement of transient electrical current and voltage

in the wire explosion by induction. The results are related in two chapters demarcated by the two coil topologies used: pancake coils and helical coils. The results describe the approaches taken to explode a wire by induction to obtain a plasma conductor. Voltage and current data are displayed and described where appropriate. Photographs of the experiments taking place also contribute to determining the outcome of experiments, and support the conclusions. Methods for obtaining the electrical current and resistance of an exploding wire with respect to time are described. This step was taken to help inform the development of a mathematical model for the exploding wire by induction.

Wires were exploded by induction in an air-cored mutually coupled coils system, and restrike of those wires was achieved. The restrike was photographed and electrical characteristics of wire explosion by electromagnetic induction are displayed and discussed based on what is known about straight exploding wires. Features of wire fragmentation, plasma bead formation and the restrike phenomenon, present in wire explosion by conduction, were also found in wire explosion via induction. Some future works are discussed in the final chapter of the thesis.

Throughout this thesis, abbreviations have sometimes been used in order to encapsulate certain concepts succinctly. Firstly, the term "exploding wire" is often referred to simply as EW. The phenomenon of "restrike" is abbreviated to RS, and "non-restrike" is termed NRS. EWs can be created by way of direct discharge of electricity from a storage element (typically a capacitor bank) into a wire. That process is regarded herein as "EW by conduction" or, CEW. Lastly, "wire explosion by electromagnetic induction" is known as IEW.

Chapter 2

Plasma Machines

"Got a spark..." - Michael Faraday

2.1 Synopsis

This chapter is a review of literature relevant to the thesis. Using an historiological perspective, wire explosion research is described beginning with the earliest experiment by Nairne through to the end of the nineteenth century. Then, modern wire explosion research is examined and important findings from both eras are described throughout. There is an explanation of recent exploding wire research activity at the University of Canterbury. The topic of plasma by induction is introduced using Faraday's law, and some examples of applications of inductively coupled plasmas are given. Both wire explosion and plasma by induction are relevant to the literature review, as the two are brought together in the subject of this thesis.

2.2 Exploding Wires

2.2.1 Historic researches of exploding wire abroad

The first exploding wire discharges were made possible with the application of currents from large banks of electrical storage elements. In the beginning, these were capacitive storage units such as the Leiden jar. Meticulously constructed machinery provided the means by which these storage elements could be charged, through accumulation of static electricity. In some later research, electrochemical Voltaic piles were used for direct application of currents to the test subjects.

In 1774, English instrument maker Edward Nairne published through the Royal Society, the first popular observation of exploding wire discharges. Nairne [1774]

conducted his exploding wire experiments with a bank of capacitors charged using his very large cylinder machine, figure 2.1. In this experimental series, he made insightful observations of how current is distributed in electric circuits and noted the effect of electrical discharges on a number of small animals and plants.

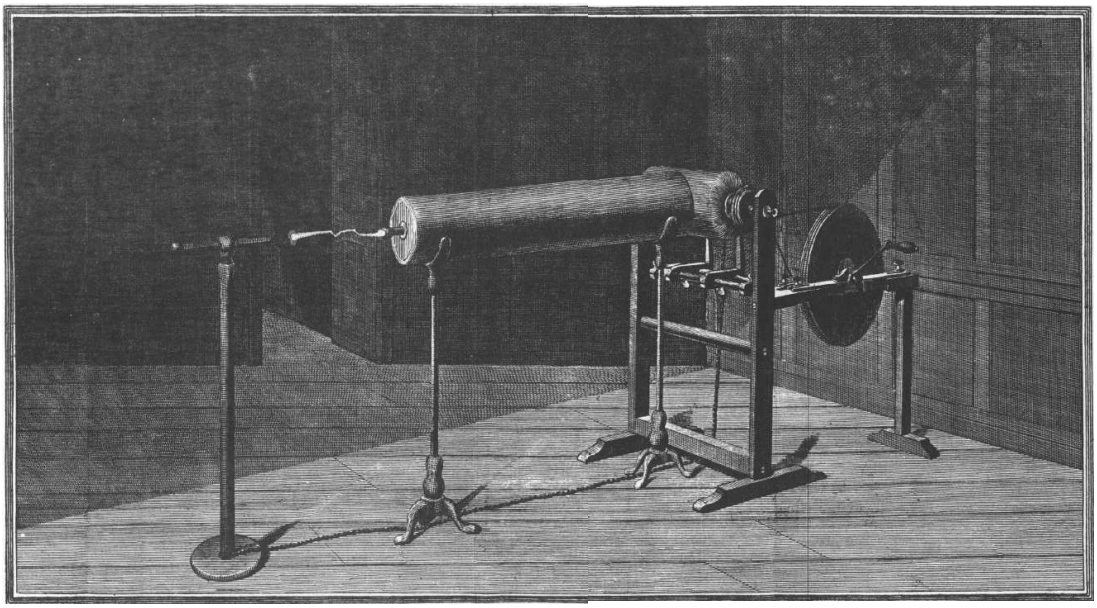

Figure 2.1: Edward Nairne's Very Large Cylinder machine, a triboelectric generator useful for making long static discharges and charging large banks of Leyden jars, [Nairne 1774].

In 1784, Dutch scientist Martinus van Marum, solicited the instrument maker John Cuthbertson to build a large triboelectric generator for the Teyler's Stichting (Teyler Foundation) in Haarlem, figure 2.2, [Hackmann 1971]. With this machine, van Marum was able to provide experimental evidence supporting Lavoisier's antiphlogiston theory, which was a crucial theoretical advancement in the understanding of oxidation-reduction reactions in the field of chemistry, [Hackmann 1974]. This was achieved in a series of experiments in the northern hemisphere winter of 1786, through explosion of wires of various metal compositions. Van Marum also recorded the first exploding wire metal oxide residues. Impressions of these residues shown in figure 2.3 were painted by an artist of natural history, J. C. Sepp of Amsterdam, [Hackmann 1974]. These experiments are related in Verhandelingen, uitgegeeven door Teyler's Tweede Genootschap by van Marum [1785].

In the nineteenth century, amateur experimenter Andrew Crosse undertook some experiments with wire explosion. These experiments were motivated chiefly out of scientific interest but were often undertaken in the manner of exposition, as in dramatic demonstrations to visitors in his well-equipped personal laboratory at his home

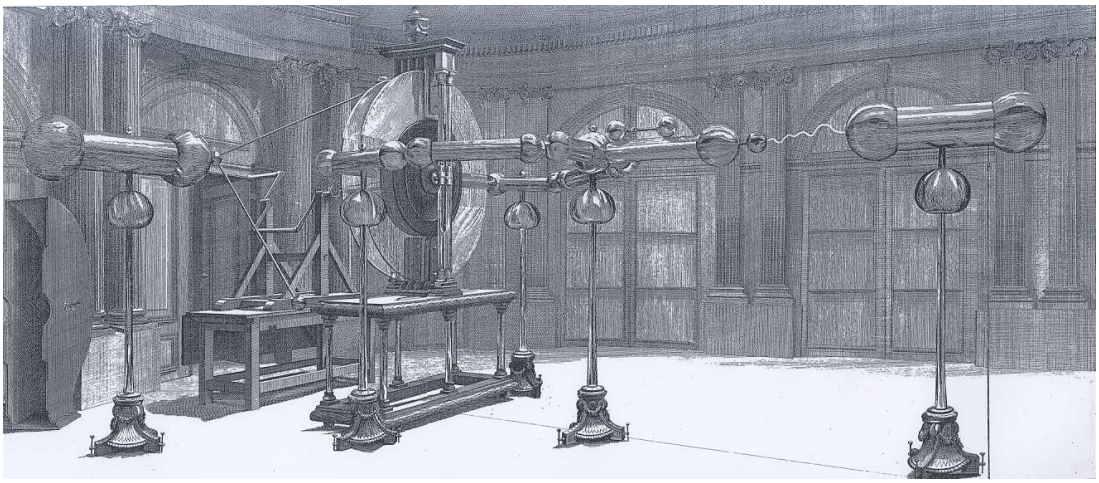

Figure 2.2: Teyler's Large Electrical machine, due to John Cuthbertson, [Hackmann 1971]. It is a twin-plate triboelectric generator useful for making long static discharges and charging large banks of Leyden jars.

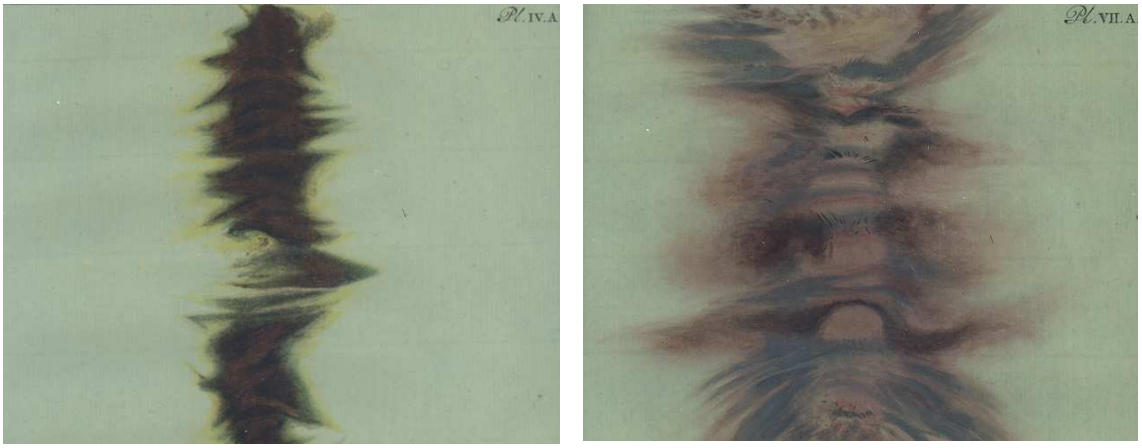

(a) Red Copper (b) Gold

Figure 2.3: Impressions of exploding wire residues painted by J. C. Sepp, from van Marum [1785].

at Fyne Court, near Bridgewater, in the United Kingdom, [Pocock 1993]. He also investigated electrical phenomena associated with atmospheric electricity, with some outdoor apparatus consisting of a network of wires strung out amongst the trees in the grounds at Fyne Court.

2.2.2 Modern research into exploding wire

Exploding wire phenomenology was pursued in the twentieth century because it allowed the investigation of physical behaviour of materials at high temperatures, and the properties of metals at these temperatures. Modern research into exploding wires is distinguished by the application of advances in electrical and physical measurement technology. The introduction of the oscillogram (oscilloscope traces) made it possible to sense and record the voltages and electrical currents of the exploding wire. The spectroscope enabled researchers to determine the chemical composition of exploding wire plasmas. In addition, one of the earliest notable film and photographic studies of exploding wires was made by Nagaoka and Futagami in the mid 1920's.

An early example of spectroscopy applied to exploding wires comes from a body of research performed by spectrographer John A. Anderson from 1919, who in one exercise exploded fine iron wires multiple times to record exposures of different sections of the absorption spectrum, [Anderson 1920]. He performed wire explosion experiments for many elements and also developed rotating mirror cameras principally used for studying exploding shells of gas to a time resolution of approximately 1 μs, [Bowen 1962]. Anderson [1922] also demonstrated that when the wires exploded, they reached temperatures in the order of 20,000 K.

Hantaro Nagaoka and Tetsugoro Futagami conducted research of the exploding wire in the mid 1920's; their photography work was important to the conclusions they drew. Their work bears close resemblance to present exploding wire research at the University of Canterbury, in regard to their methods of experimental observation. They used virtually the same capacitive discharge circuit, wire length up to 1 m, capacitance of 1.7 μF and voltages of around 40 kV. They researched the appearance and behaviour of long metallic exploded wires, as well as exploded moist threads, [Nagaoka et al. 1926]. They noticed particles of molten metal shooting off in a direction perpendicular to the wire. In Nagaoka and Futagami [1926], they were able to describe certain phases of exploding wires of various metals. They discovered "beads of light" - plasma beads - in their photographs, and also noted an "explosive condition" for the wires, the condition now known as restrike. They also mention

some cinematographic sketches made using a camera with a shutter speed of $\frac{1}{72000s}$, [Nagaoka and Futagami 1928].

From the 1950's, topics of interest in wire explosion research began to diversify, particularly in investigation of explosion dynamics, shockwave formation, and the thermodynamic states of the exploded wire. The exploding wire was attractive to physicists because of its highly non-linear physical and electrical behaviour. This natural phenomenon eluded precise explanation at that time, and formulation of a physical theory to explain it was challenging. Scientists in this era therefore met this challenge with rigorous experimentation and discussion. William G. Chace, being a prominent exploding wire researcher of the time, organised a symposium on the exploding wire phenomenon in 1959. Many researchers contributing to exploding wire literature hark back to Chace when introducing their material, and as such, Chace is regarded as the instigator of the most recent attempts to understand the exploding wire.

When a wire explodes, it undergoes several physical changes. Chace summarised the exploding wire process [Chace and Moore 1959]. The "first phase" of an exploding wire refers to the initial current conduction period (or initial current pulse) incorporating the fragmentation of the wire. The "dwell-period" (also known as "current pause") of the exploding wire is the period of ionising growth of plasma. It was also found that the current conduction during the dwell-period is small compared with the current magnitude during the first phase. At the conclusion of the dwell-period is the possibility of restrike, that is, the exploding wire response that forms a conductive plasma channel.

Vlastos later demonstrated with short exploding wires that several different types of restrike exist, and that the type of restrike depends of the average electric field (AEF) applied to the wire [Vlastos 1968]. The restrike mechanisms were achieved through AEFs much higher than 10 kV/m. Several authors have noted beads of plasma forming during an exploding wire discharge, [Nagaoka et al. 1926, Dannenberg and Silva 1969, Bhat and Jordan 1971, Taylor 2002]. Taylor introduced large inductances which reduced the dwell period duration, but did not preclude plasma beads from instigating restrike. Smith [2008] investigated restrike formation in exploding wires of varied diameters and lengths, principally between 1 m and 10 m. Sinton et al. [2011] created channels of plasma up to 36 m long using a lower AEF restrike mechanism which relies on plasma bead formation. Sinton later created a 60 m long plasma discharge, [Gautier 2011].

Chief among the factors that separate different types of EW research today is that of

the energy storage and release capability of the machine used to deliver the electrical impulse to the exploding wire. For instance, the Z-machine, based in Sandia National Laboratory, USA, is one of the most powerful machines in operation today. It is regularly used for research into exploding wire arrays. The Z machine "uses currents of about 26 million amps to reach peak X-ray emissions of 350 terawatts and an X-ray output of 2.7 megajoules", [Sandia 2011]. This research is geared predominantly toward nuclear fusion and military applications, the generation of X-rays and more powerful high energy radiation effects that wire explosions are capable of releasing, [Idzorek et al. 1999, Anderson and Briand 2003]. It is also used for experimental verification of magneto-hydrodynamic models that might describe the physical behaviour of materials being annihilated in this machine.

2.2.3 Exploding wire at University of Canterbury

The exploding wire phenomenon has been studied at University of Canterbury since at least 1998, with investigation into wire fragmentation mechanisms in an unpublished paper by David Watson and Steven Hiscock, [Mulholland 2004]. Since then, research into wire explosion has been steady, with many third professional year undergraduate projects being undertaken. In 2004, Daniel Mulholland experimented with a device called an "Arc Rifle" that fired a projectile with a trailing wire at a Faraday cage livened to a high voltage with a charged capacitor bank. He also suceeded in photographing these discharges and produced a 20 metre discharge in the laboratory [Mulholland 2004]. In 2006, Hugh Mace and David Smith carried out an applied study of the exploding wire in a remote outdoor setting. Mace was concerned with preparing the outdoor laboratory space, while Smith achieved the sucessful ignition of 10 m of wire into a plasma path. Smith went on to further study the exploding wire for the production of long-distance directional discharges. Smith et al. [2007] built a capacitor bank and discharge circuit specifically for studying the exploding wire.

Prior to the southern hemisphere summer of 2007 - 2008, collaborating artist Kerry Tunstall demonstrated that the exploding wire could be taken on curvy paths. David Smith showed the EWs could be bent around sharp corners, and from that result it was conceived that plasma helices could be formed. Further work was undertaken in this area over that summer by Mike Dalzell, who carried out research into the plasma coil. In 2008, a third professional year student, Campbell Hammond, constructed and tested the first "Plasma Transformer" in his final-year undergraduate project [Hammond 2008]. It used an exploding wire as its primary (exterior) winding, and a

secondary with a sphere-gap across its terminals. This machine successfully produced an exploding wire impulse voltage of 75 kV_{pk}, from 45 kV_{pk} applied to the input, [Sinton et al. 2009].

2.3 Plasma by Induction

2.3.1 Faraday and the magneto-electric spark

Experiments by Michael Faraday in his investigations into electromagnetic induction, produced one of the first sparks by induction, Faraday [1832]. While Faraday himself conceded that the Italian investigators Nobili and Antinori obtained the first spark by induction shortly before, Faraday was able to generate his spark by a novel set-up of his own devising, [Martin 1949]. On 1 October 1831, Faraday was searching for a way of demonstrating a spark from induced currents. He could sense the induction with his galvanometers, but he was seeking the spark that would make the phenomenon of induction tangible to the senses. His apparatus for the experiment was his now infamous iron ring transformer consisting of two coils of wire wound on opposite ends of the ring, figure 2.4. Attempting to obtain chemical decomposition, Faraday

> "Got a spark, with charcoal at the end of the inducing wires, very distinct though small - only at the moment of contact or disjunction." (from Cavicchi [2006])

Although that was 180 years ago, electromagnetic induction remains an intriguing natural property. Of critical concern to this thesis, this experiment is where wire explosion via induction, traces its origin. Moreover, it is the origin of the electric power transformer, and the technology of inductively coupled plasma.

2.3.2 Inductively coupled plasmas

Ramo et al. [1965] frames Faraday's law in a way that hints at the possibility of creating an inductively coupled plasma (ICP). In their example problem, Faraday's law is introduced as an ionising breakdown in air due to rapidly changing magnetic fields. The problem is to raise the axial magnetic field of an electromagnet to $\mathrm{d}B_z = 10$ T, linearly in time, $\mathrm{d}t$, as rapidly as possible without causing electical breakdown in air due to the electric field, E_ϑ. For their axially symmetric system, Faraday's law for a loop of radius R is,

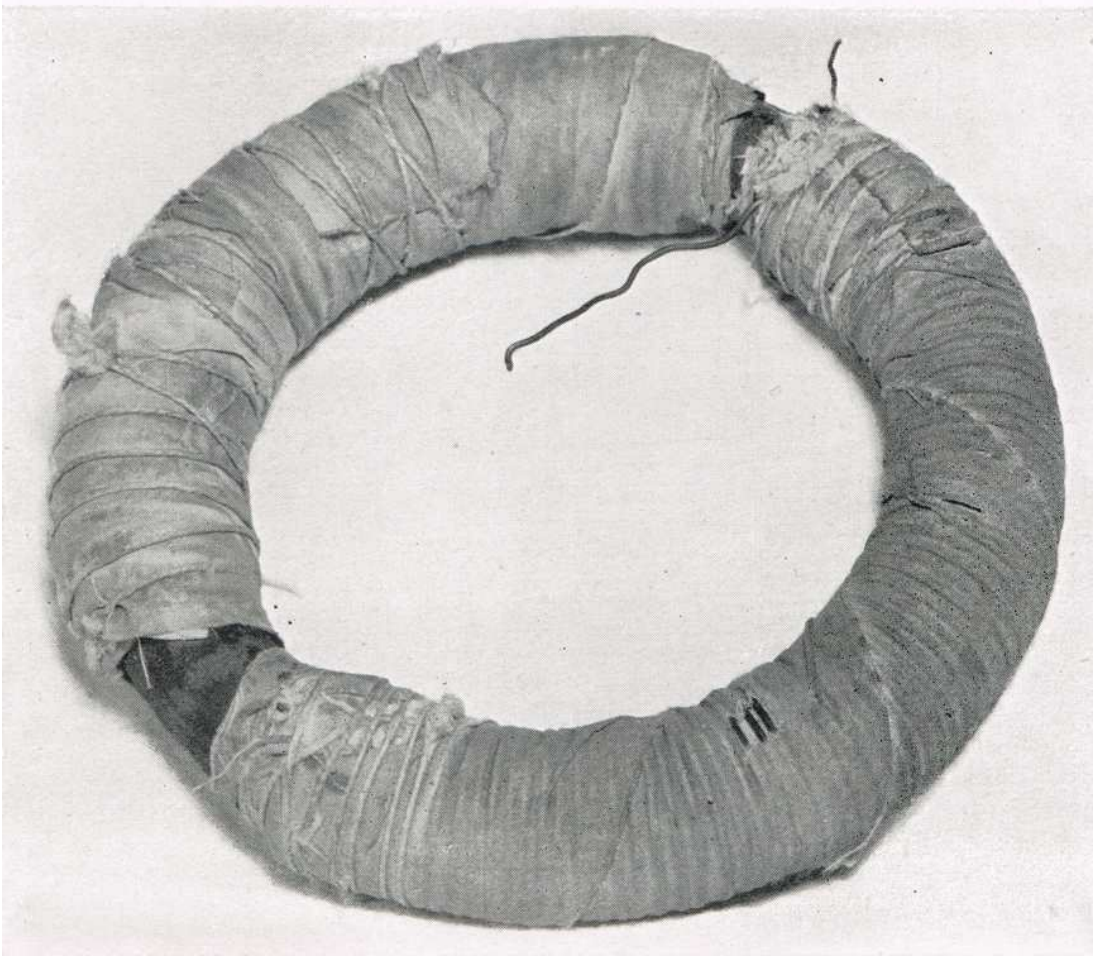

Figure 2.4: Iron Ring with Coils of Wire wound on opposite sides, 1831, from Martin [1949].

$$2\pi R \mid E_{\vartheta} \mid = \pi R^2 \frac{dB_z}{dt} \tag{2.1}$$

In equation 2.1, setting E_{ϑ} equal to the breakdown stength of the medium, and dB_z to be a maximum magnetic flux density in free-space, then the electric breakdown may be facilitated in the medium for a certain rate of change of magnetic flux. By increasing the excitation frequency of the applied magnetic field, or by lowering the pressure in the magnetic field region (increasing the mean free path of molecules), it is easier to procure ionising breakdown and thereby create an inductively coupled plasma. This is how inductively coupled plasmas are created in practice.

In this way, the ICP may be considered a relative of wire explosion by induction. ICPs generally involve the creation of ring-shaped plasmas by means of electromagnetic induction at high-frequency, bypassing the need for an exploding wire. The advantage is that it creates an electrodeless secondary circuit, normally existing in a low-pressure vessel containing a rarified gas for ionisation to the plasma state. ICPs may be found in many applications, for example in spectroscopy and mass spectrometry, pulsed inductive thruster (PIT) technology and nuclear fusion as a source of energy.

One application of the ICP is in atomic emission spectroscopy (ICP-AES). The tool is called an ICP torch and is a component to help determine the chemical compositions of minute samples of material, [Manning and Grow 1997]. The sample material is ionised upon injection into the plasma and a spectrum can be recorded from the different wavelengths of light released by the ionised sample as it cools. (So the ICP torch is basically used to identify elements in the same way a bunsen burner might be used to identify different species of salts. This seems ironic, since Faraday is known to be an inventor of an early form of laboratory gas burner as described in [Faraday 1827]).

2.3.3 Plasma thrusters for space applications

Once an external, inductively coupled plasma ring is formed, electromagnetic thrust may be generated by the Lorenz force. Using the principle of the ICP, a group of researchers devised a prototype Pulsed Inductive Thruster (PIT), figure 2.5a, for the purpose of propelling spacecraft, [Dailey and Lovberg 1993]. The PIT is designed with the intention of using it as primary propulsion in interplanetary space missions. It consists of a main excitation coil, made from parallel half-turn strands which are driven by a ring-shaped Marx-generator. The coil is protected by a dielectric shield. A thin layer of gas propellant is distributed over the coil and high currents are allowed

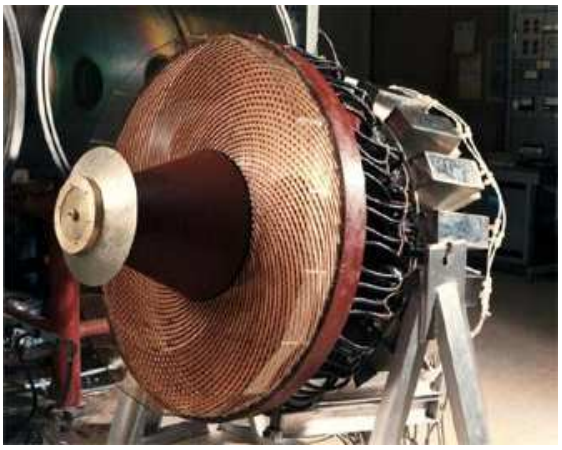

(a) The Pulsed Inductive Thruster from Dailey and Lovberg [1993]

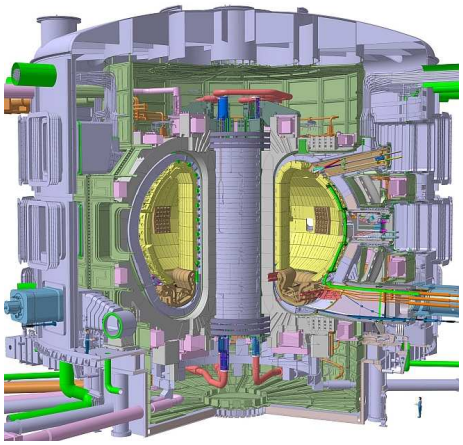

(b) The planned ITER Tokamak from Aymar et al. [2001]

Figure 2.5: Examples of plasma by induction.

to pass through the coil, generating a magnetic field which induces an azimuthal electric field above the coil. The electric field causes the rarified gas to be ionised and currents flow in the plasma ring that is produced. The currents in the coil and the currents in the plasma ring flow in opposite directions, so the plasma ring is ejected from the plate, producing thrust [Hrbud et al. 2002].

Another approach was taken by Shpanin et al. [2008]. A plasma arc was created by the rapid separation of two annular electrodes and the subsequent coupling of the resultant helically-shaped azimuthal arc column with an external coil to control the arc. The plasma can be propelled in either the positive or negative z-direction in a cylindrical co-ordinate frame, or radially, depending on the device structure.

2.3.4 Tokamak prototypes

A tokamak is a toroidal shaped room for confining plasma with external magnetic fields, and is used for the purpose of fusing light nuclei. It was inspired from an idea proposed by a Soviet soldier, Oleg Lavrent'ev, and physically realised by a cadre of Soviet scientists in the 1950s, [Bondarenko 2001]. The walls are made of electromagnets which hold the ring-shaped plasma in place in the middle of the room. The plasma can be heated to the reactor's operating temperature by varying the poloidal magnetic field to transfer energy to the nuclear reaction by transformer action. While there are many examples of experimental tokamaks in operation today, a planned tokamak project called ITER, figure 2.5b, is the latest example of this, [Shimomura et al. 2001]. The ITER project goal is to achieve a power output that is ten times

its power input, up to a plant output of 500 MW. The success of that project would demonstrate the economic viability of terrestrial controlled thermonuclear fusion as an energy source and procure the technological requirements for further plant constructions, [Aymar et al. 2001].

2.4 Hammond's Transformer - a Plasma Machine

Large-scale plasmas can be created at atmospheric pressure without rarified gases, by exploding wires, as in figure 2.6. In this thesis, the exploding wire plasma channel that forms from the phenomenon of restrike is considered as a plasma conductor.

Large-scale plasma conductors have already been used to create a machine that produces a high voltage impulse by electromagnetic induction: exploding a helical primary wire to produce measurable voltage in a solid wire secondary coil, as in Hammond's plasma-primary tranformer shown in figure 2.7 from Sinton et al. [2009]. This machine is a recent development from the research carried out in the area of exploding wire at the University of Canterbury. For a time, an explanation of how the plasma transformer worked was elusive, and would remain so until observation of EW currents could be made. The operation of the plasma transformer has been identified with the help of current waveforms obtained through the optimisation in Chapter 4.

2.5 Exploding a Wire by Induction

This thesis investigates the possibility of going the opposite way to the plasma transformer: using a high-current pulse from a solid induction coil to explode a thin copper wire loop or winding, and create a plasma conductor using electromagnetic induction.

2.6 Summary

The research into exploding wires has been detailed, beginning from Nairne's original experiments, to modern times. From the 1920s, key investigations have taken place which examine the fragmentation mechanism, plasma formation and growth, dwell period and restrike phenomena in the exploding wire. Recent research into EW at the University of Canterbury has been discussed, and the focus of this has been in scaling-up the length of the exploding wire plasma column. The inductively coupled plasma has been introduced. Various methods by which plasma is created by induction and

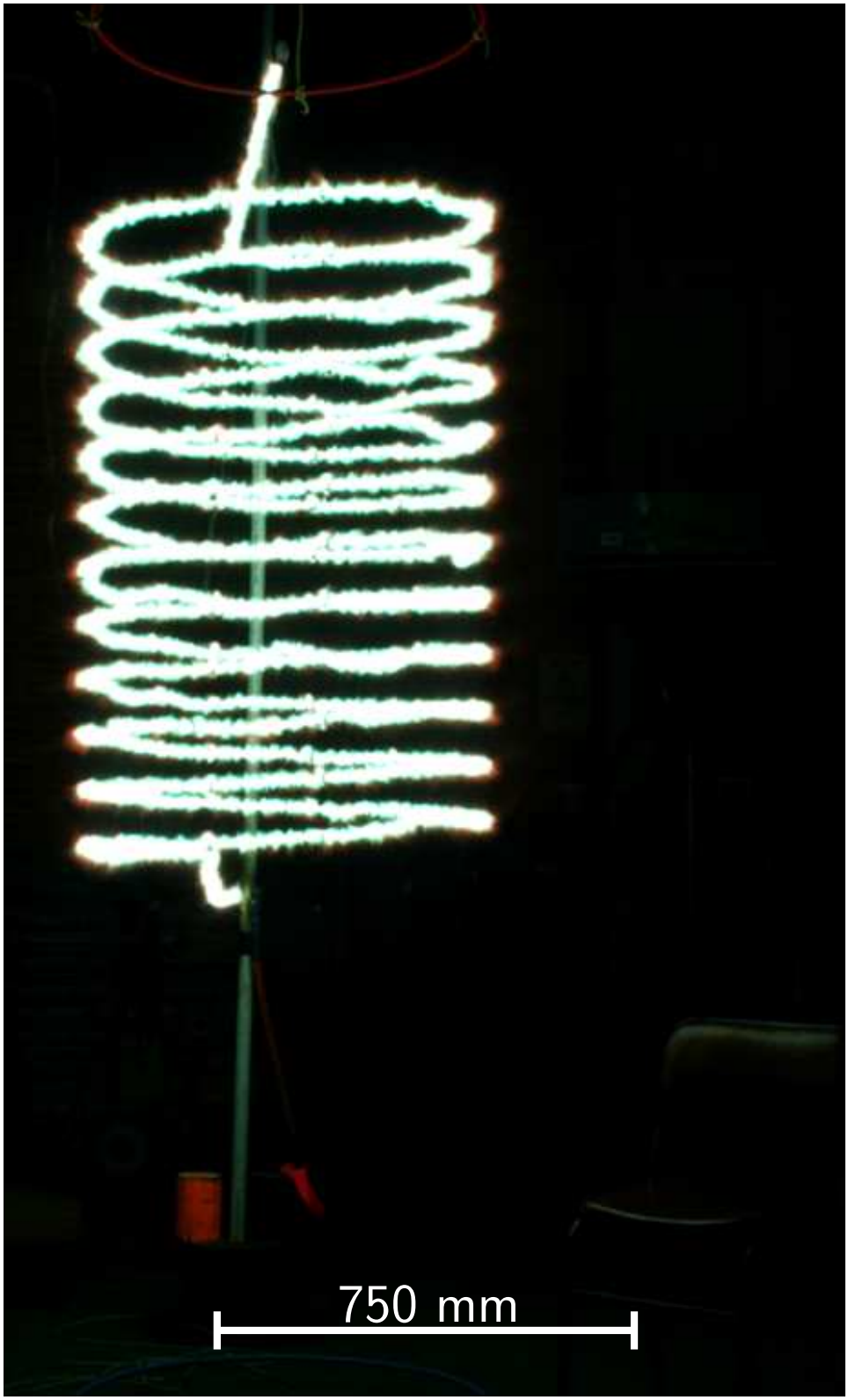

Figure 2.6: Large-scale plasma coil created by the author with Mr Sinton's Marx generator, in the high voltage laboratory.

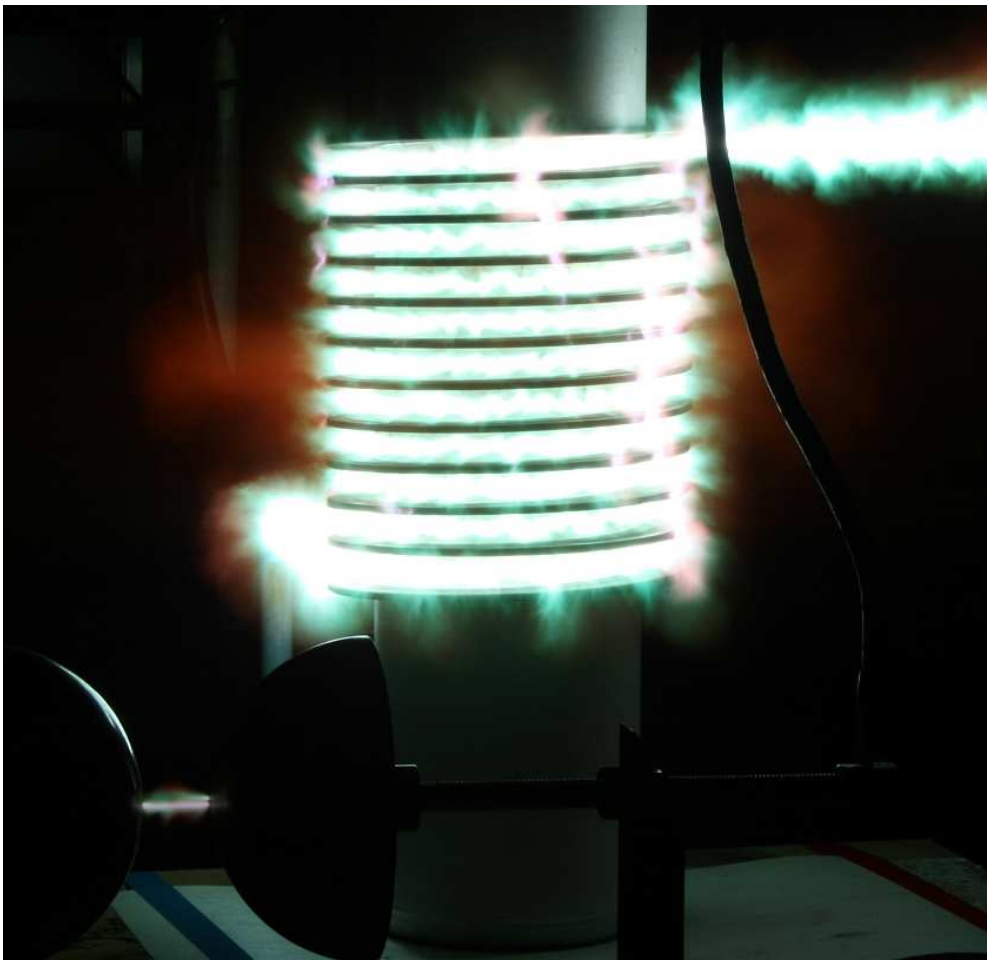

Figure 2.7: 10-turn plasma primary, 30-turn copper secondary high voltage transformer at 40 kV dc from Sinton et al. [2009]. A calibrated sphere gap set to 75 kV dc can be seen flashing over in the foreground, giving the minimum level of the secondary winding voltage output.

examples of uses for ICP's were presented. The explosion of wire by electromagnetic induction has been proposed as a novel method for creating plasma by induction.

Chapter 3

Describing Relationships

3.1 Introduction

To begin the investigation of wire explosion via electromagnetic induction, a simple model of its physical representation is developed. A straightforward winding arrangement for this purpose is a pair of mutually coupled concentric rings. One of the rings represents the field winding that creates the rapidly changing magnetic flux. The other ring is the exploding wire target which responds to the magnetic field generated by the first ring. Electromagnetic relationships between the two rings are derived. This is done without invoking Maxwell's equations from the outset, rather, it is introduced from the ideas of current paths and lines of magnetic flux. Since impulses are to be used to create the magnetic field, it would be useful to have a circuit model to examine the transient behaviour of the wire. Therefore the mutually coupled circuit parameters are derived from these relationships.

This chapter illustrates analytical methods for obtaining the self and mutual inductances of a pair of magnetically coupled concentric rings. This is explored in an arrangement where the rings are of the same radius, r, but separated by a distance, δ. It demonstrates how inductance is classified through magnetic flux concepts, and how inductance is obtained from magnetic flux density. The self and mutual inductance of the pair of rings is determined and the problem of the wire explosion by induction is summarised as an electric circit.

3.2 Electric Current Begets Magnetic Flux

The creation of a line of current also creates lines of magnetic flux, depicted in figure 3.1. These lines of flux are always perpendicular to the line of current, in all directions. As such, it is the case that lines of magnetic flux exist in closed loops,

and pervade all space. Lines of magnetic flux that pass through an area, a, have a

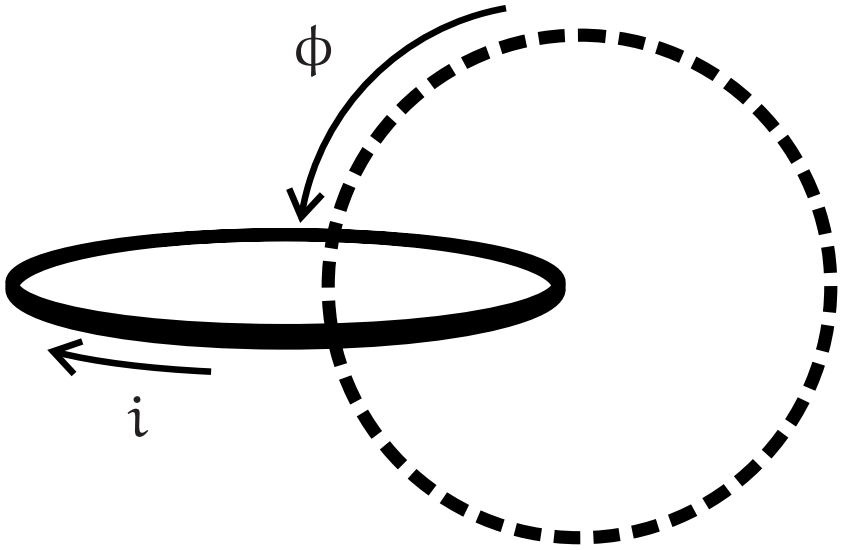

Figure 3.1: Lines of current beget lines of magnetic flux.

density, B. The more lines of flux that are drawn through the area, the greater is the magnetic flux density. This is summarised by the relationship,

$$\phi = B\ a \tag{3.1}$$

More exactly, the magnetic flux in equation 3.1 can be described as the integral of those components of the magnetic flux density that are normal to the enclosed area, S,

$$\phi = \int_S B \cdot dS \tag{3.2}$$

Due to these electromagnetic relationships, a conductor (having a current flowing in it and setting up this magnetic flux), will have a property called inductance, L. Inductance is related to the current flowing in the conductor and the magnetic flux passing through the enclosed area,

$$L = \frac{\phi}{i} \tag{3.3}$$

Putting equation 3.2 and equation 3.3 together gives a general expression for inductance,

$$L = \frac{1}{i}\int_S B \cdot dS \tag{3.4}$$

In section 3.5, this will be revisited in the approach to distinguishing the different types of inductance that are manifest in electric circuit models.

3.2.1 Magnetic field from magnetic vector potential

A magnetic field, H, is related to the magnetic flux density according to the magnetic permeability of the medium, μ.

$$\mathrm{B} = \mu \mathrm{H} \tag{3.5}$$

Throughout this thesis, μ has the value of the vacuum permeability μ_0. A vector potential for magnetism, A, is a useful device for obtaining the magnetic flux density B, (and hence magnetic field, H) by,

$$\mathrm{B} = \nabla \times \mathrm{A} \tag{3.6}$$

3.3 Magnetic Flux Density about a Ring-Shaped Conductor

The objective is to obtain a picture of the magnetic flux density due to a ring of current in free-space, in order to get an impression of the magnetic field magnitude and direction at different points away from the conductor. This is worthwhile because it helps to give a feeling for how rapidly the magnitude of the field falls away, in relation to the distance from the conductor. This is important for determining how close the first ring can be to the second ring. There needs to be separation between the coils, so they are electrically isolated, but to get good flux, mutual reluctance needs to be lessened to get more mutual induction. This is achieved by minimising the distance between the two coils.

The chosen co-ordinate frame is the spherical polar co-ordinates, (ρ, θ, φ). With the help of figure 3.2, a function for magnetic vector potential can be developed representing a circuit of current elements in space,

$$A = \oint \frac{\mu_0 i \mathrm{d}\ell}{4\pi R} \tag{3.7}$$

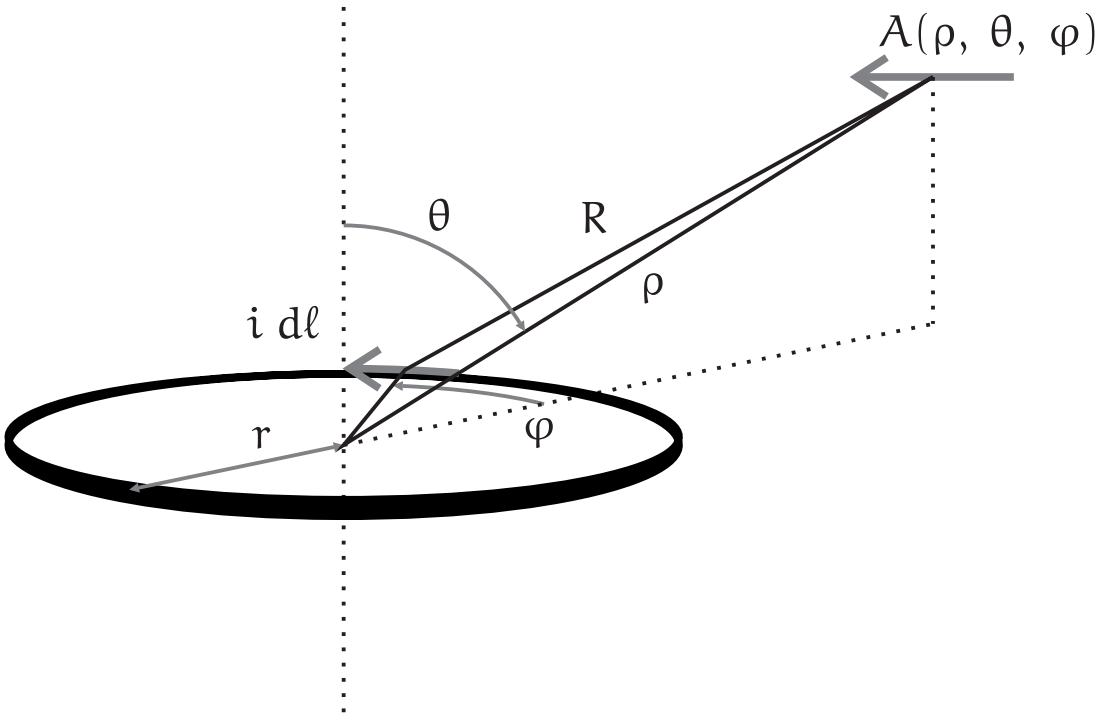

Figure 3.2: Spherical-polar coordinate system for finding the magnetic vector potential, A.

The distance R in equation 3.7 is expressed as the distance from a current element, $i\ d\ell$, in the ring, to the point (ρ, θ, φ),

$$R^2 = \rho^2 + r^2 - 2\rho r \sin(\theta)\cos(\varphi) \tag{3.8}$$

For this choice of co-ordinates, equation 3.7 becomes,

$$A = \frac{\mu_0 i r}{4\pi} \int_0^{2\pi} \frac{\cos(\varphi)}{\sqrt{\rho^2 + r^2 - 2\rho r \sin(\theta)\cos(\varphi)}} d\varphi \quad \hat{\boldsymbol{\varphi}} \tag{3.9}$$

The solution to equation 3.9 can be found through tables of integrals or be determined from a Computer Algebra System (CAS). For the sake of readability, the following substitutions may be made with reference to equation 3.9:

$$\begin{aligned} x &= \rho^2 + r^2 \\ y &= 2\rho r \sin(\theta) \end{aligned} \tag{3.10}$$

These substitutions yield the integral in equation 3.9 in the form,

$$A = \frac{\mu_0 i r}{4\pi} \int_0^{2\pi} \frac{\cos(\varphi)}{\sqrt{x - y\cos(\varphi)}} d\varphi \quad \hat{\boldsymbol{\varphi}} \tag{3.11}$$

The solution to equation 3.11 , obtained through multifarious substitutions of trigi-nometric identities is,

$$A = \frac{\mu_0 i r}{\pi} \frac{y}{y\sqrt{x+y}} \left[\frac{2}{k_1^2} E(k_1) - \frac{2 - k_1^2}{k_1^2} K(k_1) \right] \quad \hat{\boldsymbol{\varphi}} \tag{3.12}$$

where,

$$k_1{}^2 = \frac{2y}{x+y} \tag{3.13}$$

The solution is composed of elliptic integrals of the first and second kind, denoted $K(k)$, and $E(k)$ respectively.

The magnetic vector potential, A in equation 3.12, can be applied to equation 3.6 to find the magnetic flux density, B, in the vicinity of a ring-shaped conductor. Because A is φ directed, the curl of A results in a ρ and θ directed B. By the application of this approach, the magnetic flux density may be drawn. Figure 3.3 is a plot of the magnetic flux density due to $i = 1000$ amperes of current flowing in a ring shaped conductor. The assumption is that the conductor is lossless, and resides in free space. The ring is 40 mm in diameter, which is the diameter of the ring-shaped wires featured in Chapter 6. The conductor width is infinitesimal.

3.4 Faraday's Law

The static magnetic field has been obtained and the magnetic flux density has been plotted for a ring-shaped conductor residing in space. At this point, it is worthwhile introducing Faraday's Law to describe what happens when the current changes in magnitude and direction with respect to time. There are two coils residing in space. The first coil is excited with an alternating voltage so that a current flows in that coil; voltages and currents will be excited in the second coil because of electromagnetic induction. Faraday realised this in his experimental investigations on obtaining a spark by induction. The key to Faraday's discovery is that the change in magnetic flux due to the current in the first circuit, produces the voltage that can be measured

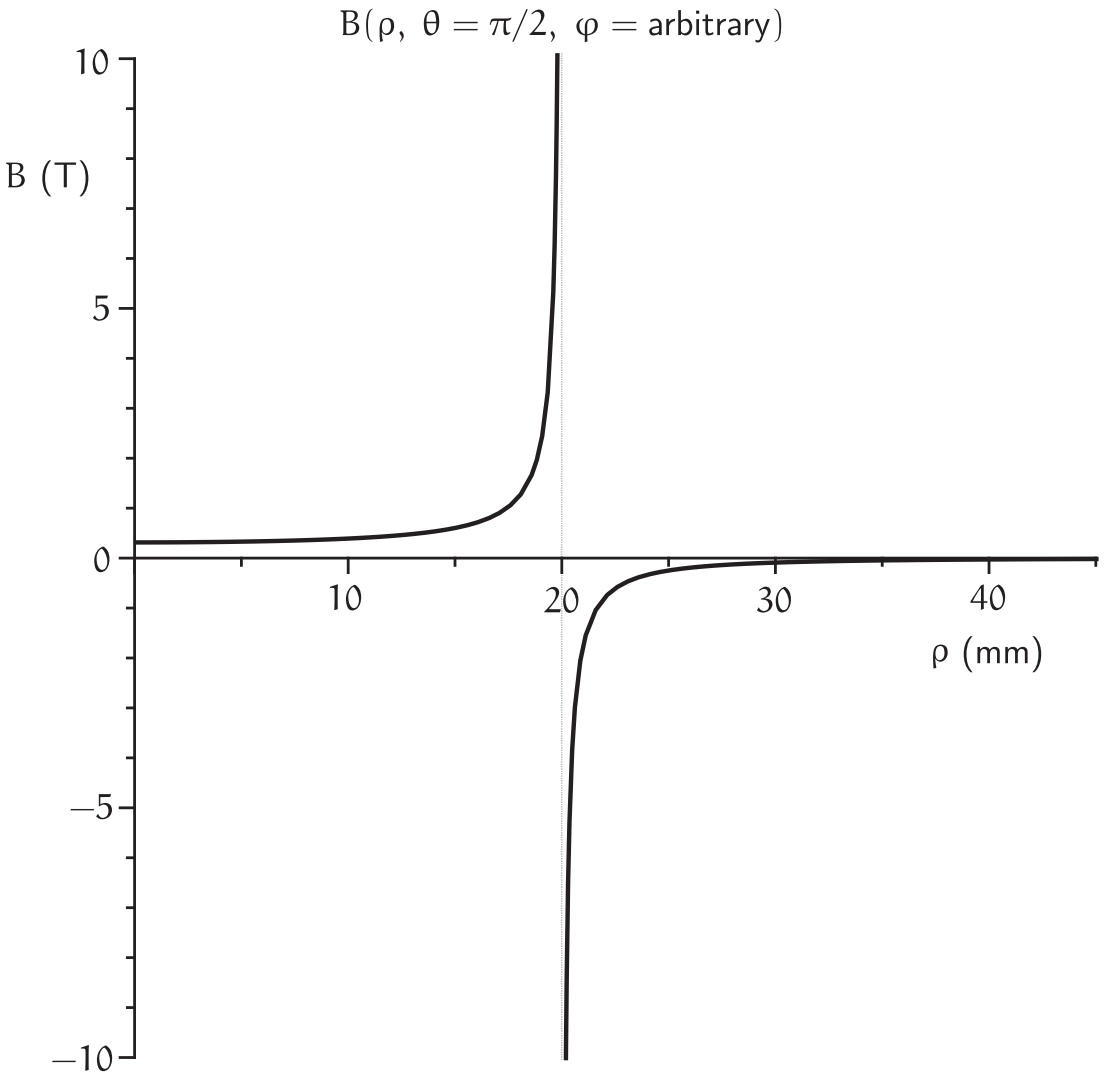

Figure 3.3: Plot of cross-sectional magnetic flux density, B, due to a ring of current carrying 1000 amperes. The ring is of infinitesimal conductor-diameter and is located at ($\rho = 20, \theta = \frac{\pi}{2}, \varphi =$ arbitrary)

in the second circuit. This observation can be embodied as a mathematical statement known classically as Faraday's Law,

$$v = \frac{d\phi}{dt} \tag{3.14}$$

It should be observed that the rule specified by Lenz is implied.

When a second circuit is introduced, it happens that the first circuit (whose flux lines pervade all space), is able to couple magnetically with that second circuit, as in figure 3.4. This will hold true if any number of circuits were introduced; each one will couple magnetically with the others. For the case of two circuits, it is a relatively simple matter to describe all the flux linkage cases. Included here is a diagram that powerfully conveys these magnetic flux relationships; its definitions are quoted in table 3.1, verbatim from Seely and LePage [1952].

Having many coils magnetically coupled together constitutes a network which can

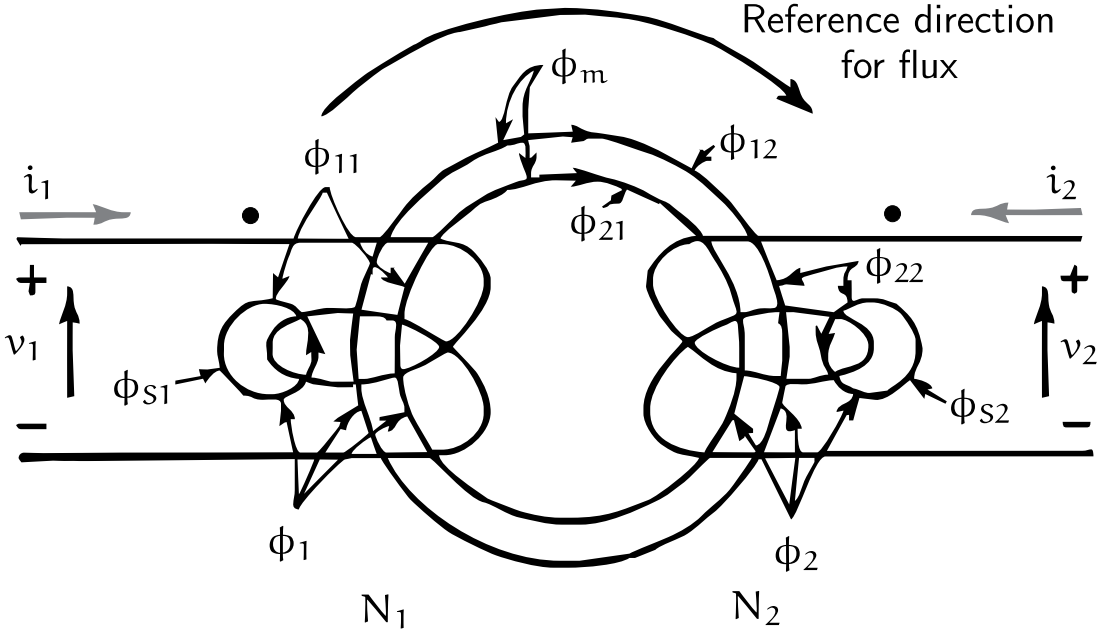

Figure 3.4: Relationships between flux paths for two coils, a figure adapted from Seely and LePage [1952]

be conveniently described as a matrix equation. From equation 3.3, it must be that flux is equal to inductance times the current,

$$\phi = Li \tag{3.15}$$

Therefore, assuming that inductance is constant with respect to time, differentiating

Table 3.1: Table of magnetic flux relationships for figure 3.4

Flux	Description
ϕ_1	Total flux linking coil 1 due to all currents
ϕ_2	Total flux linking coil 2 due to all currents
ϕ_{11}	The part of ϕ_1 which is due to i_1
ϕ_{22}	The part of ϕ_2 which is due to i_2
ϕ_{12}	The part of ϕ_1 which is due to i_2
ϕ_{21}	The part of ϕ_2 which is due to i_1
ϕ_{S1}	Leakage flux of winding 1
ϕ_{S1}	Leakage flux of winding 2
ϕ_m	Mutual flux

both sides of equation 3.15 with respect to time gives,

$$\frac{d\phi}{dt} = L\frac{di}{dt} \tag{3.16}$$

The transition between Faraday's Law from magnetic flux description to circuital description, is made from the following relations,

$$\begin{aligned} \frac{d\phi_{11}}{dt} &= L_1\frac{dI_1}{dt} \qquad \frac{d\phi_{12}}{dt} = M\frac{dI_2}{dt} \\ \frac{d\phi_{21}}{dt} &= M\frac{dI_1}{dt} \qquad \frac{d\phi_{22}}{dt} = L_2\frac{dI_2}{dt} \end{aligned} \tag{3.17}$$

Equations 3.17 can be expressed (via Faraday's Law as it is in equation 3.14), as a statement relating the voltages and currents together in a two-port network,

$$\begin{bmatrix} v_1 \\ v_2 \end{bmatrix} = \begin{bmatrix} L_1 & M \\ M & L_2 \end{bmatrix} \frac{d}{dt} \begin{bmatrix} i_1 \\ i_2 \end{bmatrix} \tag{3.18}$$

This describes the network as an inductance matrix, which can be calculated solely from geometry. A quantity, κ, that describes the magnetic coupling between the two circuits may be defined as,

$$\kappa = \frac{M}{\sqrt{L_1\, L_2}} \tag{3.19}$$

It is termed the "coupling coefficient", and shows how mutual inductance is related to the self inductance of each winding. If $\kappa = 1$, then there is perfect magnetic coupling.

3.5 Inductance from Magnetic Vector Potential

The origin of inductance by its definition from magnetic flux and its place in the electric circuit, has been established. It is necessary to go about calculating the inductance; this will be done for the case of the coupled rings in free space. A pair of conducting rings is illustrated in figure 3.5; They are concentric, each of radius $r = 20$ mm and separated by a distance, $\delta = 10$ mm. Inductance is the parameter to be used to relate voltages and currents in the coupled rings circuit, by Faraday's Law, and this was established in section 3.4. It is critical to determine whether these voltages and currents will be suitable for exploding a wire by induction. Once these inductances are specified and determined, the circuit model for magnetic energy transfer will be complete. The inductance is divided into self inductance and mutual inductance.

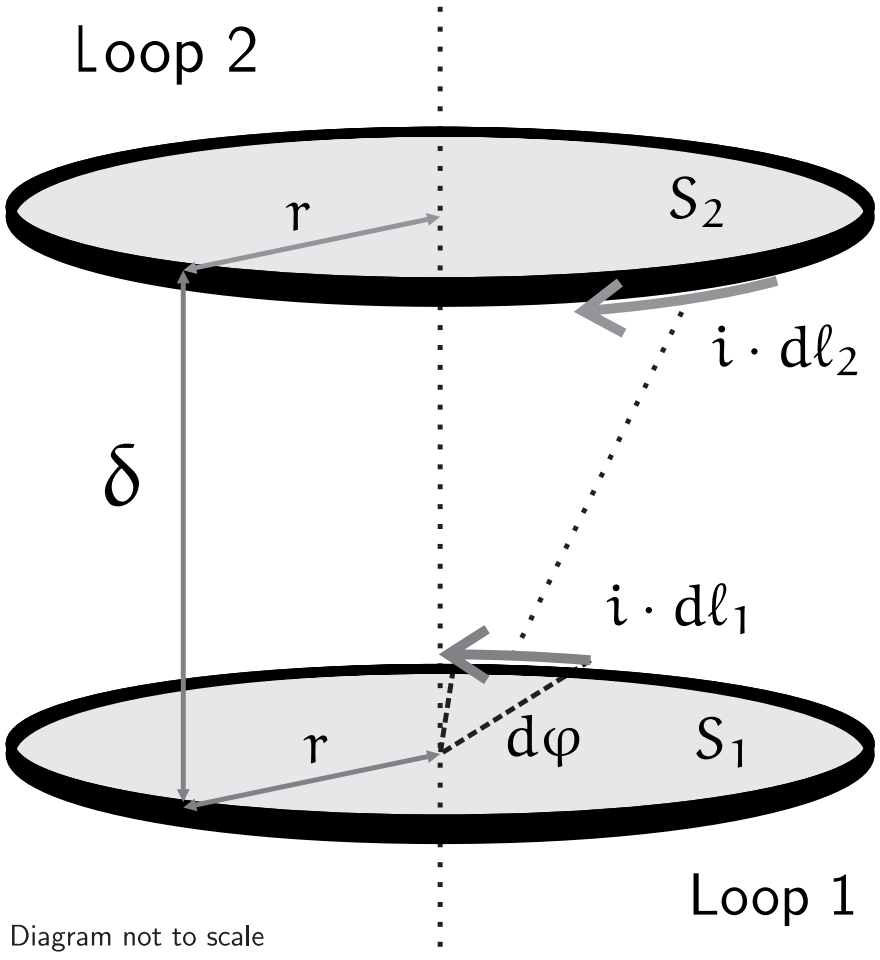

Figure 3.5: Two concentric circular conducting loops in free space.

3.5.1 Mutual inductance

The mutual inductance term, M, is due to the magnetic flux from the first circuit linking into the second circuit. It is reciprocal, in that it is also due to the magnetic flux from the second circuit linking into the first. It is this reciprocity that gives the inductance matrix in equation 3.18 its symmetry. This term is easy to calculate for the idealised coupled-rings system, but an insightful simplification is required. From equation 3.4, mutual inductance can be formulated in the sense of the reciprocal definition stated before. Thus,

$$M = \frac{1}{i_2} \int_{S_1} \nabla \times A_2 dS_1 \tag{3.20}$$

By Stoke's theorem, this is,

$$M = \frac{1}{i_2} \oint A_2 \cdot d\ell_1 \tag{3.21}$$

The magnetic vector potential given in equation 3.7 becomes

$$A_2 = \oint \frac{\mu_0 i_2 d\ell_2}{4\pi R} \tag{3.22}$$

So therefore the mutual inductance takes this form,

$$M = \frac{1}{i_2} \oint\oint \frac{\mu_0 i_2 d\ell_1 \cdot d\ell_2}{4\pi R} = \frac{\mu_0}{4\pi} \oint\oint \frac{d\ell_1 \cdot d\ell_2}{R} \tag{3.23}$$

Equation 3.23 is widely known as Neumann's form, [Nussbaum 1965]. The solution to equation 3.23 is given by Ramo et al. [1965]. The mutual inductance is described by the the equation,

$$M = \mu_0 r \left[(\frac{2}{k_2} - k_2) K(k_2) - \frac{2}{k_2} E(k_2) \right] \tag{3.24}$$

with

$$k_2{}^2 = \frac{4r^2}{\delta^2 + 4r^2} \tag{3.25}$$

This describes the mutual inductance term for the magnetically coupled rings. For coupled rings with the stated dimensions, the mutual inductance is calculated to be $M = 22.3$ nH.

3.5.2 Self inductance

The self inductance, L, is further divided into external and internal self inductances.

3.5.3 External self inductance

The external self inductance is the inductance due to the component of magnetic flux flowing normal to the area enclosed by its generating winding. The external self inductance is found by evaluating the integral,

$$L = \frac{1}{i}\int_S B \cdot dS \tag{3.26}$$

In equation 3.26, S is the element of surface area, in this case $\rho \cdot d\rho d\varphi$. Referring to figure 3.2, the flux passing through the surface S will be the theta-directed component of flux, B_θ, when $\theta = \frac{\pi}{2}$ and the integration takes place along the intervals $\rho = [0, r)$ and $\varphi = [0, 2\pi]$. Therefore the external self inductance is determined by integrating the magnetic flux density over the area enclosed by the loop of current,

$$L = \frac{1}{i_1}\int_0^{2\pi}\int_0^{r}(\nabla \times A)\rho d\rho d\varphi\Big|_{\theta=\frac{\pi}{2}} \tag{3.27}$$

The integral in equation 3.27 may be solved to obtain the value of the external component of self inductance for a ring shaped conductor of radius r. For the coupled rings, $L = 134.8$ nH and because the rings are identical, each ring has this value of self inductance. With this value of self inductance, the coupling coefficient can be calculated as,

$$\kappa = \frac{M}{\sqrt{L_1 L_2}} = \frac{22.3\ nH}{134.8\ nH} = 0.165 \tag{3.28}$$

3.5.4 Internal self inductance

The internal self inductance is the inductance due to the component of magnetic flux flowing in the wire region. It may be obtained by the equivalence of magnetic field energy in the volume of the conductor, V, with the energy stored in an inductor,

$$\frac{1}{2}Li^2 = \int_V \frac{\mu}{2}H^2 dV \tag{3.29}$$

For the coupled rings, determination of internal self inductance is pursued no further. Analytically, it is a complicated calculation. For the wire dimensions prescribed earlier, the external self inductance dominates the internal self inductance. Essentially, this term in the inductance calculation is a component in the broader definition of impedance for the wire. The wire's impedance is physically dependent on frequency, conductivity, skin depth and permeability among other things. For the purposes of wire explosion, it is made more intricate by the phase changes of the copper wire material; there is a changing conductivity during the wire explosion. Also, the radius of the plasma conductor will change, so this affects the electrical behaviour. The RLC characteristic determines the frequency, ω_d, with which the system responds, influencing the skin effect. If the frequency is relatively low, then there is scope to make assumptions about the low-frequency inductance.

3.6 The Magnetic Flux-free Electric Circuit Model

There remains the formulation of a circuit model of the exploding wire by induction. With the electromagnetic principles used to find the inductance matrix, the circuit model can now be depicted, figure 3.6, that lends physical meaning to the problem of exploding a wire by electromagnetic induction.

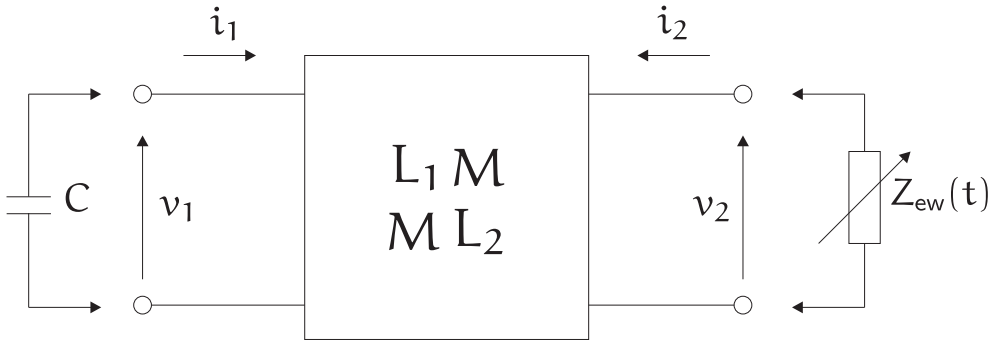

Figure 3.6: Circuit model of wire explosion by induction.

The self inductance terms L_1 and L_2 incorporate only the external component of self induction. The inductance internal to the wire has been omitted due to the small conductor size. It should not be forgotten that this omission may be a source of potential modelling inaccuracy. In the absence of a fully integrated impedance term, it is necessary to insert a component that represents the impedance of the wire. This is the impedance that varies with time, $Z_{ew}(t)$.

3.7 Summary

The problem of exploding a wire using electromagnetic induction has been characterised by a magnetically coupled pair of ring-shaped electric circuits. The consideration of the problem in this way is directly applicable to the pancake coil experiments of chapter 5, where that coil topology bears resemblance to the coupled rings.

Self and mutual inductance was found from the concept of magnetic flux. The magnetic flux density could be plotted for a steady value of current flowing through a ring shaped conductor. The self and mutual inductance of the magnetically coupled rings was determined from first principles and calculated. For the coupled rings system, with separation $\delta = 10$ mm and radius $r = 20$ mm, the self inductance is $L = 134.8$ nH and the mutual inductance is $M = 22.3$ nH. The system therefore has a coefficient of magnetic coupling $\kappa = 0.165$. A circuit model was summarised, incorporating an inductance matrix with the exploding wire represented as a varying resistance with respect to time. This is essential in examining the transient behaviour of the wire during the explosion.

Chapter 4

Exploding Wire Electrical Characteristics

4.1 Synopsis

Studies of wire explosions by conduction are conducive to the creation of plasma windings of several turns, and also aids the understanding of exploding a wire by induction. This chapter explores the electrical characteristics of long distance wire explosion. An optimisation enhanced electromagnetic transients technique was created and used to obtain time varying resistance models of the exploding wire. The optimisation is applied to voltage waveforms of 3 m long wire explosion. Measurements and modelling of voltage and current are also introduced for a set of 1 m wire explosions performed at Graz University of Technology, Austria. In Appendix A, there is an unpublished letter summarising the findings of this chapter.

4.2 Introduction

The exercise of determining electrical characteristics of current and resistance of the exploding wire is motivated in two ways. Firstly, to complete the model established in section 3.6, it is necessary to find the resistance of a wire at any given moment during its electrical explosion. Secondly, an explanation of how the plasma transformer worked, was proving elusive to its researchers as long as current measurement of EW was unavailable. A model of the exploding wire resistance, for instance, could provide clues to the shapes of the exploding wire current traces. Therefore, modelling was undertaken to find the resistance curves for the long distance exploding wire. The models were developed with an optimisation technique using only voltage waveforms and circuit impedance as model inputs. The outputs were the resistance curves.

Almost all previous modelling studies investigated bare (noncoated and nonenameled) metallic wires much shorter than 1 m in length; here the focus is on determination

of electrical characteristics of enameled wires over 1 m in length. 1 m is the shortest length of long distance exploding wire under investigation at the University of Canterbury. Modelling in works by Wall et al. [2003] and Tkachenko et al. [2004] focuses on the complex physical mechanisms present during the exploding wire process. Tucker and Toth [1975] have described a time varying resistance model for short distance exploding wires. None of these models were developed to give the electrical characteristics for long distance exploding wires incorporating the plasma bead mechanism. An ElectroMagnetic Transients (EMT) program was seen as a method to determine the electrical characteristics of long distance exploding wire experiments completed at the University of Canterbury (Canterbury) where current measurement was not available at the time. In 2009, the University of Manitoba entered a collaboration to research the exploding wire phenomenon. With knowledge of the circuit impedance values, and sets of experimental voltage waveforms, an EMT program was set up. An optimisation routine was applied to search for the exploding wire time varying resistance profile. This optimisation routine could also be used to estimate the current waveform produced by the exploding wire. This exercise was worthwhile because reliable current measurement was not available in the high voltage laboratory at the University of Canterbury until mid 2010. Also in late 2009, an opportunity transpired where some exploding wire current measurements could be made at the Institute of High Voltage Engineering and System Management at the Graz University of Technology (Graz). This provided a good opportunity to validate the EMT program predicted exploding wire currents.

Two CEW datasets are analysed; a set of five exploding wire voltage curves from Canterbury, and a set of four voltage and current traces from experiments performed at Graz. Both circuits were capacitive discharge type; the circuit at Canterbury used a 21.4 μF bank of 20 oil filled capacitors, and at Graz, a 200 kV Haefely current impulse generator configured with a capacitance of 20 μF, [Sinton et al. 2010b]. One particular result from each dataset is presented, while further results are tabulated.

4.3 The EMT Optimisation Approach

The method presented by Gole et al. [2005] was used to determine the resistance, $R_{ew}(t)$ of the exploding wire for the complete duration of the voltage waveform. The resistance was chosen as the dependent variable in the optimisation because it was believed at this stage that it was the only quantity that was changing significantly during the exploding wire experiments. Also, choosing resistance seemed to be a

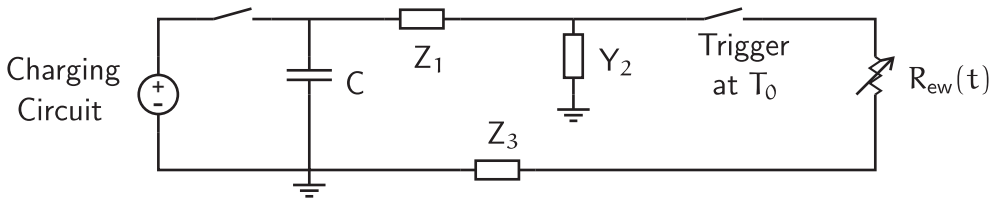

Figure 4.1: Circuit used in the optimisation enabled ElectroMagnetic Transient program.

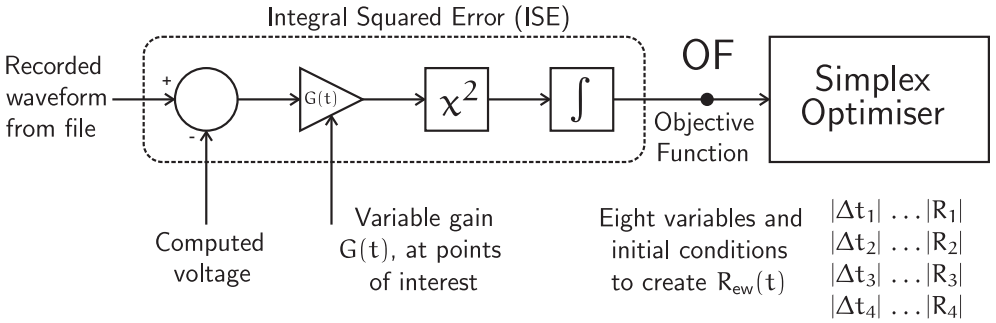

Figure 4.2: Elements of the optimisation routine.

simple way to characterise the problem. Knowing the value of the capacitor bank, C, inductances of both the delivery cables, Z_1, and the return cables, Z_3, and the capacitance to ground, Y_2, of the test set up, it was possible to draw the circuit diagram of the exploding wire in the EMT program, figure 4.1. Using the method of Gole et al., the EMT program was used to evaluate the objective function generated by the block diagram in figure 4.2.

The problem was solved in two parts; initially the program was limited to the first phase of exploding wire, i.e. all activity just prior to the restrike (figure 4.3, feature A-B-C-D). The optimisation was run until the first phase approximation was achieved within a tolerance set in the optimiser (typically 10^{-10}). The resistance values of the first phase were then recorded manually and hard-coded into the $R_{ew}(t)$ transfer characteristic. In the second sequence of the optimisation, the duration was expanded fully until the conclusion of the exploding wire restrike (figure 4.3, feature E-F-G); in this way the optimiser then operates on the restrike part of the waveform.

The Integral Squared Error (ISE) between the measured waveform and the simulated result from the circuit output was determined and passed into the optimiser routine, which attempts to minimise the objective function created by the ISE process. The optimiser routine minimises the objective function according to the simplex algorithm developed by Nelder and Mead [1965].

Within the ISE stage, it is possible to select important features of the waveform

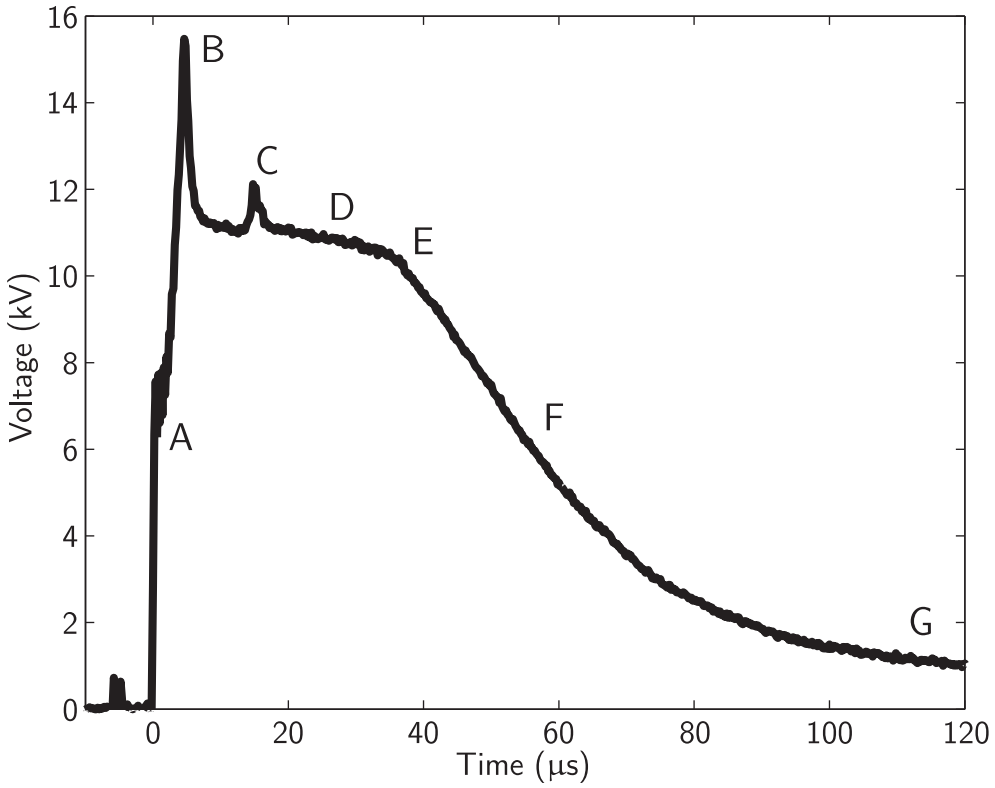

Figure 4.3: Typical exploding wire restrike voltage waveform with labelled regions: A = Initial Switching Transient, B = First voltage spike, C = Second voltage spike, D = Dwell period, E = Restrike inception, F = Conduction through the plasma path, G = Restrike conclusion

and increase the weighting on these regions to force the optimiser to work harder to minimise the error in these regions. This is achieved with the variable gain feature $G(t)$ in equation 4.1,

$$G(t) = \begin{cases} 1 & \forall t < t_1 \\ 10 & \forall t_1 \leq t \leq t_2 \\ 1 & \forall t > t_2 \end{cases} \tag{4.1}$$

The interval $[t_1 \ldots t_2]$ in 4.1 represents the region of interest. The gain for this region was typically set to a factor of ten above the other weightings in the rest of the waveform. As an example, this could be applied to ensure that the second voltage spike (figure 4.3, region C) was correctly modelled and its corresponding feature would show up in the resistance profile. Referring to figure 4.3, the selected region would be [10 μs ... 20 μs].

There are effectively sixteen variables that serve as the output from the optimiser routine. These eight points plus an initial point, [(0, T_0), (R_1, T_1), ..., (R_8, T_8)], describe $R_{ew}(t)$ at different times during the exploding wire. The absolute value of these variables is used to eliminate the optimiser attempting to select negative resistances or negative change in time values.

The time variables are represented by a change in time, Δt, and as such, require sequencing to form the non-linear transfer characteristic describing the resistance profile. This was achieved by using a set of equations in figure 4.4 to ensure the time values followed the sequence,

$$T_0 < T_1 < \ldots < T_7 < T_8 \tag{4.2}$$

4.4 Results

4.4.1 Experiments at University of Canterbury, New Zealand

The model input data was a set of five voltage waveforms from exploding wire experiments involving 3 m lengths of 0.2 mm diameter polyamide enamelled copper wire, exploded at voltages from 20 to 28 kV dc. In conjunction with the EMT program, the optimiser successfully modelled the voltage waveforms, including the first and second voltage spike, and also the exploding wire restrike. A particular comparison is shown in figure 4.5a and 4.5b. The simulations also provided predicted exploding

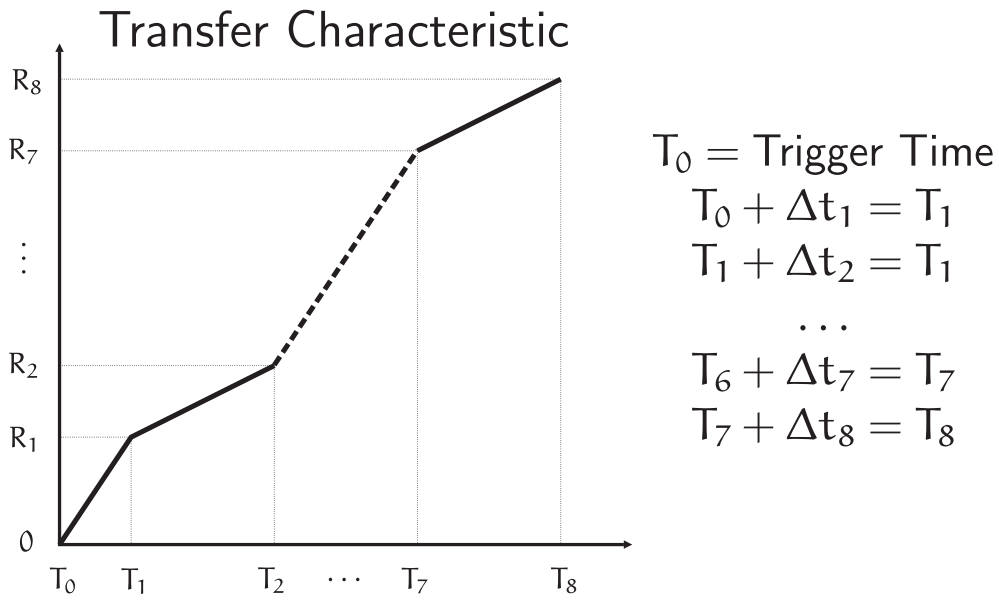

Figure 4.4: Transfer Characteristic $R_{ew}(t)$, equations and representation

wire current and resistance waveforms. The resistance of the wire had been unknown within the University of Canterbury wire explosion dataset, prior to this study. The theoretical $R_{ew}(t)$ traces are overlaid in figure 4.5, displaying the optimised points that describe the varying phases of the exploding wire.

The exploding wire current waveforms for the Canterbury dataset are displayed in figure 4.5c and figure 4.5d, and in figure 4.6 and figure 4.7. In the first phase, the Canterbury results show an impulse of rapidly changing current, of between 4.5 and 6 kA in magnitude. This evidently coincides with the first voltage spike in the voltage trace. At the conclusion of this feature is a knee-point with a rapidly falling lip as the current reduces toward zero. This coincides with the second voltage spike. Beyond this, the current rises relatively slowly during the dwell period, figure 4.3, feature D. Once the dwell period is complete the restrike occurs. In the current waveform, this is marked by the current hump rising up to between 4.5 and 12 kA.

An important result was the rate of change of current: the di/dt characteristic of the current waveforms, especially in the first phase, (figure 4.3, region A-B-C) indicated that high voltages could be produced in the plasma transformer. The plasma transformer operation appears to give two flashes over the series-connected sphere gap on the secondary, figure 4.8. Of note were the two high-di/dt events in the characteristic of the predicted exploding wire current, observed in figure 4.5d. As such, the di/dt in these features may have produced the high voltage observed in the prototype plasma transformer.

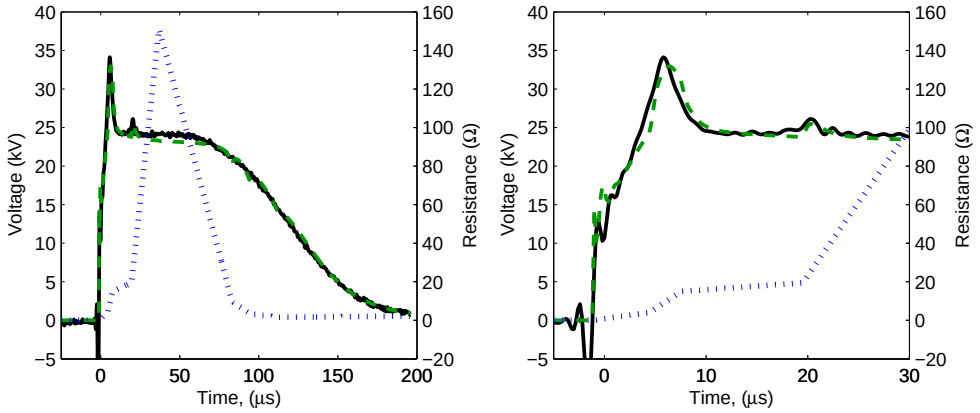

(a) Complete voltage

(b) Detail of first 30 μs voltage

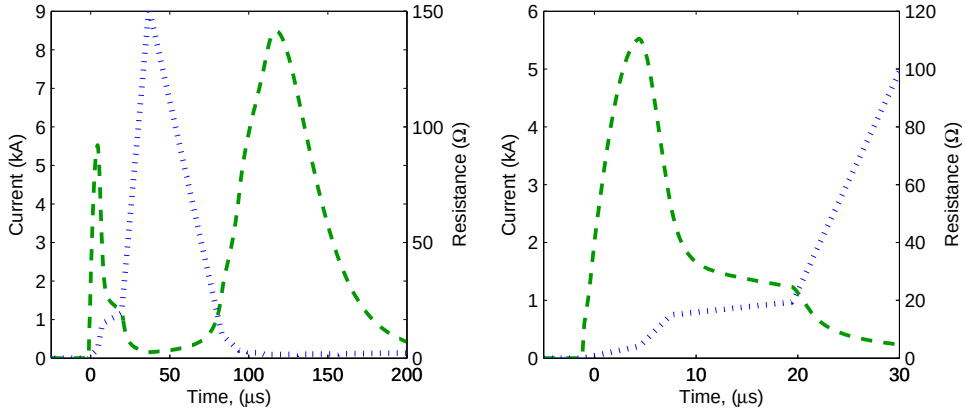

(c) Complete current

(d) Detail of first 30 μs current

Figure 4.5: Measured voltage, simulated voltage, current and resistance curves for 3 m, 0.2 mm wire exploded at 24 kV dc. The dashed traces (green) show the simulated waveforms, the solid traces show the recorded data. The dotted traces (blue) are the resistance functions, $R_{ew}(t)$.

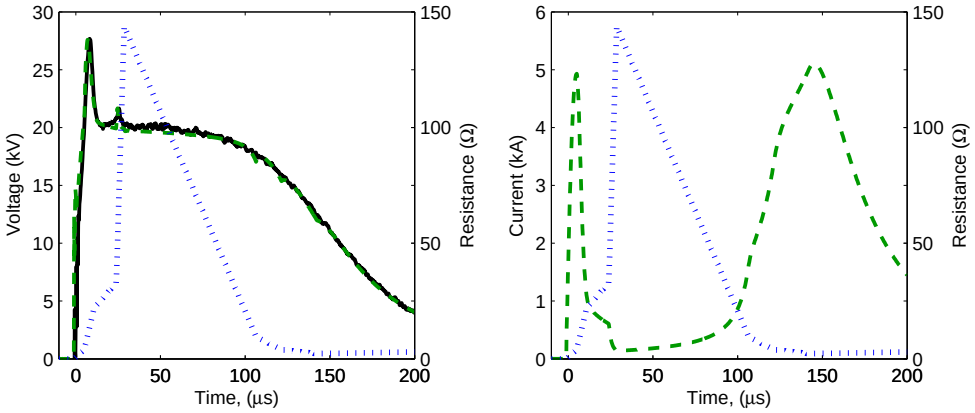

(a) Voltage; 20 kV impulse

(b) Current; 20 kV impulse

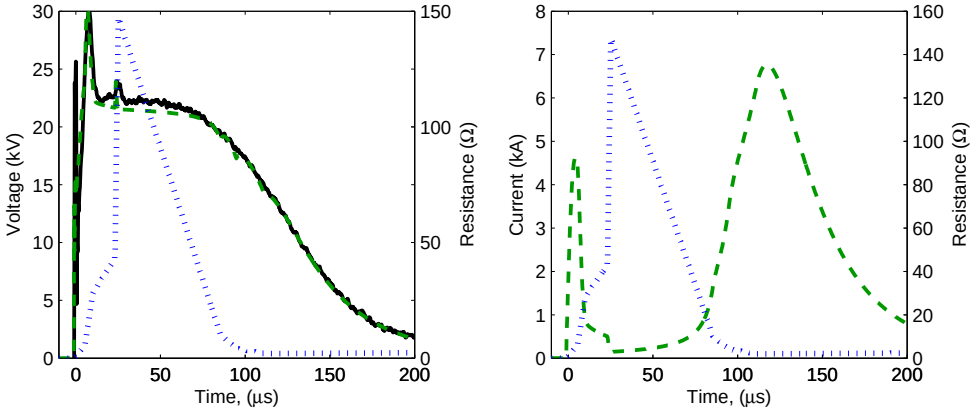

(c) Voltage; 22 kV impulse

(d) Current; 22 kV impulse

Figure 4.6: ElectroMagnetic Transient optimised exploding wire characteristics from University of Canterbury dataset, The dashed traces (green) show the simulated waveforms, the solid traces show the recorded data. The dotted traces (blue) are the resistance functions, $R_{ew}(t)$. Wire length is 3 m, wire diameter is 0.2 mm

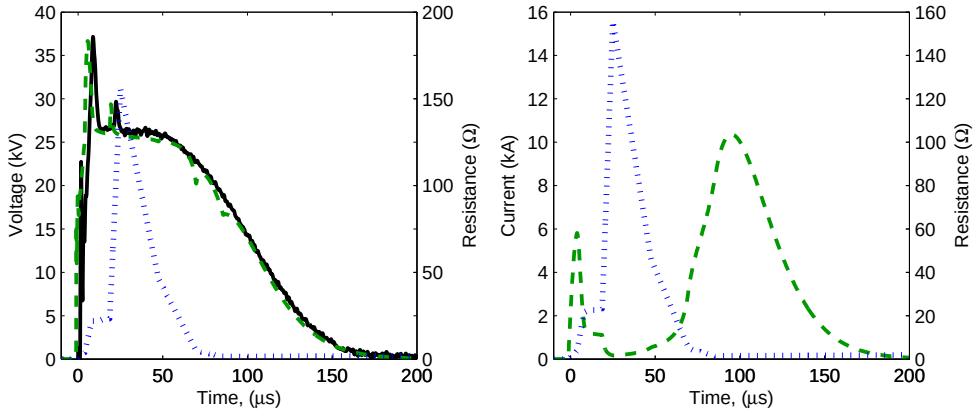

(a) Voltage; 26 kV impulse

(b) Current; 26 kV impulse

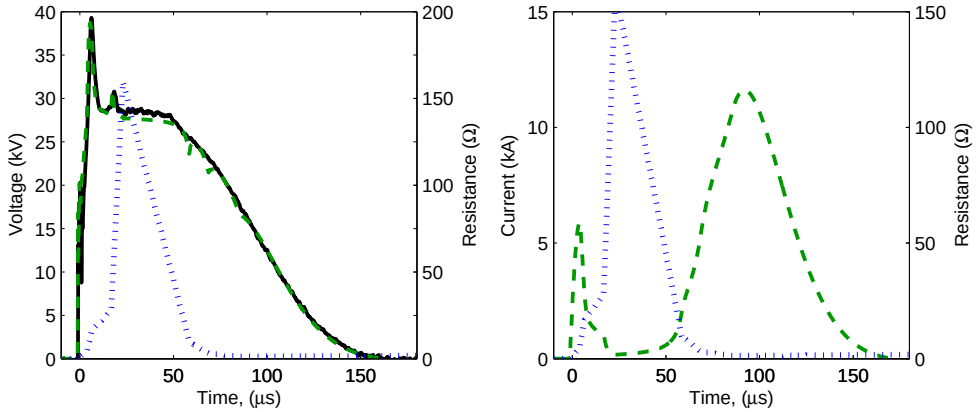

(c) Voltage; 28 kV impulse

(d) Current; 28 kV impulse

Figure 4.7: The dashed traces (green) show the simulated waveforms, the solid traces show the recorded data. The dotted traces (blue) are the resistance functions, $R_{ew}(t)$. Wire length is 3 m, wire diameter is 0.2 mm

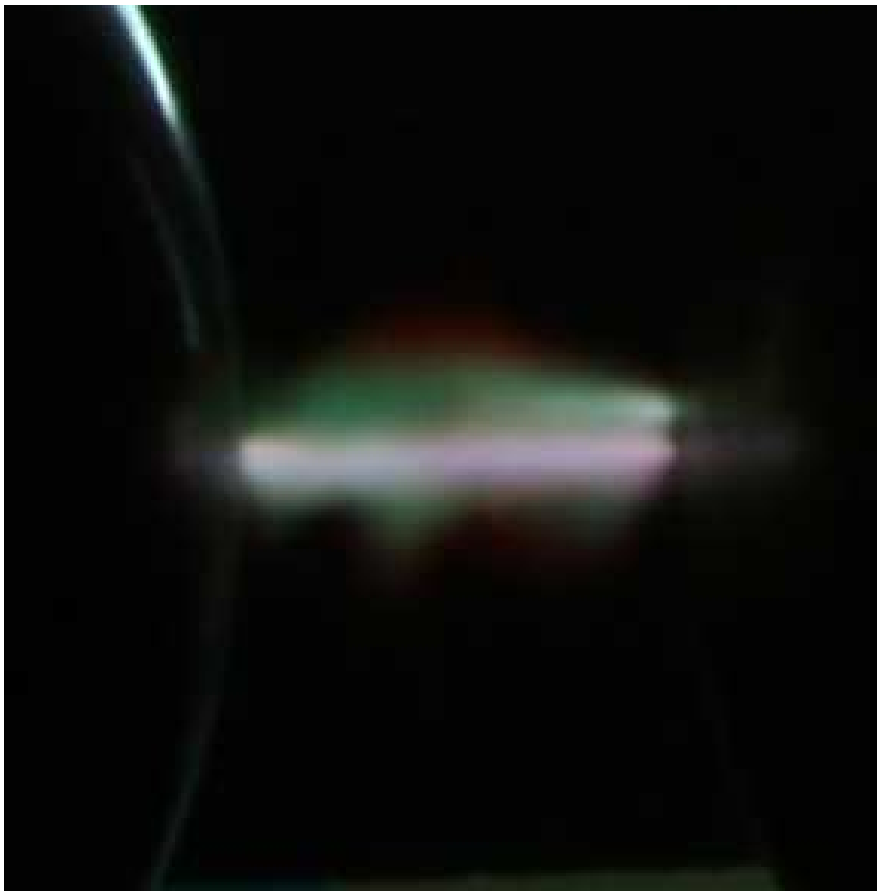

Figure 4.8: Close up of the sphere gap flashing over twice, due to voltage induction in the secondary winding of the plasma transformer in figure 2.7.

The optimisation routines produce a predicted shape of current and resistance profile. The Canterbury simulated current profiles were a significant outcome of the optimisation, because it demonstrated that Hammond's plasma-primary transformer requires large rates of change of current to produce impulse voltages over its secondary winding.

4.4.2 Experiments at Graz University of Technology, Austria

Concurrently with the modelling work of the Canterbury results, Mr Rowan Sinton was at the Institute of High Voltage Engineering and System Management at the Graz University of Technology and was able to perform exploding wire experiments with current measurement. The test subjects were 1.05 m, 0.2 mm diameter polyamide enamelled copper wires exploded at voltages from 20 to 28 kV dc.

The Graz experimental and optimised EMT model results are presented in figure 4.9, and in figure 4.10. The measured current traces exhibit many of the same features predicted by the Canterbury models. The $\mathrm{R_{ew}(t)}$ resistance curves are overlaid in each of the traces.

The current traces emerging from the optimiser resembled closely the experimental current data that was recorded at Graz. The optimiser was able to successfully model the exploding wire voltage traces. However, the current traces, while exhibiting the correct shape, were not consistent in magnitude with the current measurements of the Graz experiments.

To accurately determine the resistance of the exploding wire, the relative error in the voltage was added to the relative error in the current to produce a single overall error which was fed into the ISE step. This is shown in figure 4.11. This mode allows the optimiser to minimise error in both the voltage and current, thus providing a more faithful representation of the resistance profile for the Graz exploding wire experiments. The optimiser produced results from a small number of points that clearly showed the key features of exploding wire resistance. In comparison, applying Ohm's law to find the resistance from the voltage and current produced very noisy results.

It is within the capability of the optimiser to reproduce accurate current and voltage models from only eight points. Increasing the number of points is an option which is available, however, for the purpose of this investigation, having eight points illustrated the optimiser's principle of operation. The dual optimised Graz data illuminates a more accurate representation of the $\mathrm{R_{ew}(t)}$ profiles. These resistance traces could be

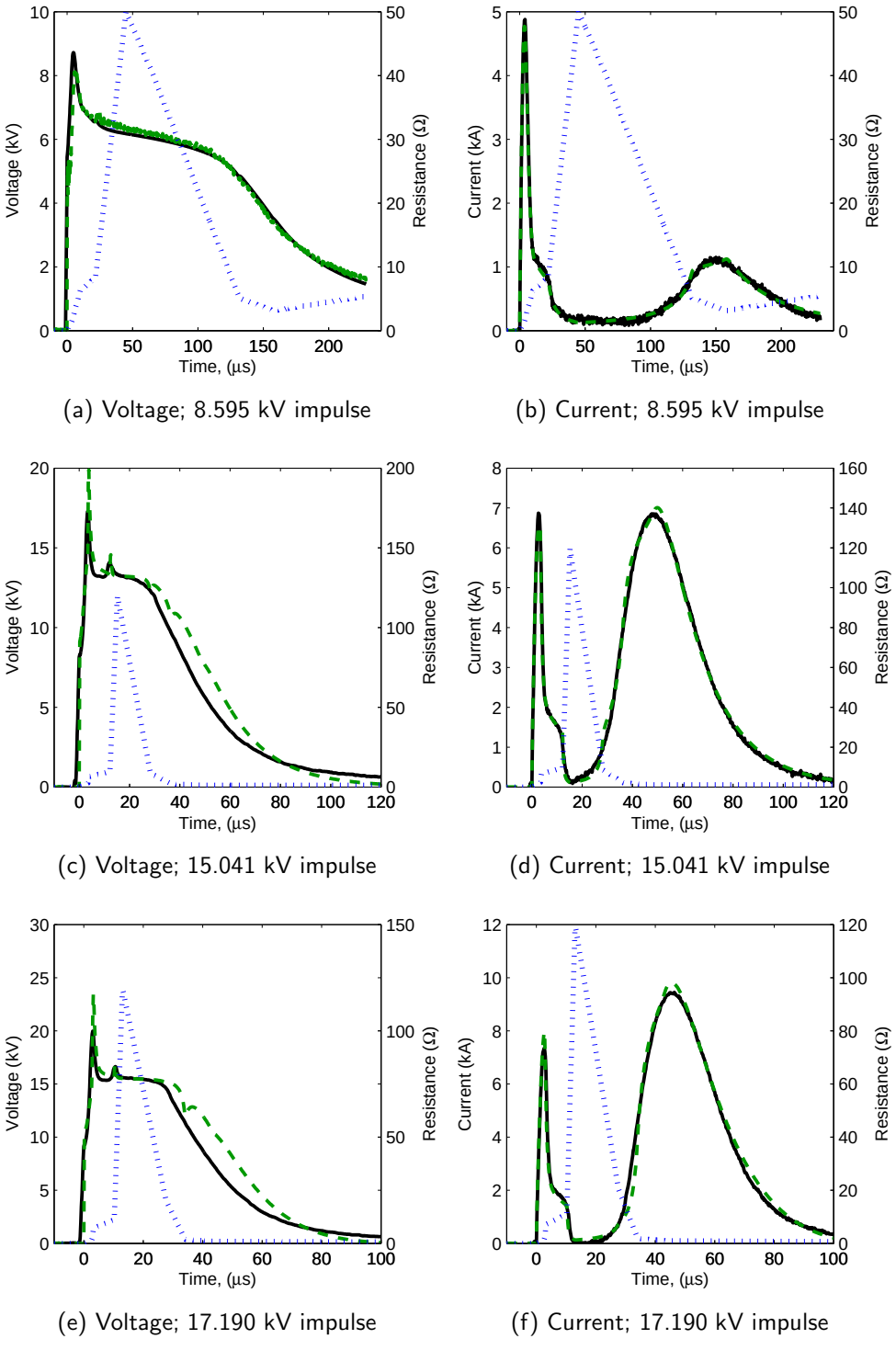

(a) Voltage; 8.595 kV impulse

(b) Current; 8.595 kV impulse

(c) Voltage; 15.041 kV impulse

(d) Current; 15.041 kV impulse

(e) Voltage; 17.190 kV impulse

(f) Current; 17.190 kV impulse

Figure 4.9: The dashed traces (green) show the simulated waveforms, the solid traces show the recorded data. The dotted traces (blue) are the resistance functions, $R_{ew}(t)$. Wire length is 1.05 m, wire diameter is 0.2 mm.

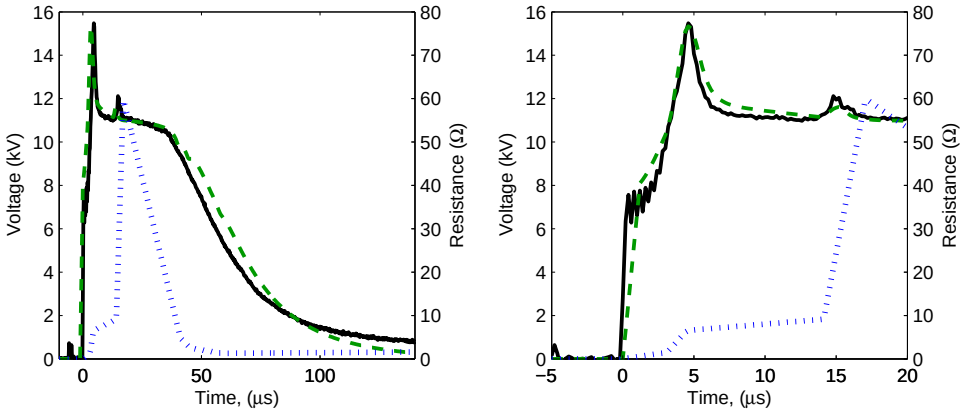

(a) Complete voltage

(b) Detail of first 30 μs voltage

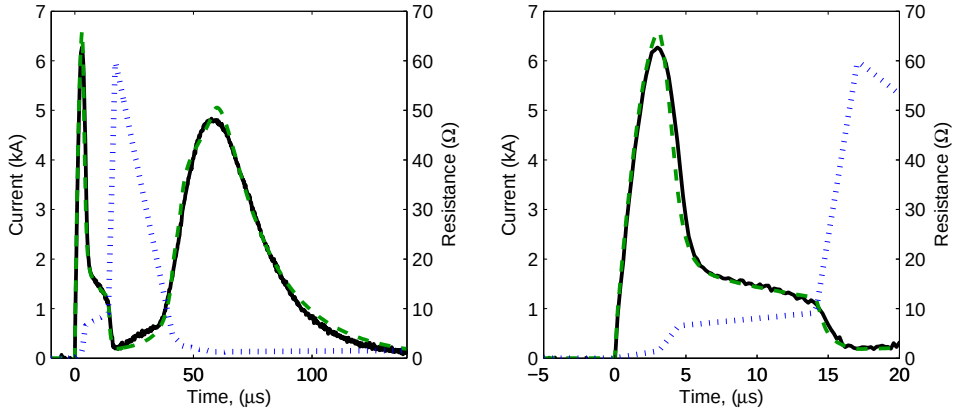

(c) Complete current

(d) Detail of first 30 μs current

Figure 4.10: Measured voltage, simulated voltage, current and resistance curves for 1.05 m, 0.2 mm wire exploded at 12.89 kV dc. The dashed traces (green) show the simulated waveforms, the solid traces show the recorded data. The dotted traces (blue) are the resistance functions, $R_{ew}(t)$.

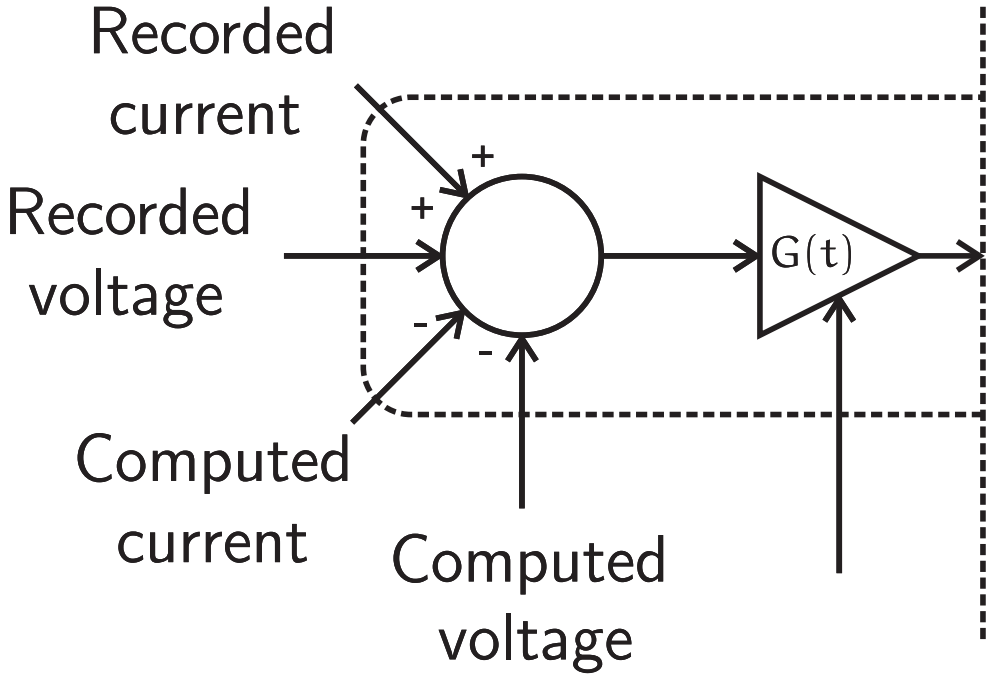

Figure 4.11: Input elements of the modified optimisation routine.

used to build up archetypal traces at theorised distances and voltages to provide a model and testable hypotheses. In turn, the optimiser could support the design of novel machinery that utilise plasma conductors.

4.5 Summary

Using recorded data from CEW experiments over 3 m and 1 m distances performed at the Universities of Canterbury and Graz, resistance models of the long exploding wire were obtained via an optimisation enhanced EMT simulation technique. With a coarse optimisation routine of only eight points, it was possible to get a detailed template for the resistance profile of long distance exploding wires. The EMT technique provided important information about exploding wire current and resistance, useful for building up the mathematical model characterising wire explosion by induction, established in section 3.6. The $R_{ew}(t)$ traces for CEW is a component in the $Z_{ew}(t)$, of that model, implying that the model for IEW is more or less complete. Another outcome was that the current traces recorded at Graz revealed the rate of change of current in the first phase of the exploding wire, demonstrating how high voltages are being produced in the plasma transformer.

Chapter 5

Experimental Environment

5.1 Introduction

A complete model of the exploding wire must certainly be useful for developing techniques for wire explosion by induction. The issue of whether this model is useful or appropriate hinges around two factors. One is voltage and current measurement. If one voltage or current measurement is missing, then the model will not be applicable to those experiments, since the system will be indeterminate. Secondly, in regard to its fragmentation and restrike mechanisms CEW should represent properly those physical properties of IEW. In essence, it should be that $R_{CEW}(t) \equiv R_{IEW}(t)$.

What remains in this thesis is predominantly experimental and empirically based methods for exploding a wire via electromagnetic induction. Further development of a model without first some experimentation would be overly philosophical for the scope of this thesis.

This section details the equipment used to provide electrical energy storage and release during exploding wire experiments, and the associated measurement techniques. Also described are the safety features and philosphy of hazard identification implemented in the laboratory during the experiments.

5.2 Equipment

5.2.1 Energy storage

Energy for the experiments on wire explosion by electromagnetic induction was stored in a bank of capacitors, with a total capacitance of 21.4 μF. The bank is comprised of 20 individual units of oil-insulated capacitors each with a capacitance of 17.1 μF. These are arranged in a stack of five units in parallel, constituting one stage, and four

(a) Capacitor Stack (b) Capacitive Voltage Divider

Figure 5.1: 21.4 μF Capacitor bank used to store electrical energy and the capacitive voltage divider used to measure the capacitor bank voltage in experiments on EW by induction

of these stages in series. The voltage rating of each capacitor stage is 15 kV d.c.; four stages therefore yield a total stack voltage rating of 60 kV d.c. The bank was built by David Smith, the details of its construction are given in Smith et al. [2007]. Figure 5.1a shows a digital image of the capacitor bank in the laboratory.

Each capacitor weighs about 60 kg so the total stack mass is therefore 1200 kg. The magnitude 7.1 (4 September 2010) and 6.3 (22 February 2011) earthquakes, that severely damaged the city of Christchurch, failed to topple the capacitor bank. Outriggers with strops tied to the top two stages had been installed by Smith to reduce the likelihood of topple over.

However, the bank did not completely escape impact. It was noted that the topmost stages (bolted to mild steel angle-section) had slid along their cylindrical culvert-piping spacers. Oil leakage, presumably from the topmost bushings, had been detected soon after significant seismic activity. The leakages did not persist after they were cleaned up, and it seems likely that the bushing movement during the heavy shaking may have released small volumes of oil from associated seals.

The capacitor bank is charged by energising with mains voltage a variable autotransformer in cascade with an 80 kV step-up transformer connected to a high-voltage half-wave rectifier. Two 50 kΩ series-connected resistors limit the charging current and thus protect the high voltage diode in the rectifier. The rectifier is connected to the capacitor bank, and operators control the charging voltage from the Faraday cage. The capacitor bank's charging voltage is measured by a resistor divider to ground, and can be read by operators from a callibrated digital multimeter.

5.2.2 Triggered spark gap (TSG)

During the experimental phase, the electromagnetic drop-switch used by Smith to trigger the capacitor bank was replaced. A three-electrode triggered spark gap (TSG) was built and used in the experiments to switch the current into the test piece. A 30 kΩ shunt water resistor was connected to the low-voltage side of the TSG to divert a low current to the earth. This was so ionisation could be maintained in the gap, during the exploding wire experiment. The TSG is detailed in Sinton et al. [2010a]. The TSG is triggered at a console by the operators via a fibre-optic cable from the Faraday cage. An automotive induction coil was used to provide the triggering spark. The electronic control circuit and ignition coil was powered by a lead-acid battery and placed in a metal box on the high-voltage side of the spark gap. The TSG operating region was determined in trials utilising capacitor-sourced high voltage d.c.

tests to find the minimum self-triggering flash-over voltage and the minimum reliable triggering voltage. The minimum difference between the operator-trigger line and the self-trigger line was 10 kV. A curve was drawn between these which was used as the reliable operating line. A chart was made with voltage on the y-axis and the gap distance on the x-axis, and this was used for setting the distance between the triggering spheres. This chart is displayed in figure 5.2. The TSG was built for triggering voltages between 10 and 60 kV d.c.

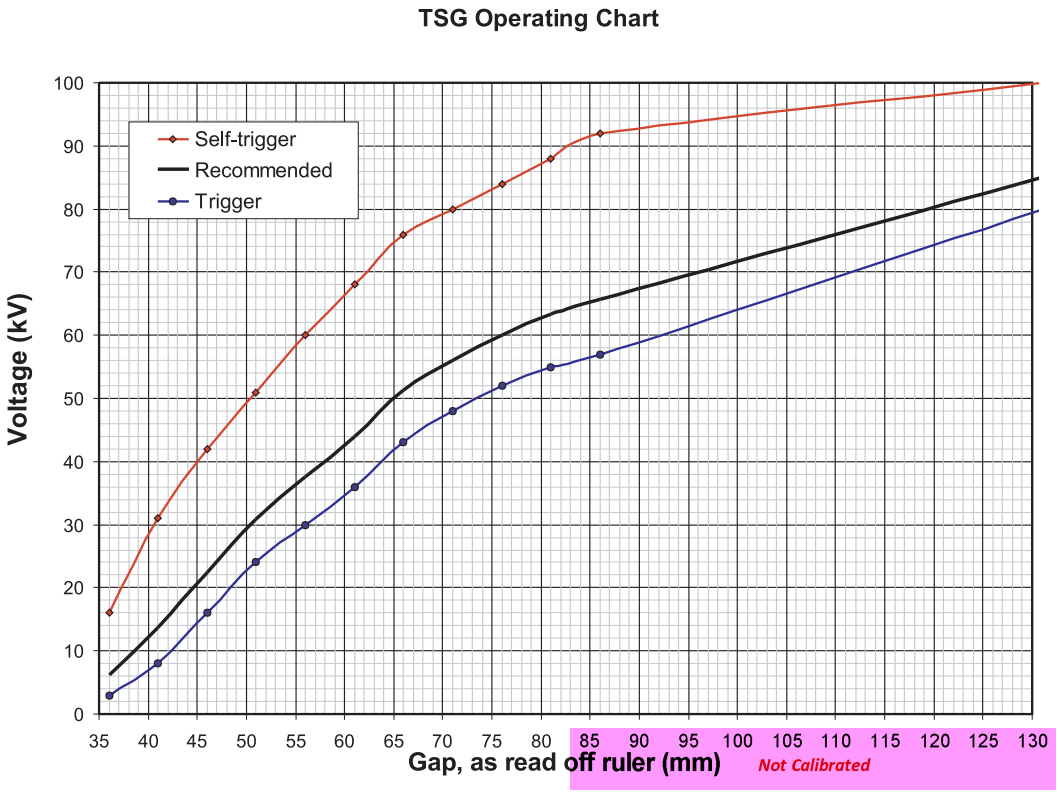

Figure 5.2: TSG operating chart depicting the operating region for reliable triggering of the wire explosion experiments

5.2.3 Types of tests

There were two main circuit configurations. Figure 5.3a shows the set-up for the pancake induction coil experiments in Chapter 6, while figure 5.3b shows the typical set-up for the experiments in Chapter 7.

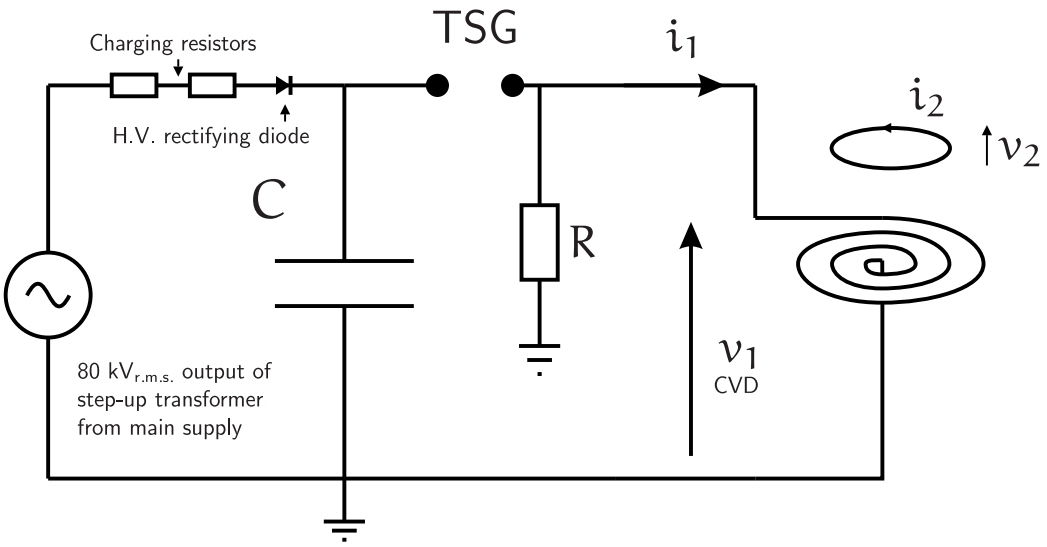

(a) Pancake IEW set-up

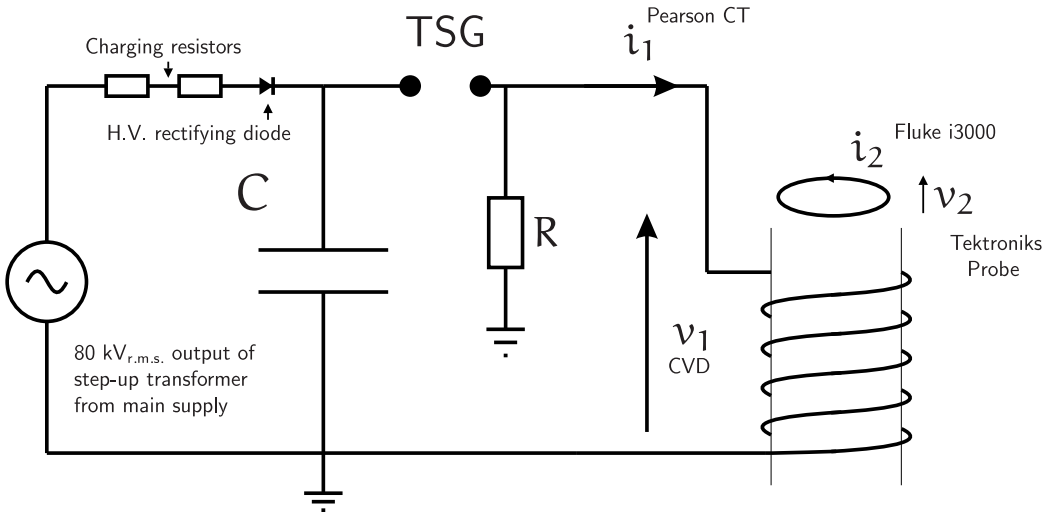

(b) Helical IEW set-up

Figure 5.3: Circuit diagrams for experiments in EW by induction. C is the capacitor bank, which is connected through a TSG to the induction winding. R is the water resistor.

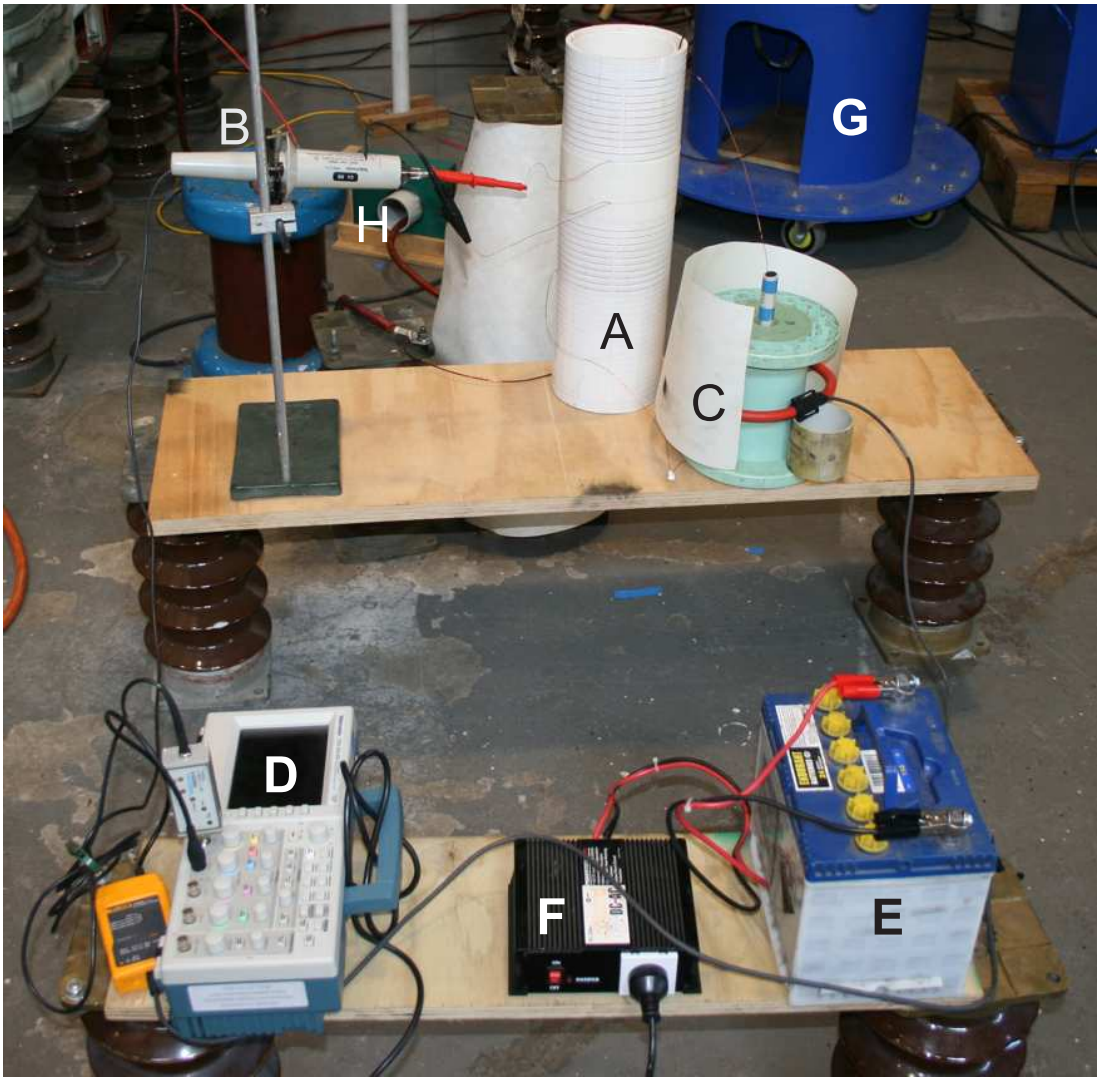

Figure 5.4: Equipment used in experiments on wire explosion via electromagnetic induction. A = a wire explosion by induction apparatus on the test bench, B = Tektronix probe measuring the exploding wire voltage, C = flexible clamp sensor measuring current flow through the wire explosion by induction, D = Oscilloscope, E = lead-acid automotive battery for isolated power supply, F = Inverter, G = capacitive voltage divider measuring capacitor voltage, H = Pearson current monitor measuring current flowing from the capacitor bank (The Pearson current monitor is the green coloured apparatus in the background)

5.3 Instruments

5.3.1 Voltage measurement

A Ferranti 600 kV capacitive voltage divider (CVD) was used to measure the capacitor-side transient voltage for the experiments. A 2 kΩ damping resistor was attached in series. The CVD was used to sense the voltage applied to the winding generating the transient magnetic field. The CVD is shown in figure 5.1b.

Exploding wire voltage waveforms were measured where possible and for this task a Tektronix 40 kV d.c. high voltage probe was used. The probe was mounted at the handle on a laboratory clamp-stand. The probe's ground electrode was suspended with an insulating string so that there was acceptable clearance between the probe contact points. The Tektronix probe is shown on the test bench in figure 5.4, feature B.

The oscilloscope models used were the Tektronix TDS-2022B 200 MHz two-channel scope and TDS-2014B 100 MHz four-channel scope. Figure 5.4, feature D shows the oscilloscope in place in an experiment. Where only capacitor discharge voltage and current were measured, these were recorded on the two-channel scope. For both capacitor discharge traces and exploding wire traces, two separate oscilloscopes were used. All oscilloscopes measuring exploding wire current and voltage activity were powered using an isolated supply from an automotive lead-acid battery and inverter. The second scope and battery-inverter supply was always isolated from the earth on insulator stands so that the exploding wire voltage was floating from ground. This was to minimise the chance of electrical energy being discharged through the instruments to ground. The battery-inverter set comprises features E and F in figure 5.4.

The voltage measurements were used by the oscilloscopes for triggering the scopes to record the transients. The traces were written to data files immediately after the energy supplies were isolated and earthed. Recordings were stored on a 500 MB universal serial bus flash drive.

5.3.2 Current measurement

Capacitor current measurement was made via a 50 kA Pearson 301X ferrite-cored high frequency current transformer (CT). The CT was situated near the earth connection to the neutral cable returning to the bottom electrode of the capacitor bank. It is depicted in figure 5.4, feature H. The 95 mm^2 return cable from the experiment was

run through the CT, with the sense of the current pointing towards the earth. The CT was isolated from the ground to a voltage rating of 20 kV r.m.s. An insulating sheath, rated continuously to 20 kV r.m.s, was made from a section of polyvinylchloride drainpipe to isolate the conductor from the ferrite chassis of the CT. This would minimise the possiblilty of inadvertent capacitor discharge to earth through the instrumentation. The CT was connected to the capacitor-side oscilloscope through a UHF to BNC adaptor.

Exploding wire transient current measurement was made via a Fluke i3000 flexible a.c. current sensor. The sensor was set to the 3000 A range which gave a voltage output of 100 mV/A. This current monitor was connected to the same oscilloscope as the exploding wire voltage measurement from the Tektronix probe. It is shown in figure 5.4, feature C. Care was taken to ensure the exploding wire and capacitive discharge portions of the experiment were electrically isolated from the current monitor. The flexible current clamp was wrapped around a plastic insulating reel to prevent electrical contact with the exploding wire circuit. The insulating reel was tested to withstand a voltage of 40 kV r.m.s for a duration of 60 s. The sensor's cables were suspended from the earth by looming them over PVC culvert piping insulators, known to withstand peak voltages of 40 kV r.m.s for a duration of 60 s.

5.3.3 Photographic observation

Photography was made with a Canon 400d digital single lens reflex camera with ND8 darkening filters attached to prevent overexposure. Options for long-exposure and momentary photography were available. Co-ordination with TSG was made possible by setting a triggering signal to the camera before the TSG's triggering signal was sent. The delay between the camera trigger time and TSG trigger signal was configurable from the TSG console in the Faraday cage. This enabled the camera shutter to be open at the instant the experiment took place.

5.4 Layers of Safety

5.4.1 The Minimum Approach Distance (M.A.D)

One method of operator protection from high voltage hazards was the minimum approach distance (M.A.D). This is the minimum allowable safe distance for competent operators to approach live conductors. The M.A.D is the first line of defence against

the high voltage hazard. If M.A.D's for particular high dc voltages are unavailable, the M.A.D is determined by choosing the distance from ac tables specified by equation 5.1,

$$V_{ac} = \frac{V_{dc} \times \sqrt{3}}{\sqrt{2}} \tag{5.1}$$

The minimum approach distance tables are found in Electricity Engineers Association of New Zealand (EEA) 'Safety Manual - Electricity Industry', ([Safety Manual - Electricity Industry 2009]), a copy is kept permanently in the High Voltage Laboratory. It was important to keep the camera used for long exposure shots further than the minimum approach distance since the camera's triggering cable is brought into the cage where the operators are situated.

5.4.2 De-energisation and earthing

The capacitor stack, charged to 60 kV, can store 38.5 kJ of energy. In the event that the TSG cannot be triggered, or for some reason the experiment must be aborted, then the capacitor bank needs to be de-energised safely. This is achieved by applying a water resistor to the topmost electrode of the capacitor bank, and observing with a fixed multimeter that the charge voltage returns to zero. Originally, the capacitor bank was discharged by an operator applied water resistor. In order to isolate the operators from further risk of the high voltage hazard, this de-energisation system was replaced with an automated remote switch. The switch consists of an electromagnet and aluminium rod and counterweight. When power is applied to the electromagnet, it causes the earthed rod to detach from the electrode connected to the water resistor and capacitor bank. After this, the charging may commence. To remove energy from the capacitors, power to the electromagnet is switched off and the rod falls into position to connect the capacitor bank and series water resistor to earth. The remote switch was not considered to be truly fail-safe, because it was not set-up to trigger automatically with a gate interlock system, for example. To reflect this, the remote switch is termed a 'de-energise-closed' switch because when power is disconnected from the switch, it closes and consequently the capacitor bank gets de-energised. The de-energise-closed switch is shown in figure 5.5a.

5.4.3 Faraday cage

A Faraday cage was used to provide isolation of operators from high voltage hazards. The Faraday cage works by surrounding its contents with an equipotential electric

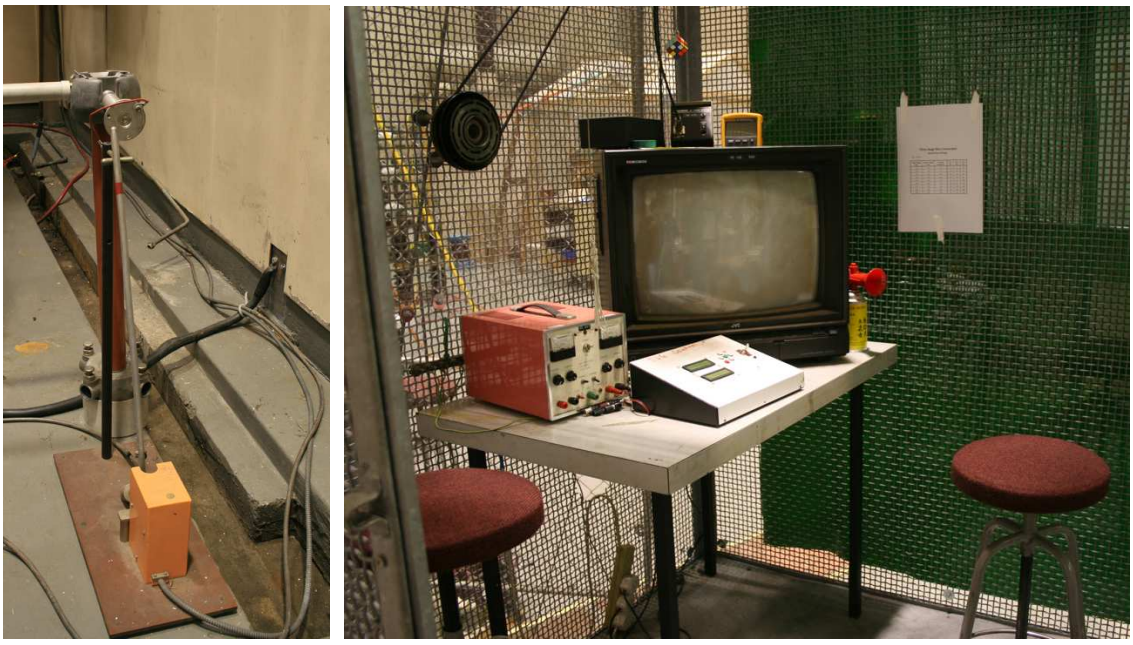

(a) Remote de-energise-closed switch

(b) Faraday Cage

Figure 5.5: Layers of safety in the high voltage laboratory

field. This eliminates the possibility of step and touch potentials due to earth potential rise (EPR) occuring inside the cage, in turn minimising the likelihood of operators being affected by that hazard. The charging circuit and de-energise-closed switch were activated by insulated pull-switches. The pull switch string was tested to withstand a voltage of 100 kV r.m.s over a length of 40 cm. The variable autotransformer used to charge the capacitor bank was external to the cage. The handle for the autotransformer was manipulated with an insulated rubber belt. The TSG console was situated in the cage, and the charging circuit voltmeters and ammeter could be monitored via a closed-circuit television camera. Control circuits for the de-energise-closed switch, circuits for charging and voltmeters with leads were not brought into the cage. This minimised the risk of high voltage being present inside the cage where the operators were situated. The Faraday cage interior is shown in figure 5.5b.

5.5 Management of Hazards: The Hazard Identification Procedure

Over the course of this research, health and safety procedures were being continually reviewed by the high voltage research group. The purpose of introducing the additional safety controls was to enable comfortable observation of the experimental

outcomes without concentrating on hazard management. During this period, layers of safety were incorporated into the design of experimental equipment in the high voltage laboratory. A hazard identification procedure was undertaken daily to ensure that operators were aware of the various hazards in the laboratory, their risk category and the means by which the hazards were to be controlled. It is of critical importance to understand the hazard identification process because without it, experiments could not be undertaken.

Prior to any experimentation, the safety procedures are reviewed and a hazard identification (hazard ID) sheet is filled out before proceeding. Table 5.1 summarises the hazards that were identified during the course of experiments. It describes the controls that were applied to treat the hazard. There are three categories of hazard treatment:

Eliminate The hazard has been eliminated on this occasion

Minimise The danger presented by the hazard has been minimised as much as possible, but some risk remains

Isolate The operators have been isolated from the hazard

Categorising hazards in this way adds clarity to how the hazard can be treated and managed by operators. The hazard treatment was determined by way of operator consensus, during the hazard ID process.

The high voltage hazard was controlled by isolating the operators in the application of the M.A.D. Operators were isolated from stored energy by applying the de-energise-closed water resistor, and electrically and physically isolating the charging supply and earthing the conductors and storage elements before handling them again. EPR was managed by situating the operators inside the Faraday cage. All protective earths including operator applied earth-sticks were tested each week to measure less than half an ohm. This reduced the risk of exposure to EPR if an earth was applied to a fully energised storage element. Explosion and debris was minimised by triggering the experiment from inside the Faraday cage which had been fitted with 4.5 mm thick polycarbonate screens. Operators would wear personal protective equipment consisting of grade-5 hearing protection, face shields and cotton overalls. An area where high voltage is present should have only one entry and exit point. Additional points of entry were eliminated. Procedures for fire and earthquake were implemented when appropriate, and summary details of those matters can be found in the table of hazards.

Table 5.1: Table of Hazards for all IEW experiments

Hazard	Treatment	Control
High voltage up to 60 kV dc	Isolate	Maintain M.A.D of 1 metre
		Includes camera cable back to cage
Stored electrical energy	Isolate	Apply de-energise-closed water resistor
		Isolate and earth prior to touch
Earth potential rise	Isolate	Operators in Faraday Cage
		Operator applied earths tested weekly $<0.5\ \Omega$
Explosion and debris	Minimise	Operators in Faraday Cage
		Operators behind polycarbonate screen
		PPE, hearing and eye protection
		Covered-in arms, wear natural fibre
Fire	Minimise	De-energise, isolate and earth, raise alarm
		Fight fire if comfortable
		Evacuate if uncomfortable
Second point of entry	Eliminate	Closed - cannot open from outside
Seismic aftershock	Minimise	Activate remote water resistor
		Stop charging, operators to remain in cage

5.6 Summary

This section described the energy sources and switching apparatus used to explode a wire by induction. Voltage and current measurement apparatus were described. A hazard identification procedure was used to protect operators during experimentation. Examples of different types of hazards and the management of those hazards were summarised in a table of hazards.

Chapter 6

Experiments with Pancake Coils

6.1 Synopsis

Plasma beads were produced from wire explosion by induction using a pancake induction coil topology, where the target was a ring-shaped copper wire. In some experiments the wire target was segmented so that the plasma spots were spread around the circumference of the wire ring. Full restrike of the wire was not encountered in these experiments.

6.2 Introduction

This chapter is about exploding a wire by induction using pancake-shaped induction coils to produce a transient magnetic field due to a capacitor discharge. Experimental surveys were undertaken to create a full plasma ring by the induced explosion of a ring of copper wire. The ring-shaped copper wire used as the target for the IEW was placed directly above the induction coil to maximise the coupling, κ. A current from the 21.4 μF capacitor bank was discharged through the induction coils, which transferred energy magnetically to the ring-shaped copper wire target, in order to explode that wire.

6.2.1 The pancake-winding arrangement

A pancake coil is a spiral-shaped conductor wound in a single plane, such that the resulting winding is shaped like a pancake. The pancake coil topology was chosen because it was easy to build, the windings can be brought close together and it would be easy to bring a ring-shaped copper wire target close to the face of the coil.

Figure 6.1 depicts a sectional elevation of a typical pancake-coil experiment, as it was set up in the laboratory prior to the discharge of energy through the induction winding. The induction coil is wound from 0.25 mm x 4.5 mm flat copper conductor. The copper conductors are embedded in a fold of Nomex tape, which are taped over the edge of a strip of Nomex-Mylar-Nomex (NMN) 5-10-5 insulating paper. There is another wider strip of NMN 5-10-5 stuck onto the strip with the winding on it. The NMN strips are sandwiched together during the winding process using double-sided Nomex tape (a strip of tape folded in on itself), to form a band. The band is wound five times around a polyvinylchloride (PVC) former of 48 mm diameter to produce a five-turn coil. NMN 5-10-5 was chosen because the mylar has good electrical insulation properties and the nomex layers have good thermal properties such as fire resistance.

The IEW ring was initially made from 0.2 mm enamelled copper wire. For subsequent sets of experiments, the copper ring was made by placing a sheet of copper circuit-board material in a lathe. The chisel pointed toward the copper layer, and so a ring shaped pattern was etched by scratching off the layer of copper on the board. The width of the remaining copper wire-track was normally 0.3 mm, but could vary by $\pm$ 0.1 mm. This variability in the wire width turned out to be an important factor in determining where the plasma beads would appear along the ring.

6.3 Experiments

Many experiments were undertaken to investigate the possibility of creating a plasma ring from the induced explosion of a copper turn. Experiments that produced the most notable outcomes are mentioned in table 6.1. These experiments all used induction coils described in section 6.2.1, which correspond to specimens C, D and F in the table. With each experiment, the winding condition would deteriorate because of the magnitude of the current pulse, so that is why new coils had to be wound occasionally. All the experiments used some variation of the single copper ring to produce different exploding wire plasma-by-induction effects.

6.3.1 Diamond ring effect

On 10 May 2010, 10 kV was discharged into a pancake coil. The copper wire ring target produced some spots of plasma. When 20 kV was applied to Coil C, it resulted

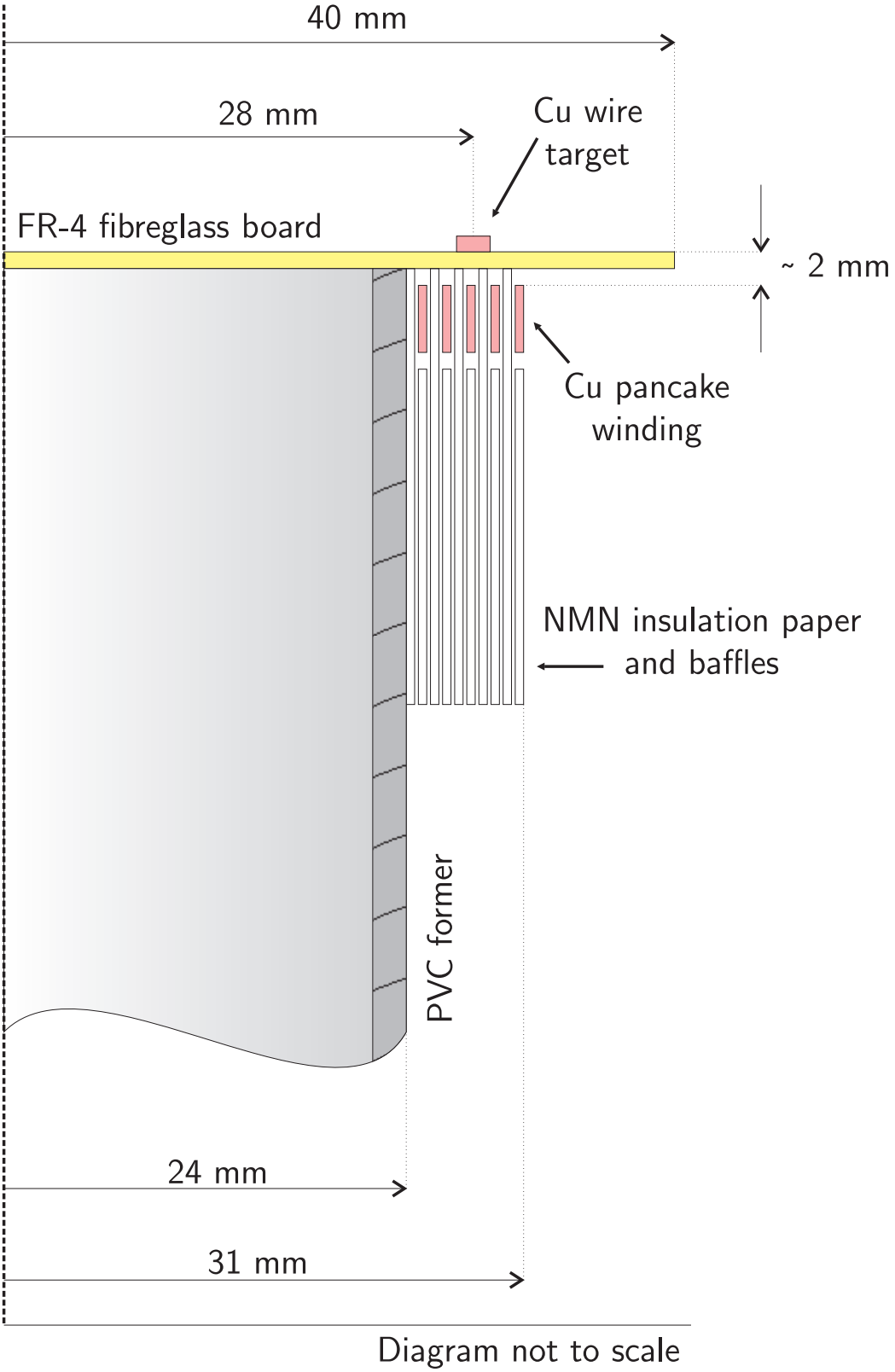

Figure 6.1: Cross sectional elevation of the winding arrangement for the planar-coil experiments on exploding wire by induction.

Table 6.1: Table of pancake coil experiments

Date	Apparatus	Summary
10 May 2010	Coil C	Single turn of wire explodes at soldered connection
	Coil C	Coil flashover destroys Coil C
26 May 2010	Coil D	"Diamond Ring" effect observed
28 May 2010	Coil D	5 out of 8 discontinuities form plasma
3 June 2010	Coil D	7 out of 8 discontinuities form plasma
20 July 2010	Coil F	12 out of 32 discontinuities form plasma
	Coil F	Forces on target wire observed

in an inter-turn flashover which destoyed that coil, figure 6.2. It was determined that this was a good start, so further experiments were pursued.

The first sign that plasma was being created in the inductive explosion of copper wire was the "diamond ring" effect depicted in figure 6.3, which is a photograph of the experiment performed on 26 May 2010. This particular copper ring was etched onto a fibreglass board, and was noted to have some variation in the wire width. One side of the wire-track was 0.2 mm across, while the other side of the ring was 0.3 mm across. The voltage applied to the induction coil from the 21.4 μF capacitor bank was 10 kV.

It is known that the resistivity of a solid conductor increases with decreasing cross-sectional area, therefore, the thinnest part of the ring has more resistance initially. Assuming a uniform current is generated in the ring, the high resistance region will experience the most power dissipation according to $P = I^2R$ for a solid coductor, where P is the power dissipated, R is the resistance of the thin section, and I is the current circulating through the ring. The thin section of wire then experiences all the heating effects, melting and eventually vapourising. Upon vapourisation, the wire forms an open circuit and a voltage will appear across the breakage, facilitating the electrical breakdown of the exploding wire section, and eventual plasma formation. This produces the elongated bead of plasma that can be seen in the photograph.

6.3.2 Seeding plasma beads by adding discontinuities to the copper ring

In the experiment that produced the diamond-ring effect, it appeared that once a plasma bead had formed, it constituted a short-circuit and as such the voltage would collapse and ionisation would cease. If the circuit was broken at this point, then

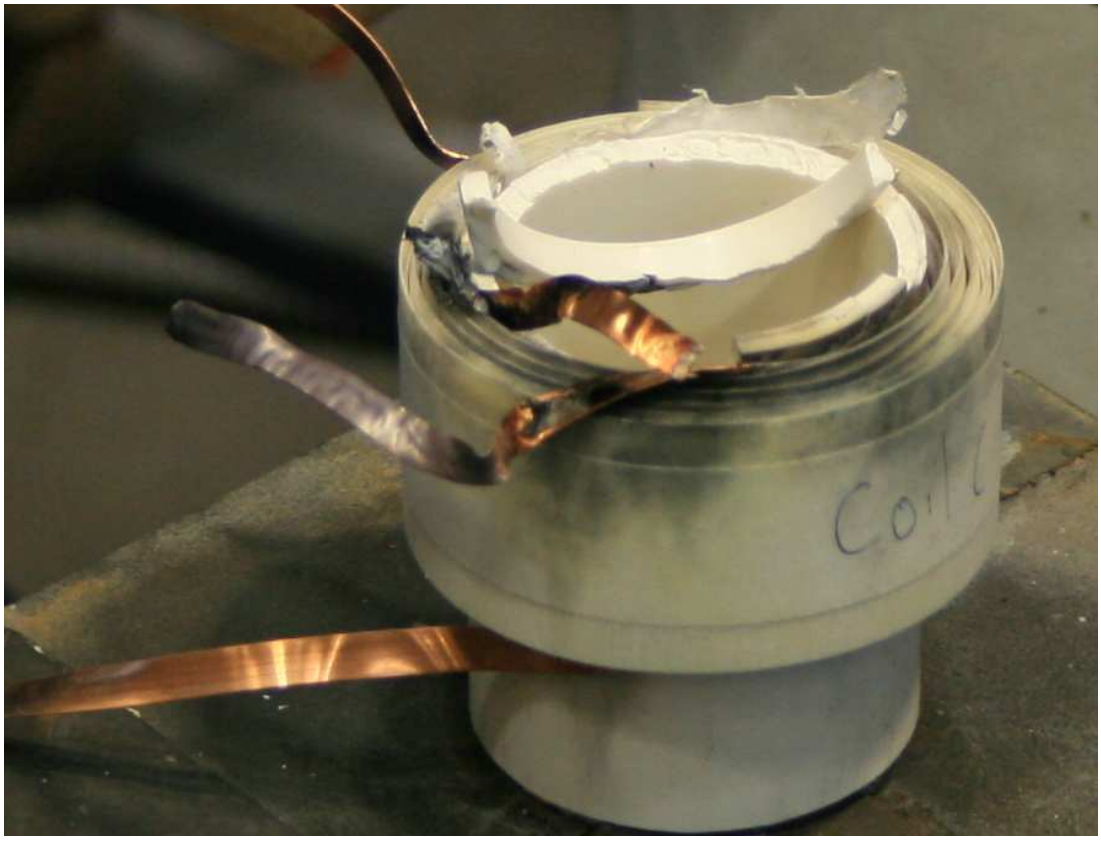

Figure 6.2: Result from pancake coil experiment of 20 kV discharge into Coil C.

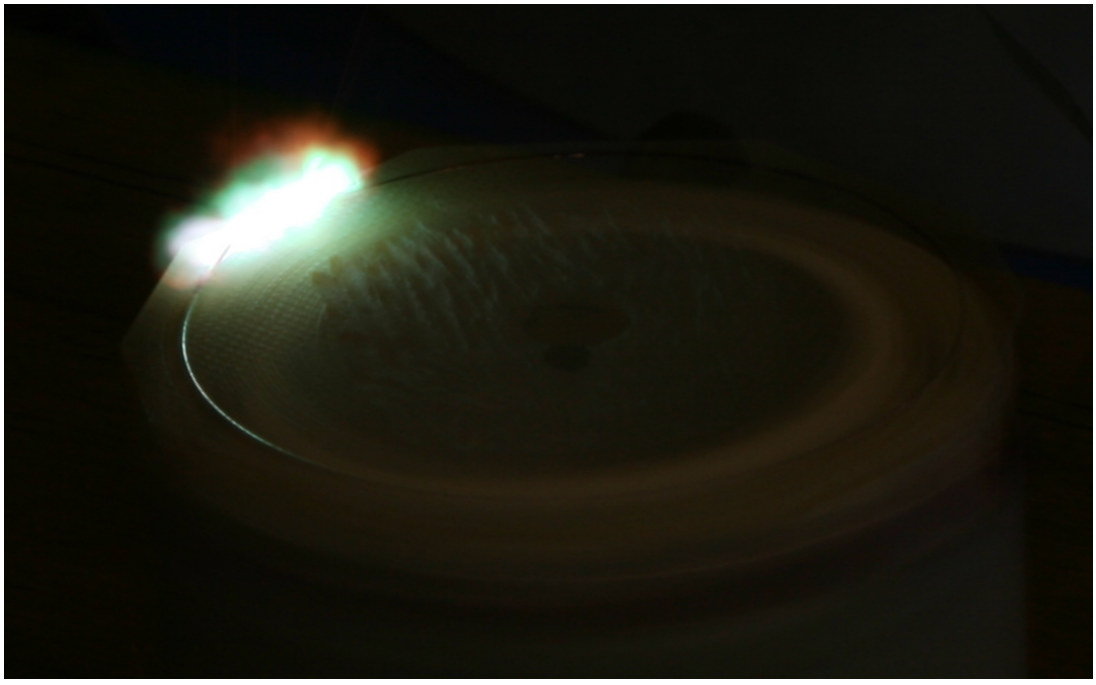

Figure 6.3: Pancake coil experiment of exploding wire plasma creation by induction, resulting in a 'diamond ring' shaped pattern.

currents would cease to flow in the ring, and the wire explosion processes would finish. Because of this, it also appeared that plasma beads would occur only in the most resistive part of the ring, and nowhere else.

It was conceived that because the plasma beads formed at the most resistive part, it might be possible to seed plasma beads about the circumference by inserting equally spaced notches, or discontinuities, on the copper wire. This technique was applied by MeBar and Harel [1996] to achieve different modes of exploding wire restrike. In that work, a series of segmented straight wires was exploded by direct connection to the capacitor banks, and results compared with smooth wires. It was found that while the smooth wires disintegrated completely, the segmented wire sections formed plasma in their interstices, and conduction took place within the shroud of plasma and metallic vapour that had formed around the remaining segments. Those results suggest the larger segments do not explode when a plasma shrouds those segments, providing an alternative path that diverts current away from the metal segment.

This strategy was attempted in experiments from 28 May 2010 to 20 July 2010. The discontinuities in the copper ring were inserted using a scalpel. In the first of these experiments, the wire-track width was 3.5 mm in diameter on average, with eight discontinuities of half the wire width, forming the vertices of an octagon. The test voltage was 10 kV, directly applied to the induction winding. That experiment is shown in figure 6.4, where five out of the eight discontinuities sucessfully ignited into bright plumes of plasma.

This was an important experiment demonstrating that the segmented exploding wire technique was able to produce plasma in the interstices of the discontinuities in different parts of the ring. This result differed from the diamond-ring effect since it showed that the plasma can be distributed evenly about the ring. As per the explosion of segmented straight wires, the segments of larger diameter remain, whilst the segments of smaller diameter have vanished.

Figure 6.5 shows a photo of part of the ring before the experiment. This photograph illustrates the variability of the wire width due to scratching off the copper plane on the lathe. If the lathe face is not true, then the width of the wire that remains will vary.

Having a variable wire diameter also means the discontinuities are of varying width. This is illustrated in figure 6.5, where subsequently the left-hand discontinuity had ignited, the right-hand discontinuity had not. This is because the width of the left-hand discontinuity is smaller than that of the right-hand discontinuity, and therefore the former is the more resistive of the two. As such, the former is more likely to

experience more power dissipation, melting and eventual electrical breakdown.

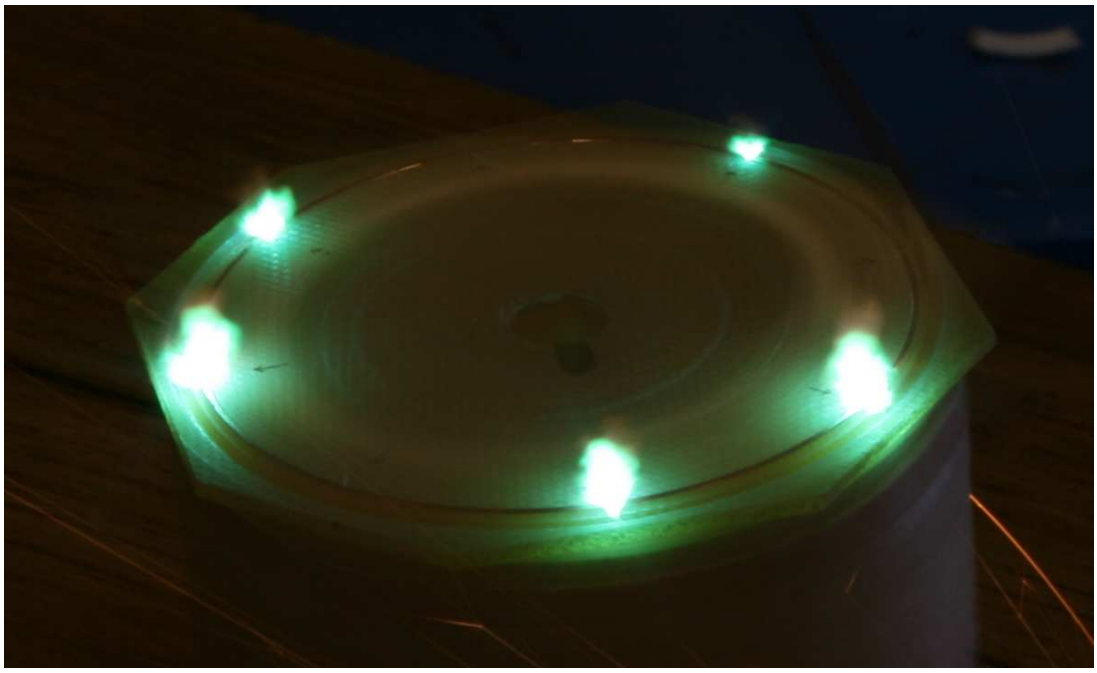

Figure 6.4: A 5-turn pancake induction coil, 1-turn copper etched target IEW seeded plasma-by-induction experiment. Five seeded plasma beads can be seen igniting on the surface of the board.

Another attempt was made on 3 June 2010, in an effort to reproduce the result of 28 May 2010, but this time with more plasma. The test voltage was increased to 12.1 kV. On this occasion, seven out of eight discontinuities had formed plasma beads as shown in figure 6.6. Therefore, for the pancake coil experiments, a higher initial capacitor voltage corresponds to a greater quantity of plasma produced. Some damage was noted on the induction coil, where a section of the innermost conductor on the coil had popped out of the plane of the coil. This was a sign that the thermal capacity and transient current carrying capability of the coil's conductor had been exceeded. This marked the end of experimentation with Coil D.

With the improvement in plasma formation from the 3 June 2010 experiment, a copper ring target was produced with 32 discontinuities carefully hand-etched into the conductor. By increasing the number of discontinuities, it was conjectured that the plasma beads could coalesce into one circular plasma conduit, shrouding the wire and linking together to form a plasma ring. The voltage applied to the induction winding on this occasion was 11 kV. Twelve of the 32 discontinuities were ignited into plasma spots, figure 6.7, but a full plasma ring was not realised.

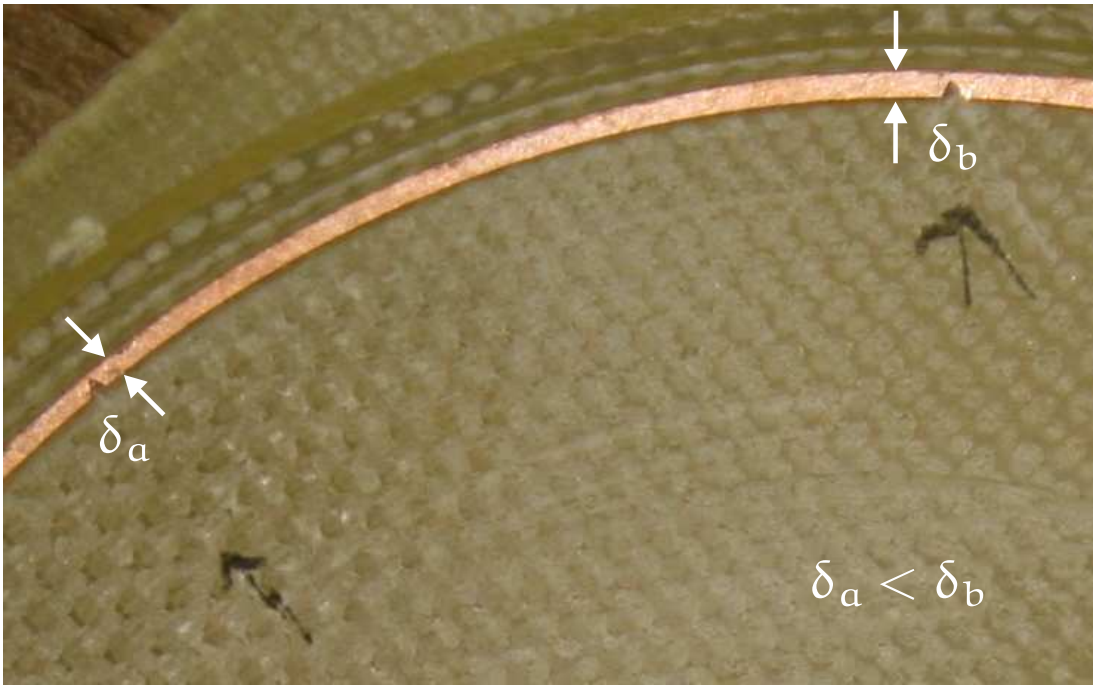

Figure 6.5: Photograph showing two discontinuities in the 1-turn copper etched IEW target prior to ignition in the seeded plasma-by-induction experiment. The left-hand discontinuity ignited into plasma, whereas the right-hand discontinuity did not. The wire comprising the copper ring was also of variable width. On the left-hand extremum, the wire width δ_a is thinner than the wire width, δ_b, in the right hand extremum. This contributed to non-uniform plasma distribution about the ring for both continuous and discontinuous wire types, producing the "diamond ring" and seeded plasma effects respectively.

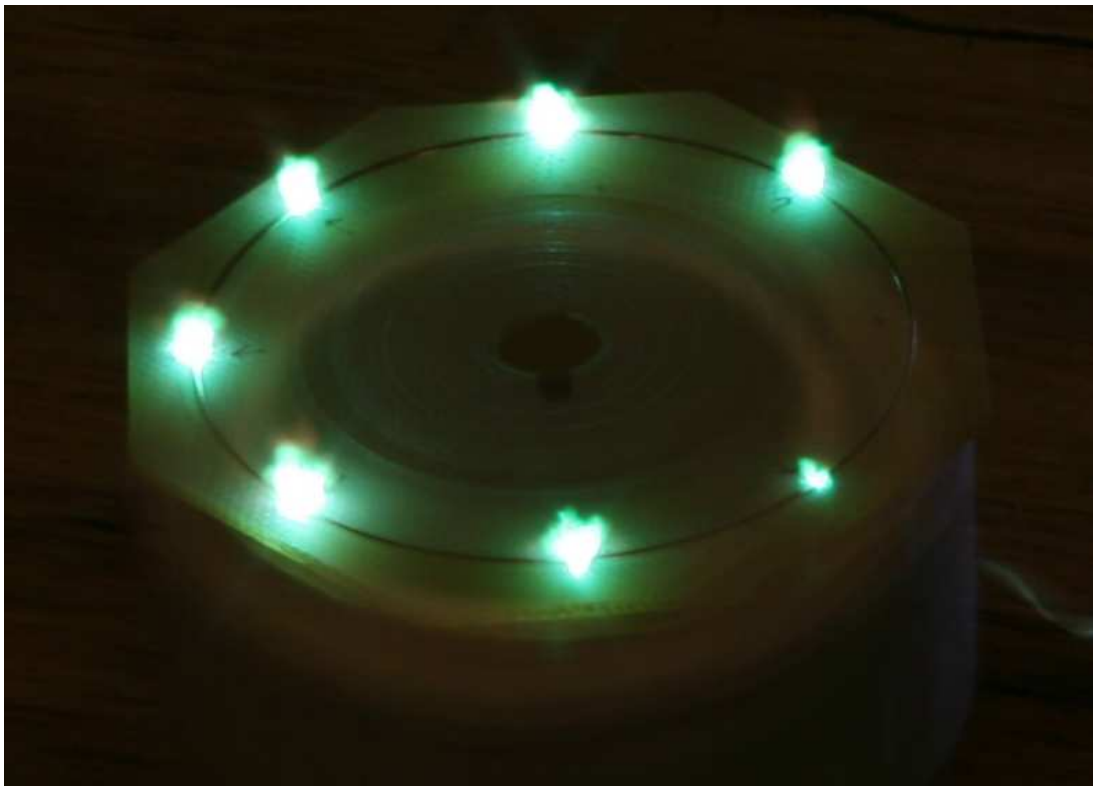

Figure 6.6: A 5-turn pancake induction coil, 1-turn copper etched target IEW seeded plasma-by-induction experiment. Seven seeded plasma beads can be seen igniting on the surface of the board.

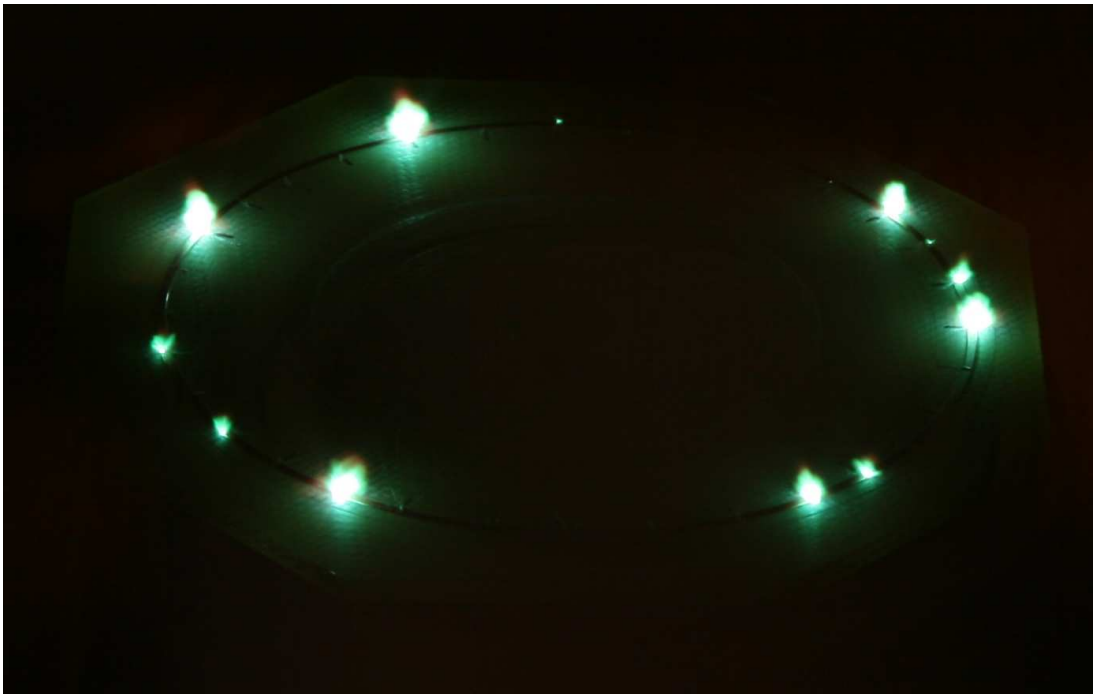

Figure 6.7: A 5-turn pancake induction coil, 1-turn copper etched target IEW seeded plasma-by-induction experiment. Twelve spots of plasma can be seen igniting on the surface of the board, from 32 discontinuities

6.3.3 Observations of forces acting on the wire

This experiment demonstrated the direction of forces acting on the IEW turn. The test subject was a single turn, 56 mm across, of enamelled 0.2 mm diameter copper wire, glued down at intervals onto a bare fibreglass board. The test voltage was 10 kV. There was no plasma formation, however, the wire exhibited high heating stresses and sufficient radial expansion due to thermal heating to blow its enamel layer off. The most critical result was that the wire ring had collapsed inward, forming a star-shaped pattern. In the wire explosion via induction, there are radial forces present in the IEW turn, implying the wire carries a lot of current. The wire collapsing inward means the area through which the mutual flux passes is decreasing, which therefore reduces the magnetic coupling. Instead, if the wire was supported by a sturdy former, it could solve the flux collapse problem. If the wire was supported, then possibly the wire may break under the crushing-force and form electrical arcing in the breakages in the wire. These ideas were not tested in the experiments.

6.4 Discussion of the Method

The pancake coil topology was used to create plasma by induction via the induced explosion of wire. The resulting beads of plasma were able to be distributed around the circumference of the copper ring by etching equidistant discontinuities along the length of the wire.

The first outcome was that of plasma creation by induction. By recording the condition of the test target prior to explosion, it was discovered that the plasma would form at the thinnest part of the target wire - in electrical terms, the part of the target with the highest resistance (hence all the electrical voltage stress would appear at this point, facilitating plasmafication). Following this it was conceived that the target wire could be etched onto a thin copper sheet attached to a fibreglass substrate. With discontinuities spaced equidistantly about the wire, spots of plasma were seeded at these sites, demonstrating that the plasma could be spread out along the circumference of the ring. This result is concordant with those obtained in straight segmented wires by MeBar and Harel [1996].

The plasma generated in these experiments was sparse, and the typical wire explosion effects of fragmentation were virtually absent. It became apparent that insufficient voltage and current was being delivered to the wire target during the impulse. Only capacitor voltage measurements were made, from which very little information could be discerned about the wire explosion. The test subjects were poorly sized in comparison to the capacity and physical size of the energy storage elements. Crucially, the impedance of the induction coil was comparable to the impedance of the supply cables. This had the effect of increasing leakage inductance in the experiment.

A key problem for this experimental series was the lack of electrical voltage and current data in the results. At the time these experiments were taking place, a current monitoring device was not yet installed for use on the capacitor discharge circuit. For the ring-shaped copper wire targets, because the ring diameter was so small it was physically difficult to measure the current and voltage with available probes. As such, lack of electrical measurement made it difficult to determine the power being delivered to the wire target, or the exploding wire's resistance with respect to time. Furthermore, it was not known whether the wire explosion behaved differently to a capacitively exploded wire, as the wire was ring-shaped and being excited by a magnetic field. These factors made it impossible from this position to build a model of a wire exploded by induction, using the experimental methods of this chapter.

While all these pancake-coil experiments were capable of producing some plasma effects, it never seemed as if they had the potential to create enough plasma to form a complete plasma ring. While photographic evidence suggested that there was a lot of plasma being created, the experiments themselves did not substantially explode the wire. Only small portions of the wire were actually ionising into plasma beads, even in the case of a smooth wire target. The wire needed to undergo a more complete explosion than what the experiments were producing, and Laithwaite [1967] suggests that the physical size of the induction windings (in relation to the capacitor bank) needed to be scaled up, id est, the induction winding producing the rapidly changing magnetic flux needed to be of a size comparable to the capacitive energy storage element [1].

The elements of the circuit that needed scaling up were the coupling ratio, κ, and the physical size of the excitation coil. The coupling ratio between the induction and IEW coils was low. This means there is more leakage flux and therefore more inductive losses. Secondly, the induction coil is physically smaller than the rest of the circuit, particularly when compared with the electrical delivery and return cables between the capacitor bank and the coil. The pancake coils used in the experiments had an inductance of 3.43 μH, as measured with a Hewlett Packard 4192A Low Frequency Impedance Analyzer. This means the self inductance represented by the coil is comparable to the inductance of the return cables, which in turn also represents an inductive leakage term. This consequently reduced the total voltage across the induction coil, by the action of voltage division between the coil and the cables. This reduces the overall energy transfer from induction coil to the target wire, meaning that the wire has less power available with which to explode itself.

Another advantage of scaling-up the dimensions of the device is that voltage and current probes can be more easily inserted into the experiment.

6.5 Summary

Ring-shaped copper wires were exploded by induction using pancake coils impulsed with current from a capacitor discharge. Plasma beads were produced from the explosion of wire by induction, and in some experiments the wire target was segmented so that the plasma spots were spread around the circumference of the wire ring. It

[1] Laithwaite was alluding to the phenomenon of resonance, which was the key to his magnetic levitation demonstrations. It is what he meant by things being "the right size".

was found that variations in the wire's width was an important factor in seeding the plasma beads. Wires were etched onto virgin printed circuit board using a lathe.

Chapter 7

Experiments with Helical Coils

7.1 Synopsis

This chapter begins with an experimental survey of techniques for wire explosion via electromagnetic induction, using helical coils. From those experiments, an experimental strategy is identified for the purpose of creating a plasma turn via the restrike of the exploding wire. A conductive plasma channel in the shape of a helical arc is created via the mechanisms of electromagnetic induction and exploding wire. The main results are the electrical characteristics, in the form of voltage and current waveforms for the induction coil and exploding wire.

7.2 Introduction

It was apparent in Chapter 6 that the quantity of plasma needed to be improved if the restrike phenomenon was to be achieved from IEW. This was achieved by constructing a larger induction coil, and a larger-scale exploding wire target made from an increased number of turns. This increased the coupling between the coils, making more energy available to the exploding wire. Experimental work migrated from the pancake induction coils to using helically shaped coils, ultimately with the exploding wire target being coupled in series to a "receiver coil" to produce a machine that could yield the restrike of the wire.

During the experimental survey, a number of findings were made, and these arose out of the simple act of winding the exploding wires into coil shapes. The capacitor bank was used to supply electrical impulses to an air-cored induction coil, which provided a transient magnetic field. This coil was coupled in each experiment with different helical exploding wire targets, connected in short-circuit, to create plasma via electromagnetic induction. These prototypes built from thicker wires, were found

to produce a higher quantity of plasma than was possible with the pancake coil prototypes, by simply increasing the magnetic coupling between coils. It was later found that a thin exploding wire section connected between two coil sections of larger conductor diameter, given the term "receiver coil", could explode instead of the whole coil exploding. Plasma generated in the explosion of copper wire would sometimes trigger an electrical breakdown across the whole receiver coil winding. This was eliminated by increasing the distance between the exploding wire terminals.

Finally, a machine is described in detail, whose operation facilitates the creation of plasma by induction due to restrike of the exploding wire. The apparatus is a pair of mutually coupled helical coils, arranged on cylindrical polyvinylchloride formers, with a capacitor bank as the energy source. The restrike mechanism is documented for a single turn of 0.2 mm diameter copper wire, exploded via electromagnetic induction. Voltage and current waveforms are presented. The wire explosion by induction exhibits key features that exist in conventional wire explosion by conduction, namely wire fragmentation, dwell period and restrike phenomena. Photography, visual observation and copper oxide residue patterns helped to determine whether a restrike took place.

7.3 Experimental Surveys with the Helical Coil Prototypes

It was not a straight path to obtain a restriking IEW, so this section gives the detail of the series of experiments performed on helical coil prototypes, revealing the incremental progress toward the restrike. The rationale of using helical coils was to increase the coupling between the mutually coupled coils. This was done in several ways. The receiver coil was wound with multiple turns, as many turns as the induction coil. This increases the ampere-turns of each coil. Another way was to wind the receiver coil out over the surface of the induction coil, that is, leakage flux would be minimised by ensuring that as much of the induction coil was covered up by the receiver coil. Lastly the distance between the two coils would be kept to a minimum.

7.3.1 Revisiting Mr Dalzell's experiments

As mentioned in the literature review, Mr Dalzell had performed some experiments at the University of Canterbury during the summer of 2007/2008. Those results were recorded in a notebook and may be found in Appendix B, and there is also a low frame-rate video recording of the experiments taking place. There were two key experiments involving a helical induction coil measuring 420 mm in height and

(a) Target wire before placement inside the induction winding

(b) Rod-shaped EW fragments

Figure 7.1: Helical exploding wire experiment to explode 10 turns of 0.375 mm diameter enamelled copper wire by electromagnetic induction. The target wire was interior to the induction winding. Also depicted are the remanent copper fragments.

200 mm across, 20 turns of 2.125 mm diameter copper wire wound with a 21 mm pitch. These experiments were repeated because they were considered to be a good starting point. They were repeated as closely as possible, but this time with the digital SLR camera trained on the experiment, with a long-duration exposure time. The induction coil was connected to the capacitor bank.

In the first experiment, the target was 10 turns of 0.375 mm diameter on a 180 mm diameter former, with a winding pitch of 5 mm, figure 7.1a. The terminals were shorted together and it was placed inside the air core of the induction coil, about the magnetic centre. The test voltage was 45 kV. Upon discharge, there was a flash and an explosion could be heard. After the experiment, the formers were removed. It was apparent that the wire had exploded, leaving behind rod-shaped copper fragments, and bits of the wire's enamel, figure 7.1b. It could not be established whether plasma had formed from this wire explosion.

The second experiment was therefore to determine what was going on in the last experiment, by placing the target wire on the exterior of the induction coil. The target wire was 10 turns of 0.375 mm diameter enamelled copper wire wound on 220 mm wide PVC former. The ends of the target wire were bared and shorted by braiding them together. Again the target was placed in concentricity with the induction coil, and placed about the magnetic centre. The test voltage was 45 kV. On this occasion, there was a bright flash and many plasma beads were captured in the photograph, figure 7.2. This indicated that plasma had formed in this wire explosion, and that there was some considerable quantity of it. Another feature observed in the photograph was the radial bursting forces on the exploding wire target. This is due to the Lorenz force, and the effect is exacerbated by the ohmic heating of the wire

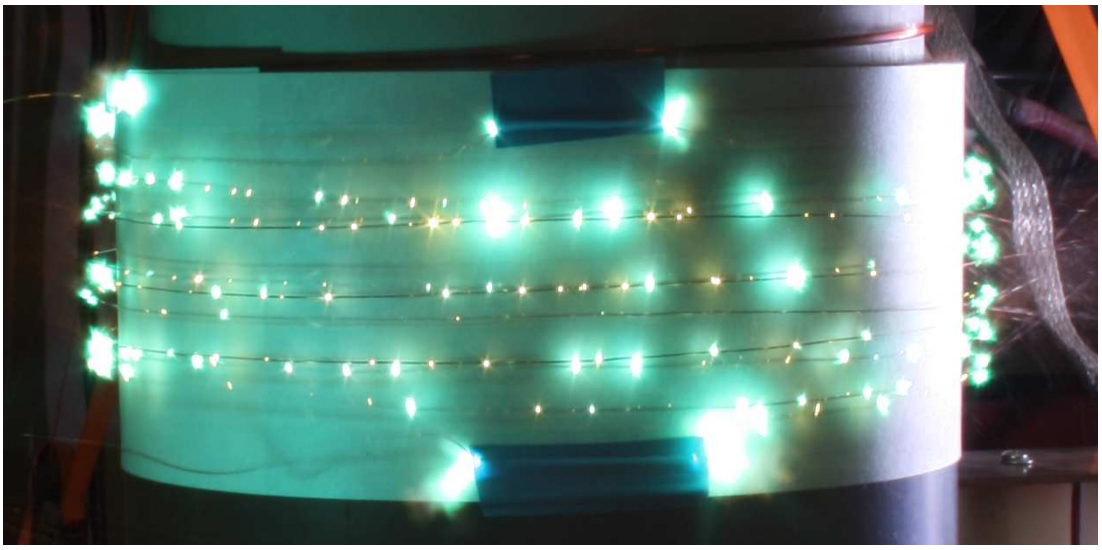

Figure 7.2: Explosion of copper wire with the target wire exterior to the induction coil. Plasma formation occurred in this IEW experiment.

causing expansion of the copper conductor.

7.3.2 Experimental development: An exploding wire section, straddling two sections of receiver coil

It happens that a section of thin wire which is connected in series to a slightly thicker section will, upon electric discharge, experience explosion to the plasma state, while the thicker wire remains intact. This was used successfully in the atmospheric partial discharge experiments (using exploding wires) detailed in an article by Gautier [2011]. It was therefore conceived that a thin wire connected between two thicker receiver coil sections could be made to form a complete plasma channel. A 19 turn receiver coil was wound on a 220 mm wide former from 0.63 mm diameter copper wire, with 1 turn of 0.2 mm enamelled copper wire connected in series with the receiver coil, around the middle of the former. The test voltage was 45 kV. The photograph of the experiment, in figure 7.3, revealed movement of the winding during the explosion. Because there were no darkening filters on the camera, the image was saturated where a large explosion occurred due to the receiver coil being shorted out. In spite of this, the image revealed a faint halo of plasma bursting forth from the site of the exploding wire section, which can be seen in figure 7.4.

During the experiment, the sections of 0.63 mm diameter receiver coil would always snap together toward the magnetic centre of the coil, since the large-scale winding force points to the centre of the coil. If the receiver coils failed electrically, they were

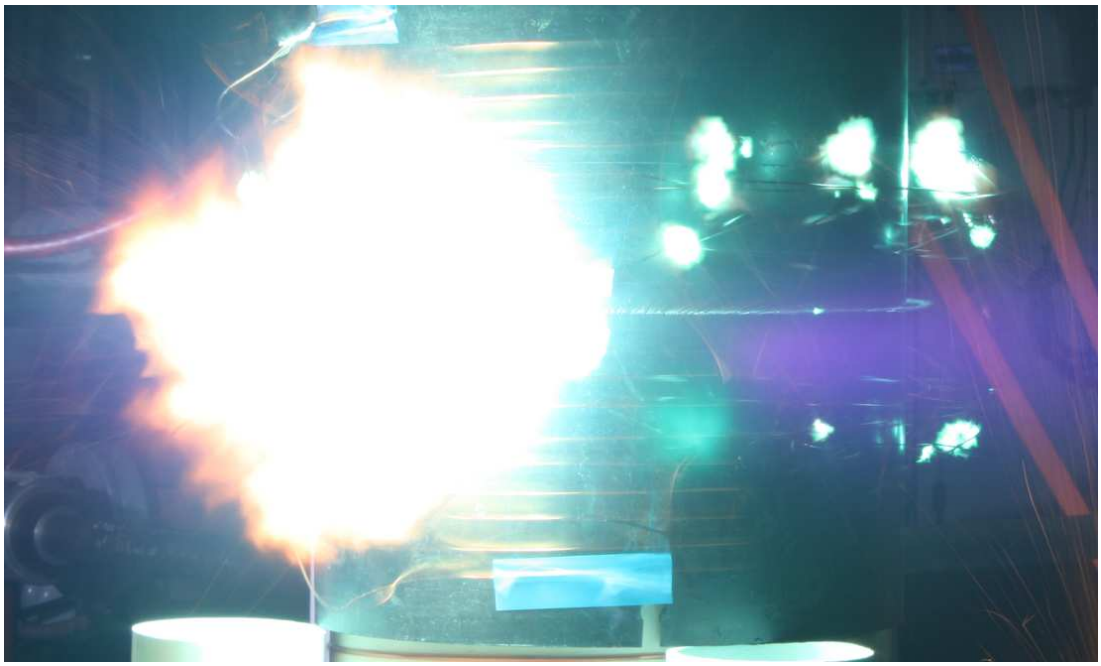

Figure 7.3: Explosion of copper wire with the target wire straddled between two receiver coils. Plasma formed in this IEW experiment shorted out the windings.

Figure 7.4: A faint halo of plasma can be seen in figure 7.3, where the 0.2 mm diameter exploding wire section was situated.

observed to form crinkly and burnt-out bird's-nest-shaped wire remnants.

The immediate problem with this approach was that plasma generated in the explosion of copper wire would trigger an electrical breakdown across the receiver coil winding. To avoid electrical failure of the coil, there would need to be increased separation between the exploding wire and the receiver coil. In addition, fragments of copper wire from the receiver coil were found all over the lab, having been ejected from the outer PVC former during the experiment. To mitigate this, further experiments were physically contained using a cylindrical polycarbonate screen.

At this stage the PVC former was also being coated in conductive copper oxide residues, so the former was covered with Nomex paper, which has suitable fire resisting properties. A prototype receiver coil with target wire and Nomex paper barrier is shown in figure 7.5a.

(a) Exterior receiver coils with exploding wire section

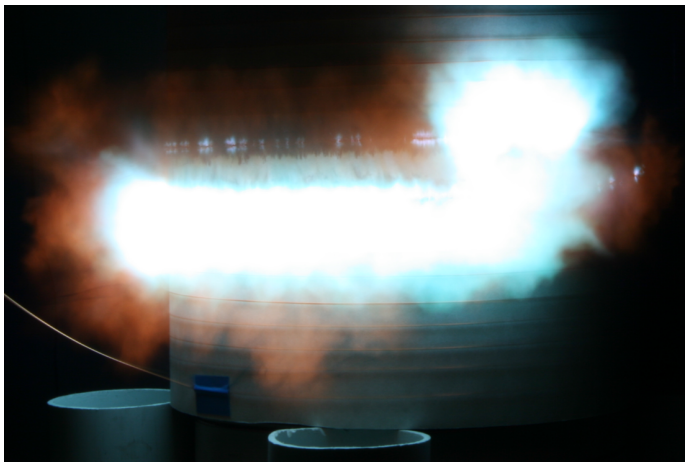

(b) Partial restrike of an IEW prototype helical coil experiment

Figure 7.5: Exterior receiver coils with exploding wire, prior to IEW experiment, and the outcome of the test performed on 10 August 2010.

Two further experiments were carried out with the exterior receiver coil prototypes. At 25 kV of capacitor voltage, with a target wire length of 1.5 turns, there was a partial restrike of the wire which can be seen in figure 7.5b. Initially it was thought that the 0.2 mm diameter target wire section had formed a complete "plasma-turn", but examination of the photograph of the experiment indicated that this was not the case. It was clear that a section of the wire had formed a plasma, but this had been shorted out. The plasma that was created in this experiment was reminiscent of the straight-wire explosion experiments.

The final experiment in this series was a repeat of the previous experiment, but this time with a nomex baffle placed between the overlapping exploding wire sections. This approach worked in the Plasma Transformer experiments to segregate the plasma turns from inter-turn failure, [Sinton et al. 2009]. The experiment was performed and there was no restrike, while the exploding wire residues captured on the Nomex paper indicated there had been some plasma bead formation.

7.3.3 Bands of exploding wire residue

The EW leaves behind copper metal and oxide residues on any surface which the explosion comes into contact with. For the EW by induction machine, a paper sheath was used to protect the PVC former from being coated with conductive residues. Residues captured on the paper in the helical coil experiments produced some interesting looking patterns, as in figure 7.7. The paper types that were used were

Nomex, and also ordinary 80 gsm white paper from a bookshop. A wire explosion creates a suspension of hot material. The copper vapours and oxides that condense on the paper behave like an extremely fine powder. Nomex paper is best for capturing residues, but fingerprints tended to show up in the residue pattern if the paper had been handled prior to the experiment. It is a worthwhile exercise to coat the paper with shellac or spray-on enamel after the experiment, in order to preserve the pattern. This additional precaution will prevent it from further oxidation.

In the main experiments, the visual continuity of the band of residue helped to indicate if a restrike had occurred. The residue colours are suggestive of the type of copper oxides formed, and these in turn suggest the temperature of the plasma at different parts of the band, [Taylor 2002 - 2003]. The residue contains copper(I) and copper(II) oxides, but it is principally composed of black copper(II) oxide, figure 7.7. Here the bands of residue are restricted to the paper sheath.

Figure 7.6: Copper oxide residues found in EW by induction.

7.3.4 Dust-trees

A dust-tree is a type of Lichtenburg figure that was noted during the experiments. After a discharge, rows of dust-trees were found to have sprouted perpendicular to the non-exploding copper conductors of the receiver coils, figure 7.8. In these experiments, the dust-trees typically formed in the presence of the copper suspension, and must arise due to the high electric fields along the profile of the receiver coils. They appear in neat rows where the receiver coils are located. While the main results

Figure 7.7: Copper oxide residues from NRS EW by induction.

of this thesis are not dependent on this observation, it was a reliable and curious observation made during the IEW experiments.

Figure 7.8: Dust trees collected on the surface of the outer PVC former. The trees have appeared between the turns of the receiver coils.

7.4 Main Result: Restrike of Exploding Wire via Induction

From this point forward, it was determined that a new machine be built for the purpose of exploding a wire via electromagnetic induction, incoporating all the mechanisms

that worked in the prototypes. This would also improve the repeatablility of the experiments, making it convenient to perform research into the IEW mechanisms by controlling as many variables as possible. Furthermore, exploding wire voltage and current would be measured for the first time, for IEW. This choice meant that a new induction winding would be built, as well as a new set of exterior receiver coils.

The restrike mechanism in wire explosion by electromagnetic induction is documented here. It was found that a number of physical features of IEW are common to CEW, such as wire fragmentation, the dwell period (also known as current pause) and restrike. The IEW apparatus used to facilitate creation of plasma by induction via the EW restrike, is described in this section. Enamelled copper wires 0.2 mm in diameter were exploded in the magnetically coupled coils system for eight different discharge voltages. Observation methods and waveforms are presented for these discharges, with accompanying descriptions of the EW response. The plasma formed by IEW has the advantage of being magnetically coupled to, but electrically isolated from the discharge circuit. However, IEW still requires connection to a receiver coil structure.

7.4.1 Circuit description

In figure 7.9, the circuit elements are shown, and the winding sets are laid out to show the relationship between magnetic flux density, B, and the voltages and currents that are generated in the machine. The high voltage energy supply for the discharge is the 21.4 μF bank of oil-insulated capacitors, C. This is connected to the L_1 winding through the three-electrode TSG. A water resistor, R, is connected in shunt across the L_1 winding to maintain minimum current flow through the TSG once it has triggered.

7.4.2 Machine description

The IEW machine is an air-cored, helical, concentrically-wound set of mutually coupled coils. The windings are arranged on cylindrical PVC formers, in order to maximise the magnetic flux coupling between them. Figure 7.10 shows the cross-section of the IEW machine, depicting the layout of the conductors. The inside winding, L_1, is 140 mm in diameter and is wound from 20 turns of 2 mm diameter, enamelled copper wire, with an 18 mm winding pitch. The outside winding is composed of two receiver coils and the IEW turn, spanning a diameter of 160 mm. The receiver coils are each wound from 10 turns of 0.63 mm diameter enamelled copper wire, with a

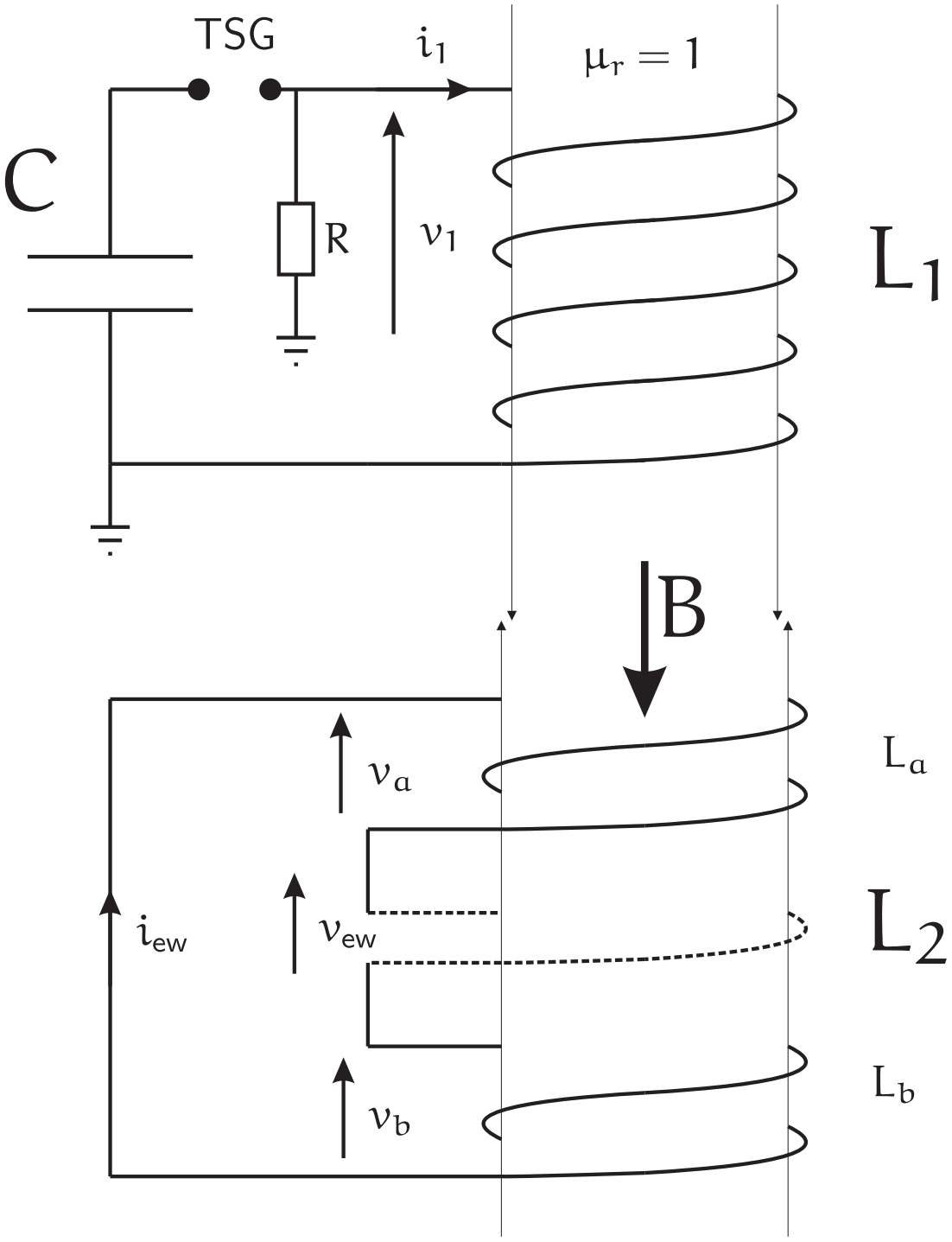

Figure 7.9: Helical windings arranged in exploded view, depicting a single axis of magnetic flux through an air-core and corresponding senses of voltage and current.

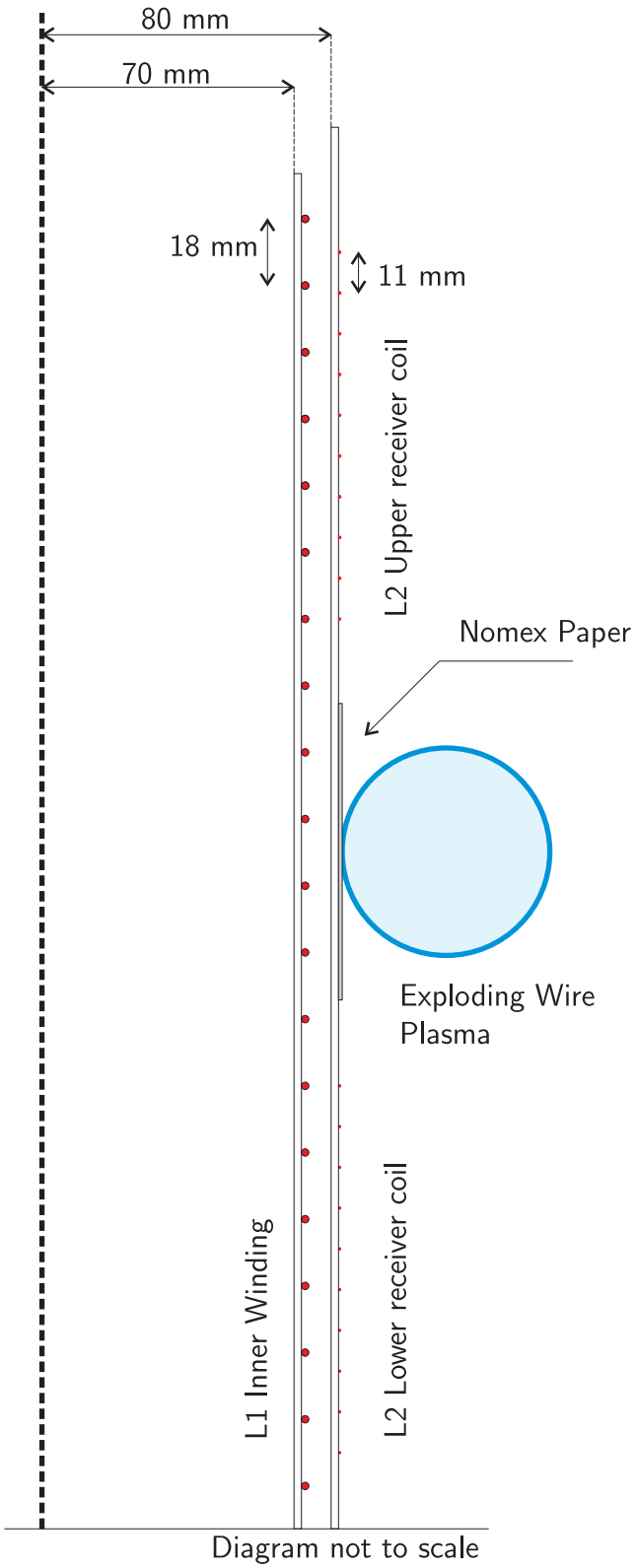

Figure 7.10: Sectional elevation of the EW by induction machine.

winding pitch of 11 mm. These are situated at the top and bottom of the device, with the EW straddling the intervening space. The EW is a single turn of 0.2 mm enamelled copper wire with a winding pitch exceeding 56 mm. This is so there is enough electrical clearance to avoid shorting the terminals out before the EW has an opportunity to form a restrike. The inside winding is connected to the capacitor bank, while the outside windings are connected together in short circuit. The IEW machine is shown in figure 7.11, in the laboratory prior to experimentation.

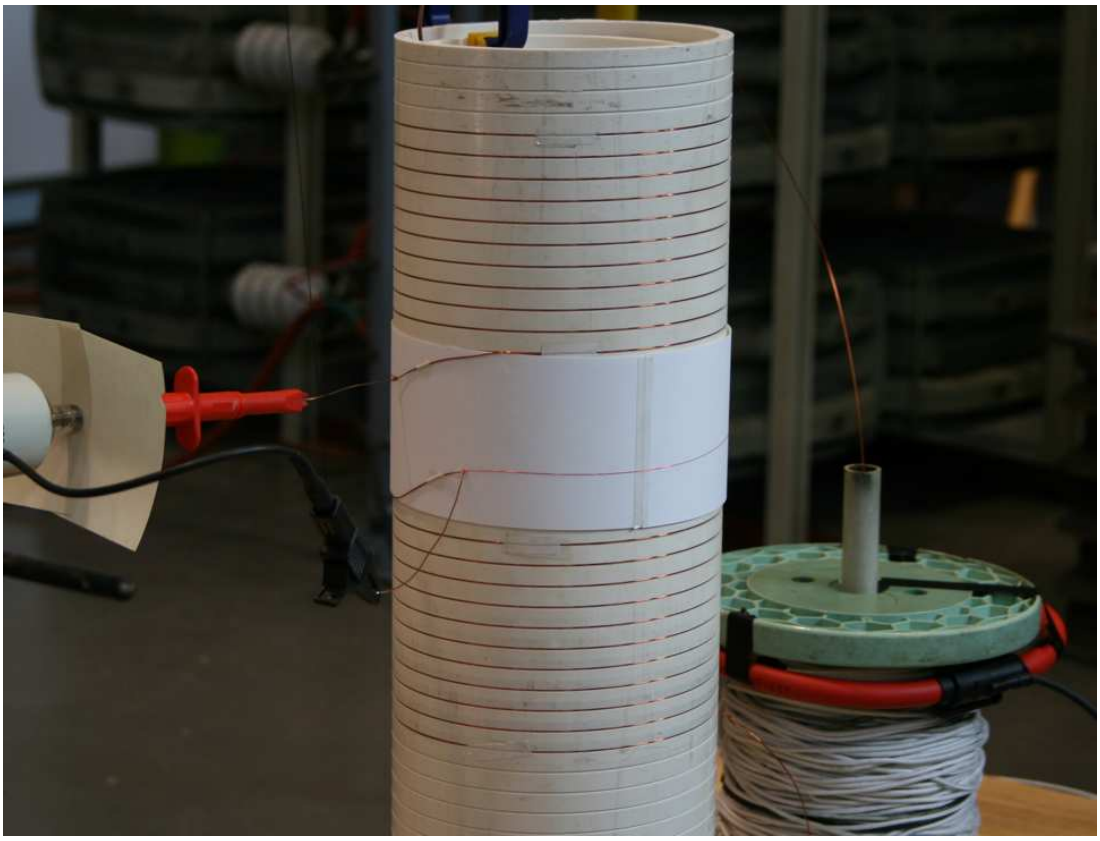

Figure 7.11: Mutually coupled coils set-up prior to experimentation, in the high voltage laboratory. The outside winding consisting of the two receiver coils and the exploding wire can be seen. The inside winding is obscured from view. The connection from the EW to the Tektronix high voltage probe can be seen in the foreground.

7.4.3 Instrument description and observation methods

With reference to figure 7.9, voltage v_1 was measured with the 600 kV Ferranti capacitive voltage divider (CVD), current i_1 was measured using the 50 kA Pearson ferrite-cored high frequency current transformer. The EW voltage, v_{ew}, was measured with a Tektronix 40 kV d.c. high voltage probe, the EW current, i_{ew}, was measured with a Fluke i3000 flexible current clamp.

A Canon 400d digital single lens reflex camera was used to capture still photographs in syncronism with the TSG's triggering signal. The photographs help to confirm visually the outcome of the experiment; whether there was a full plasma discharge or only partial plasma formation. Qualitative methods were also used to record experimental outcomes, for instance: that of listening to the loudness of the discharge, observation of bright flashes, observation of winding condition and inspection of metallic-oxide residue patterns left behind by the wire explosion.

7.5 Results

7.5.1 Experimental results

Conductive plasma channels in the shape of a 360 degree helical arc were created via the mechanisms of electromagnetic induction and exploding wire, as shown in figure 7.12. Wires were exploded by induction for eight different initial capacitor voltages, v_0, between 14 kV and 27 kV. There were two broad cases of outcome for the EW test wire: that of plasma channel formation, known as restrike (RS); and that which does not produce a plasma channel, called non-restrike (NRS). Five of these experiments produced NRS behaviour, figure 7.13a. The 23 kV to 27 kV experiments produced a restrike, figure 7.13b.

7.5.2 Electrical characteristics

In the capacitor voltage waveform, v_1, in figure 7.14, an oscillation is apparent, which is typical of an underdamped RLC response. This is similarly true for the capacitor current i_1, figure 7.15. In these inside-winding waveforms, some effect of to the EW can be seen. For instance, in figure 7.16, there is a voltage spike at about 30 μs, at which point there is a corresponding change in current in figure 7.17. Between the NRS and RS experiments, there appears to be a difference in the exponential damping envelope. The damping factor α for a parallel RLC is $\alpha = \frac{1}{2RC}$. R is the exploding wire resistance, C is the capacitance of the capacitor bank, and L is the leakage inductance of the mutually coupled coils system. Once the EW forms a restrike, it is known that the plasma resistance drops from nearly open circuit to a low resistance. This resistance change is detectable by observing the change in the exponential envelope of the underdamped RLC response in the inside winding, between RS and NRS outcomes. Exponential damping envelopes, $(\pm v_0\, e^{-\alpha t})$, were

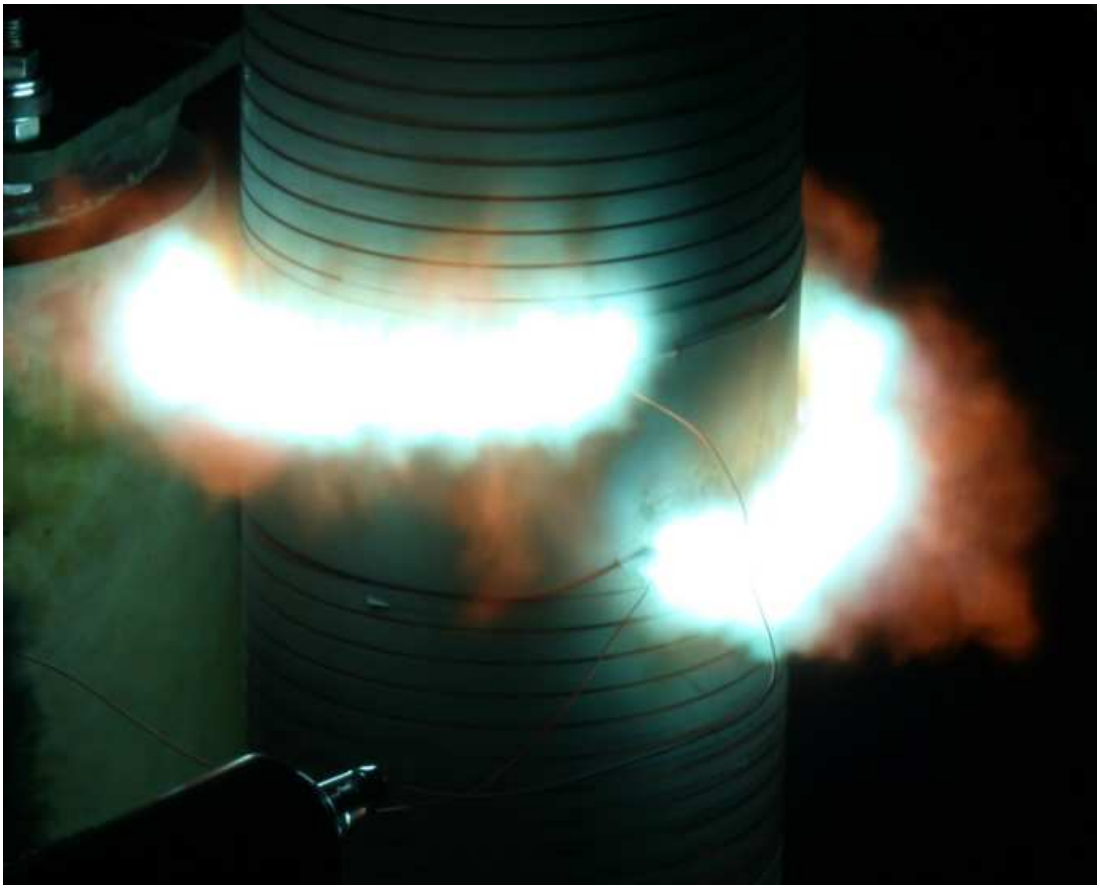

Figure 7.12: Explosion of copper wire by electromagnetic induction.

(a) Partial plasma formation in IEW, 14 kV discharge

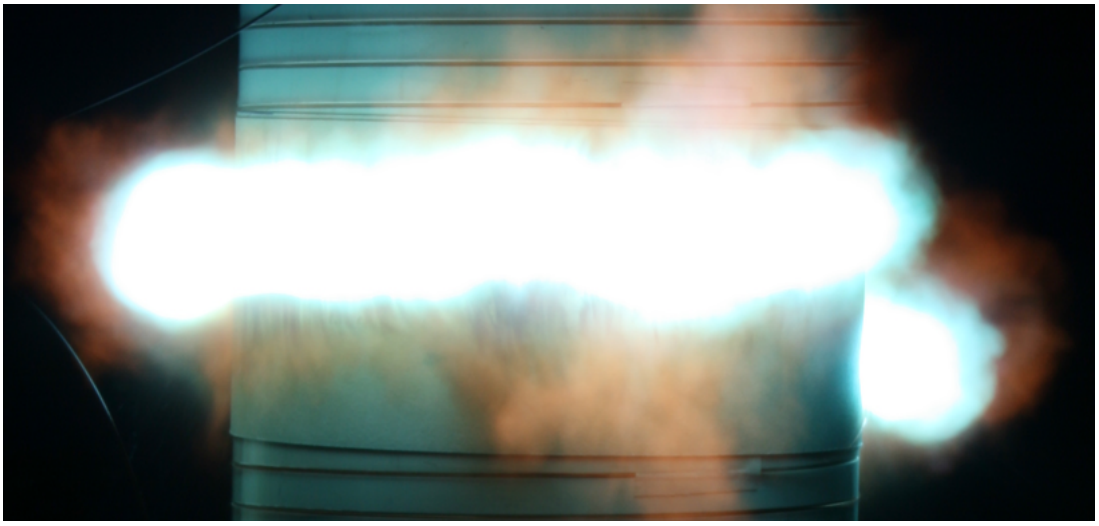

(b) Restrike of IEW

Figure 7.13: Outcomes of IEW.

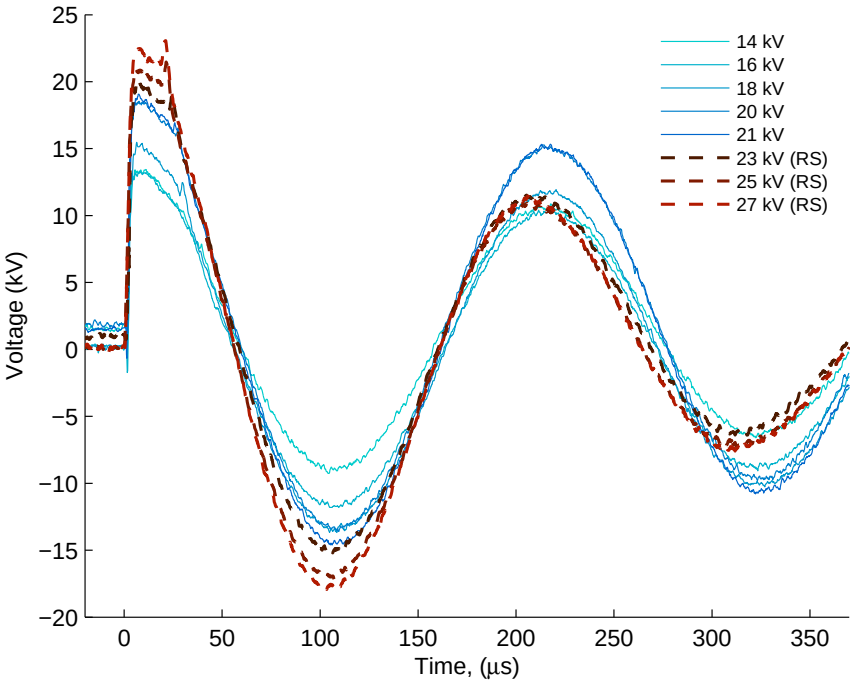

Figure 7.14: Voltage across the inside winding, v_1.

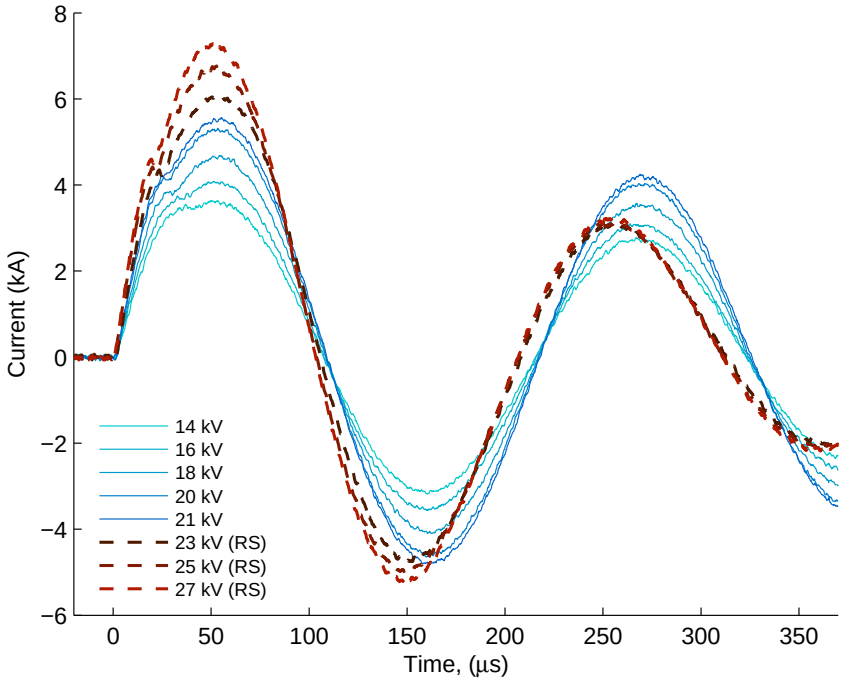

Figure 7.15: Current flowing in the inside winding, i_1.

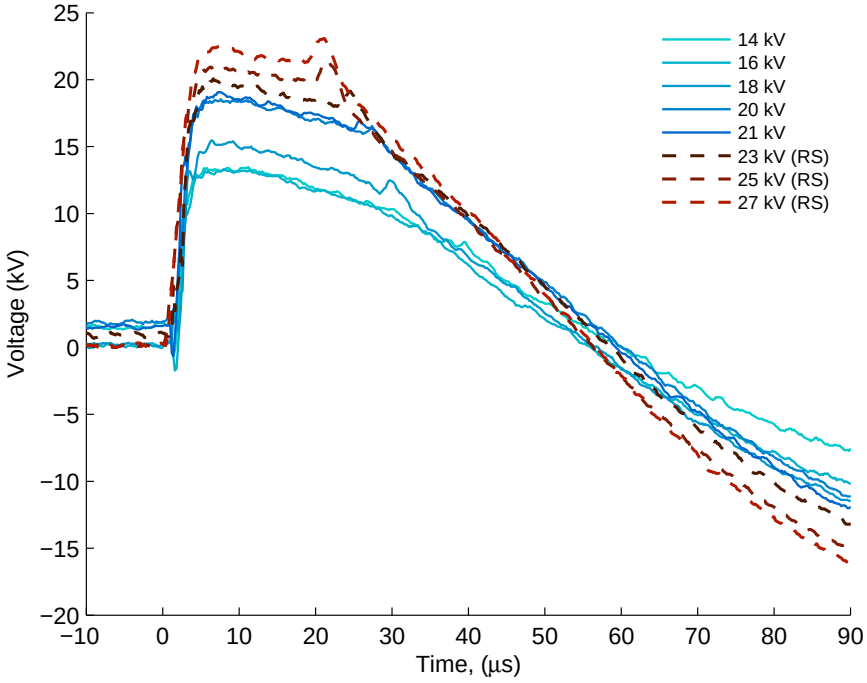

Figure 7.16: Voltage across the inside winding, v_1, first phase

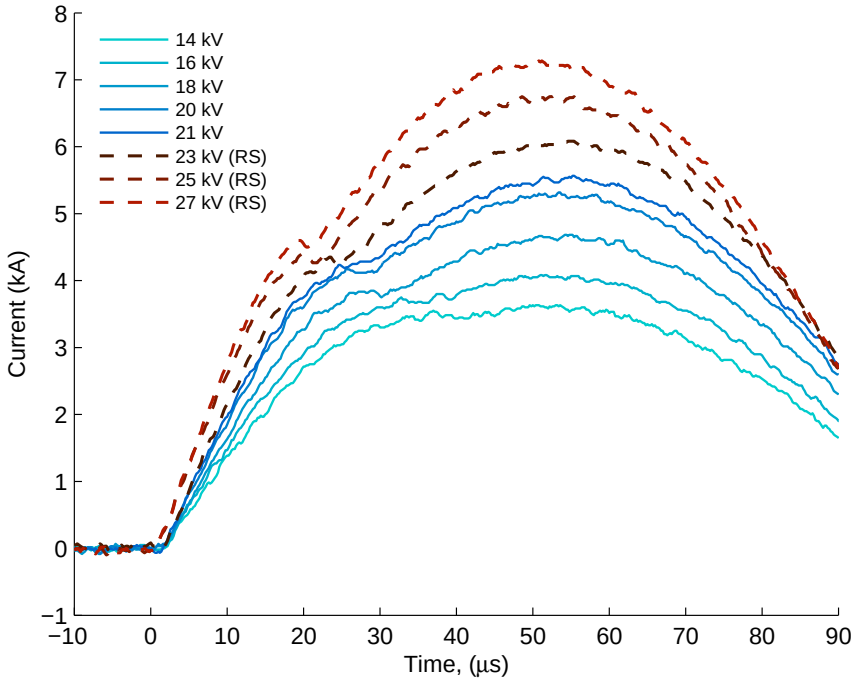

Figure 7.17: Current flowing in the inside winding, i_1, first phase

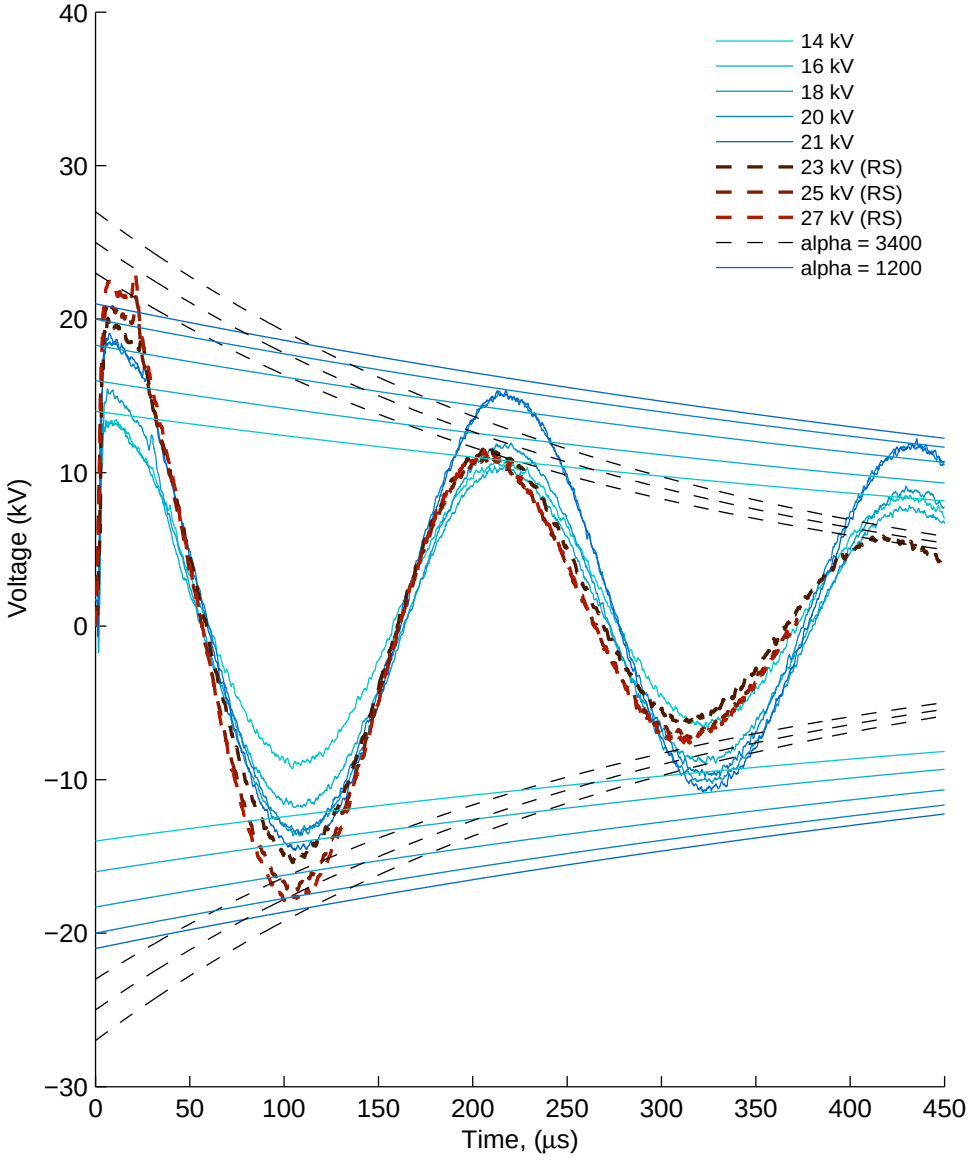

Figure 7.18: Voltage across the inside winding, v_1, with exponential damping envelopes displayed.

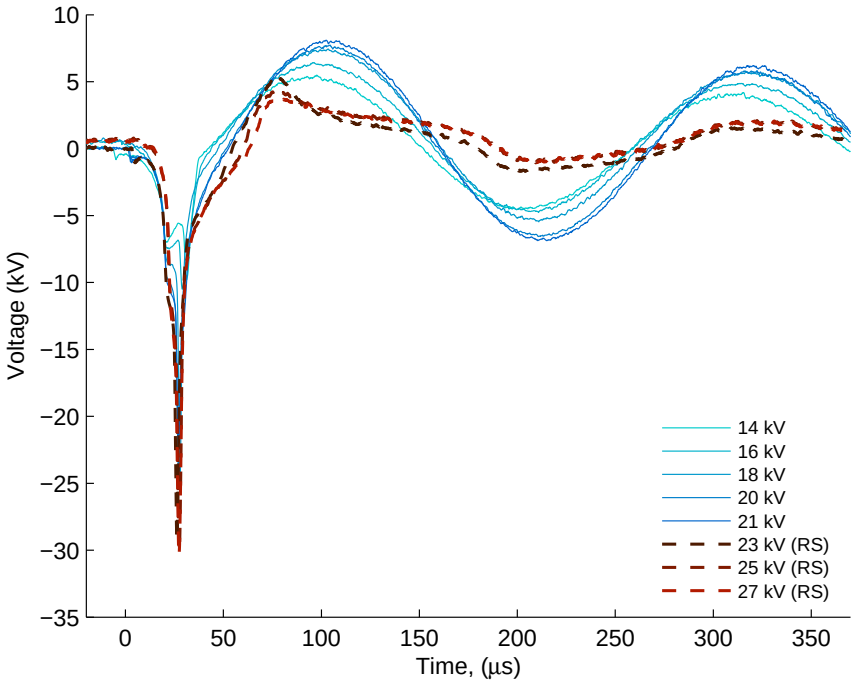

Figure 7.19: Voltage across the exploding wire, v_{ew}

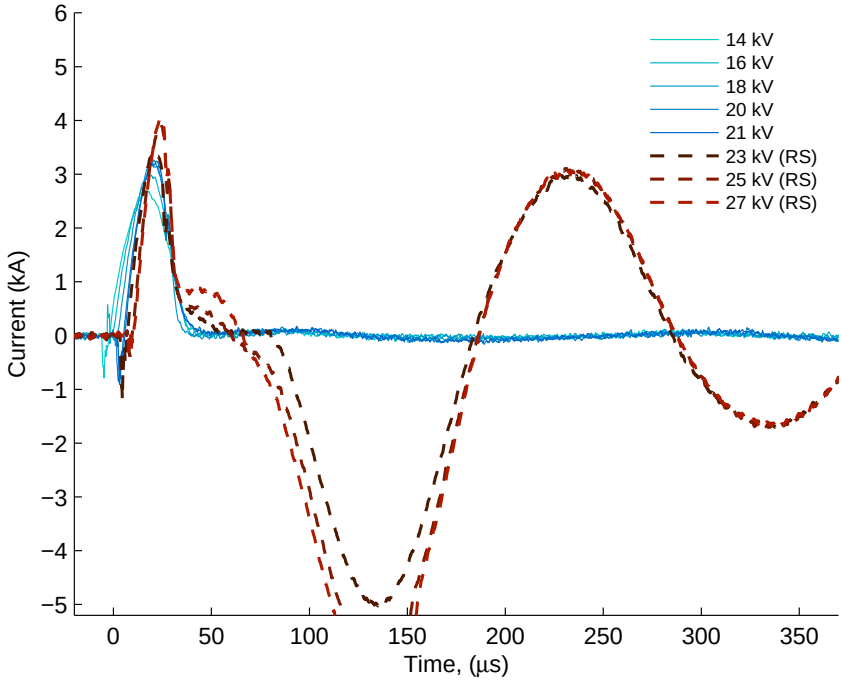

Figure 7.20: Current flowing in the exploding wire, i_{ew}

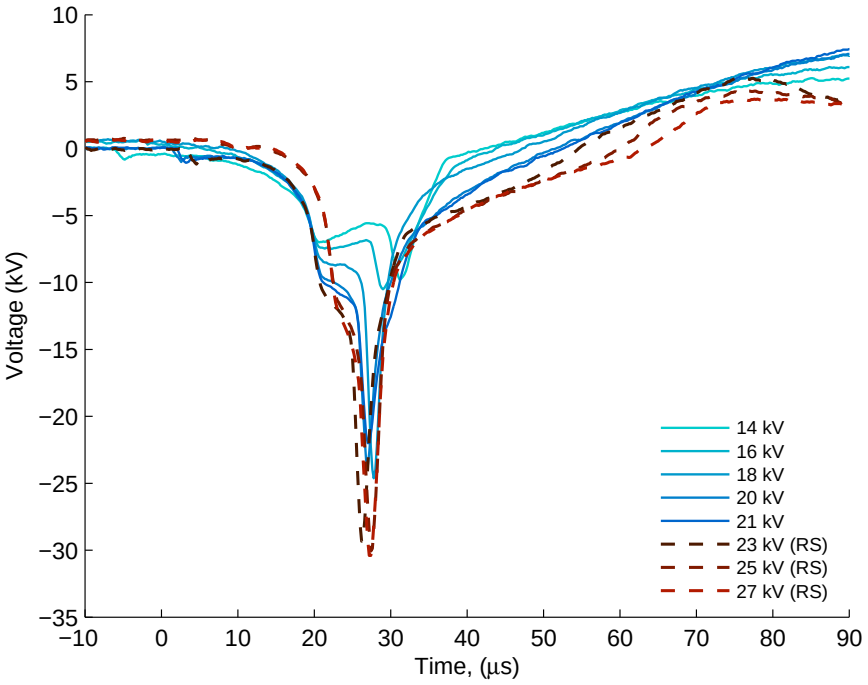

Figure 7.21: Voltage across the exploding wire, v_{ew}, first phase

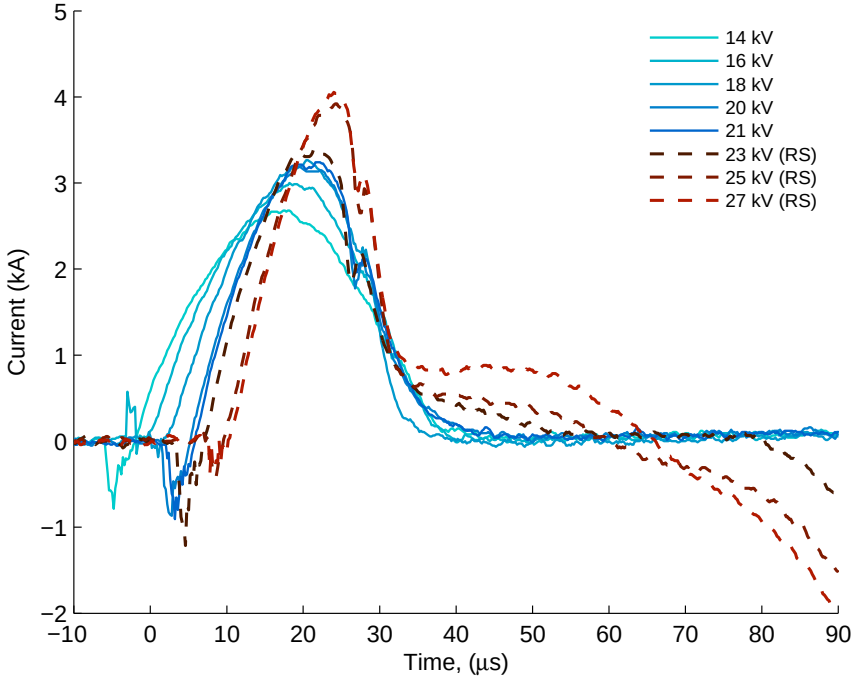

Figure 7.22: Current flowing in the exploding wire, i_{ew}, first phase

applied graphically to the v_1 voltage waveforms, as in figure 7.18. In the NRS case, $\alpha = 1200\ s^{-1}$, while in the RS case, $\alpha = 3400\ s^{-1}$. That result indicates that where the EW reaches the RS condition, then the coupled coils system enters a more conductive state than is maintained in the NRS response.

The voltage across the EW, v_{ew}, figure 7.19, shows a large negative polarity initial voltage spike. In the detail of the first-phase voltage, figure 7.21, it is observed that the first-phase EW voltage spike increases in magnitude with respect to the applied capacitor voltage and current. This is because the corresponding higher current flowing through the exploding wire during fragmentation, figure 7.22, drives the resistance change of the wire more quickly. After the initial spike, NRS EWs become open circuit, and so there is maximal voltage swing, figure 7.19. In the RS case, the voltage after the spike continues to increase through its dwell period. Once the dwell time has elapsed, the EW has formed a complete plasma path. When this EW restrike is created, it acts like a short circuit across the L_2 winding. This causes the voltage to collapse, figure 7.19, as high current conducts through the plasma channel, figure 7.20.

In the exploding wire current waveforms, i_{ew}, figure 7.20, the first phase of IEW appears similar to the first phase of EW by conduction in Sinton et al. [2010b]. For the NRS case, the EW undergoes fragmentation, and there is some conduction for a time, before the ionisation mechanism ceases. Upon failure of that mechanism, the EW enters an open-circuit state depicted by the collapse of current which indicates loss of conduction. In the RS case, the initial current conduction period again resembles the first-phase current of the straight EW by conduction. After the EW dwell period, the plasma conduction channel is formed, and the current rises to a maximal oscillation. Most notably, the restrike current flows through several zero-crossings, in an underdamped oscillatory response. For the 25 kV and 27 kV discharges, the current magnitudes in the initial restrike maxima were above 5.4 kA, which exceeded the measuring capability of the Fluke i3000 sensor. Therefore that detail is omitted in the current traces of figure 7.20.

7.6 Summary

This chapter has introduced and described new experiments that produce plasma from wire explosion by electromagnetic induction. The helical winding topology was used to perform preliminary investigations into the possiblility of exploding a 0.2 mm diameter wire, by induction. Several important observations were made to determine

the most suitable way to procure plasma. It was noted that thicker wires could be exploded into the plasma state by improving the coupling between coils. The quantity of plasma produced was on a scale consistent with that in other straight-wire experiments. It was determined that a section of the exploding wire could straddle two sections of the receiver coil, and that the thin wire could explode while the thicker wire remained intact. Plasma generated in the explosion of copper wire was found to trigger an electrical breakdown across the receiver coil winding. Therefore the separation between the exploding wire and the receiver coil was increased. It was determined that the best way to protect the PVC formers from being coated in conductive copper oxide residues was to cover them with Nomex paper, which has suitable fire resisting properties.

Conductive plasma channels in the shape of a 360 degree helical arc were produced. The apparatus was a pair of mutually coupled helical coils, arranged on cylindrical PVC formers, with capacitor discharge as the energy source. Several techniques were employed to make physical observations of the wire explosion. Waveforms of voltage and current of the EW were presented. The IEW exhibits key features that exist in CEW, namely wire fragmentation, a dwell period and restrike phenomena. Copper oxide residue patterns helped to determine whether a restrike took place. Lichtenburg figures in the form of dust-trees were found to form some time during the IEW discharge.

Chapter 8

Conclusion

A review of the literature revealed investigations made into the exploding wire historically, and more recently at the University of Canterbury. The review also explored the various applications of electromagnetic induction involving creation of plasma. In this thesis, electromagnetic induction was used for the task of exploding a wire. This was achieved by an electrical current impulse from a capacitor bank, into a magnetic field-generating winding, which couples into the wire. The investigation of wire explosion by induction and the background on the mathematical relationships related to this topic provided a basis on which to build further research into wire explosion via induction. A circuit representation for the problem of wire explosion by induction was proposed. This was developed from first principles using the idea of flux linkages and Faraday's law. The experimental environment was considered, with particular attention paid to safety in the laboratory and the types of instruments used to record voltage and current transients in the experiments.

The pancake coil topology was investigated experimentally. Ring-shaped wires were etched onto a copper-clad fibreglass board and plasma beads could be seeded by introducing discontinuities in the wire. It was difficult to make electrical measurements of the wire during the explosion, and it was felt that the experiments needed to be scaled up in order to create more plasma, and to make it easier to insert measuring instruments. In the helical winding experiments, the wire targets were wound helically and placed concentrically to their induction windings. The wires in these experiments exploded producing fragmentation, plasma beads and restrike phenomena, which are common to wire exploded by conduction. The preliminary investigations helped to guide the development of a machine for producing restrike of a wire exploded by electromagnetic induction. It was demonstrated that a wire could explode in this configuration and experience enough ionisation to form a plasma channel for discharging electrical energy. IEW voltages and currents were measured for the first

time in these experiments. Some characteristics of the restrike were investigated, and it was determined that a restrike could be detected from the primary voltage waveform, by comparing the difference in the exponential damping co-efficient, α, between restrike and non-restrike outcomes. A higher value of α indicated that the system had entered a more conductive state, which was consistent with the observation that a restrike had taken place. This could be a useful strategy for investigating IEWs, where direct observation of the wire voltage and current is difficult.

A number of extra observations of wire explosion by induction were made. The copper oxide residues left behind by the wire explosion formed interesting patterns on the Nomex paper. Some Lichtenburg figures were also found on the PVC formers where the receiver coils were situated. These figures were dubbed "dust-trees" because they could be rubbed off easily, suggesting they were comprised of copper metal and metal-oxides in the suspension created by the wire explosion.

8.1 Future Works

8.1.1 The plasma ring from exploding wire

The plasma ring from wire explosion via electromagnetic induction remains a future research goal. A way of creating a plasma ring from the methods achieved in Chapter 7, is shown in figure 8.1. The exploding wire plasma could be used as a way of switching in other sources or conductors. As the plasma conductor grows radially, it can make electrical contact with an externally placed conductor. An exploding wire "shorting-bar" is set across the turns of the plasma winding to convert it into a plasma ring. In this way huge currents could also be induced in the plasma by way of transformer action, once it is shorted out to form a continuous ring.

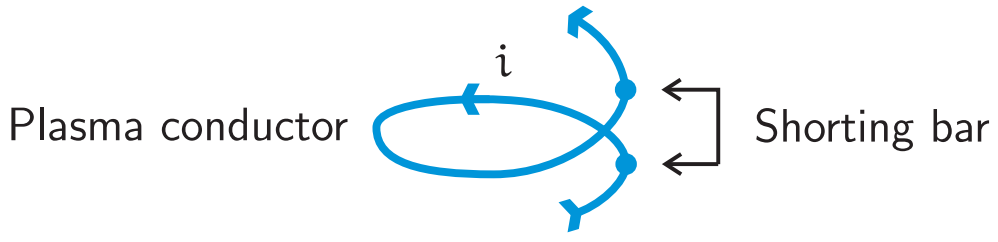

Figure 8.1: An exploding wire shorting bar is placed across the turns of the plasma winding to convert the plasma turn into a plasma ring.

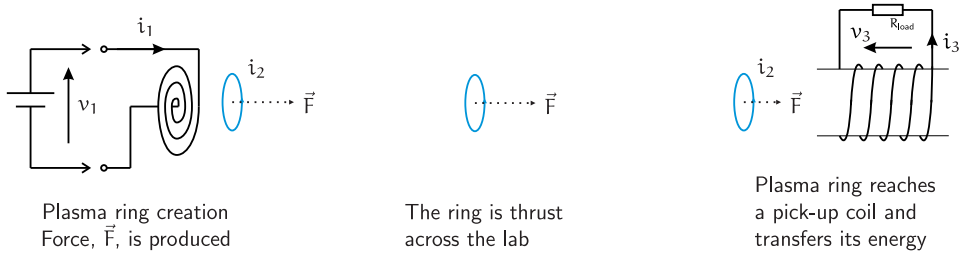

(a) Creation (b) Thrust (c) Transfer

Figure 8.2: Formation of a plasma ring by induction, and some of its uses. Once the plasma ring is formed, it could be kicked through free-space to a receiver, thus transfering its stored energy without wires. The coil types are representative.

8.1.2 Kicking the plasma ring using electromagnetic force

Once the plasma ring has been created, figure 8.2a, researchers could use the magnetic field of the induction winding to move the plasma ring along its axis in space. By natural transformer action, there will be a net force exerted on the plasma ring, creating thrust as in figure 8.2b. In this way, the plasma ring could also be used to store energy as a packet for wireless transmission of power across the laboratory. It could be thrust, say, toward a loaded receiving coil or antenna and deposit stored energy to the pick-up circuit, figure 8.2c.

8.1.3 Characteristics of exploding wires in vacuum

Restrike of the exploding wire has already been demonstrated for IEW. It has the advantage of being electrically isolated, but magnetically coupled from the induction winding. This allows the IEW to be placed inside a vacuum chamber. Thrusters could be developed for applications in space technology. The IEW could be used in manufacturing in zero gravity, zero atmosphere and low temperature environments.

References

Anderson, J.A. (1920), 'Spectra of explosions', *Proceedings of the National Academy of Science*, Vol. 6, pp. 42 – 43.

Anderson, J.A. (1922), 'The spectral energy distribution and opacity of wire explosion vapors.', *Proceedings of the National Academy of Science*, Vol. 8, pp. 231 – 232.

Anderson, D. and Briand, D. (2003), 'Zr reliability and operations analysis', In *Digest of Technical Papers. Pulsed Power Conference.*

Aymar, R., Chuyanov, V., Huguet, M., Shimomura, Y., Team, I.J.C. and Teams, I.H. (2001), 'Overview of iter-feat - the future international burning plasma experiment', *Nuclear Fusion*, Vol. 41, No. 10, p. 1301.

Bhat, B.K. and Jordan, I.B. (1971), 'Explosion of bare and insulated copper wires', *Journal of Applied Physics*, Vol. 42, No. 2, p. 809.

Bondarenko, B.D. (2001), 'Role played by o a lavrent'ev in the formulation of the problem and the initiation of research into controlled nuclear fusion in the ussr', *Physics-Uspekhi*, Vol. 44, pp. 844 – 851.

Bowen, I.S. (1962), *John August Anderson 1876 - 1959.*, National Academy of Sciences, Washington D.C.

Cavicchi, E. (2006), 'Nineteenth-century developments in coiled instruments and experiences with electromagnetic induction', *Annals of Science*, Vol. 63, pp. 319 – 361.

Chace, W.G. and Moore, H.K. (1959), *Exploding wires*, Plenum Press, New York.

Dailey, C.L. and Lovberg, R.H. (1993), *The PIT MkV Pulsed Inductive Thruster*, Nasa Contractor Report 191155, NASA, July.

Dannenberg, R. and Silva, A. (1969), 'Exploding wire initiation and electrical operation of a 40-kv system for arc-heated drivers up to 10 feet long', *NASA TN D-5126*.

Faraday, M. (1827), *Chemical Manipulation, Being Instructions to Students in Chemistry*, Royal Institution of Great Britain.

Faraday, M. (1832), 'Experimental researches in electricty', *Philosophical Transactions of the Royal Society of London*, Vol. 122, pp. 125 – 162.

Gautier, R. (Ed.) (2011), *Australian Power Technologies Transmission and Distribution*, February - March.

Gole, A.M., Filizadeh, S., Menzies, R.W. and Wilson, P.L. (2005), 'Optimization enabled electromagnetic transient simulation', *IEEE Transactions on Power Delivery*, Vol. 20, No. 1, January, pp. 512 – 518.

Hackmann, W. (1971), 'The design of the triboelectric generators of martinus van marum, f.r.s. a case history of the interaction between england and holland in the field of instrument design in the eighteenth century', *Notes and Records of the Royal Society of London*, Vol. 26, No. 2, December, pp. 163 – 181.

Hackmann, W. (1974), 'An early attempt to oxidise gold', *Gold Bulletin*, Vol. 7, pp. 80–83. 10.1007/BF03215043.

Hammond, C. (2008), 'A plasma primary high voltage transformer', In *Third Professional Year Projects*, University of Canterbury, Department of Electrical and Computer Engineering.

Hrbud, I., LaPointe, M., Vondra, R., Dailey, C.L. and Lovberg, R. (2002), 'Status of pulsed inductive thruster research', In *AIP Conf. Proc.*, American Institute of Physics, January 14, pp. 627 – 632.

Idzorek, G., Chrien, R., Matuska, W., Peterson, D., Swenson, F., Chandler, G., Porter, J. and Ruggles, L. (1999), 'Radiation experiments on the z-machine', In *Digest of Technical Papers. 12th IEEE International Pulsed Power Conference*, pp. 1060–1062.

Laithwaite, E.R. (1967), *The Engineer in Wonderland*, English Universities Press.

Manning, T.J. and Grow, W.R. (1997), 'Inductively coupled plasma - atomic emission spectrometry', *The Chemical Educator*, Vol. 2, pp. 1 – 19.

Martin, T. (1949), *Faraday's Discovery of Electromagnetic Induction*, Edward Arnold & Co.

MeBar, Y. and Harel, R. (1996), 'Electrical explosion of segmented wires', *Journal of Applied Physics*, Vol. 79, No. 4, pp. 1864–1868.

Mulholland, D. (2004), 'Explosion of 10m of copper wire', In *Third Professional Year Projects*, University of Canterbury, Department of Electrical and Computer Engineering.

Nagaoka, H. and Futagami, T. (1926), 'Instantaneous photographs of electrically exploded wires', *Proceedings of the Imperial Academy (Tokyo)*, Vol. 2, pp. 387 – 389.

Nagaoka, H. and Futagami, T. (1928), 'Cinematographic sketch of electrically exploded wires', *Proceedings of the Imperial Academy (Tokyo)*, Vol. 4, pp. 198 – 200.

Nagaoka, H., Futagami, T. and Machida, T. (1926), 'Electric explosion of wires and threads', *Proceedings of the Imperial Academy (Tokyo)*, Vol. 2, pp. 328 – 331.

Nairne, E. (1774), 'Electrical experiments by mr. edward nairne, of london, mathematical instrument-maker, made with a machine of his own workmanship, a description of which is prefixed', *Philosophical Transactions*, Vol. 64, pp. 79 – 89.

Nelder, J.A. and Mead, R. (1965), 'A simplex method for function minimization', *The Computer Journal*, Vol. 7, No. 4, pp. 308 – 313.

Nussbaum, A. (1965), *Electromagnetic Theory for Engineers and Scientists*, Prentice Hall.

Pocock, R.F. (1993), 'Andrew crosse: Early nineteenth-century amateur of electrical science', *IEE Proceedings - A*, Vol. 140, No. 3, pp. 187 – 196.

Ramo, S., Whinnery, J.R. and van Duzer, T. (1965), *Fields and Waves in Communication Electronics*, Wiley.

(2009), *Safety Manual - Electricity Industry*, Wellington.

Sandia (2011), *About Z - Z Pulsed Power Facility*, May. Accessed 2 May 2011.

Seely, S. and LePage, W.R. (1952), *General Network Analysis*, McGraw-Hill Book Company Incoporated.

Shimomura, Y., Aymar, R., Chuyanov, V., Huguet, M., Matsumoto, H., Mizoguchi, T., Murakami, Y., Polevoi, A., Shimada, M., Team, I.J.C. and Teams, I.H. (2001), 'Iter-feat operation', *Nuclear Fusion*, Vol. 41, No. 3, p. 309.

Shpanin, L.M., Jones, G.R., Spencer, J.W. and Djakov, B.E. (2008), 'Control and propulsion of an atmospheric pressure plasma ring', *IEEE Transactions on Plasma Science*, Vol. 36, No. 5, October, pp. 2795 – 2800.

Sinton, R., Hammond, C., Enright, W. and Bodger, P. (2009), 'Generating high voltages with a plasma coil transformer', In *Techcon Asia Pacific*, Sydney, pp. 211–219.

Sinton, R., van Herel, R., Enright, W. and Bodger, P. (2010a), 'Design and construction of a triggered spark gap for long distance exploding wire experiments', In *20th Australasian Universities Power Engineering Conference (AUPEC)*.

Sinton, R., van Herel, R., Enright, W. and Bodger, P. (2010b), 'Investigating long-distance exploding-wire restrike', *Plasma Science, IEEE Transactions on*, Vol. 38, No. 4, april, pp. 1015 –1018.

Sinton, R., van Herel, R., Enright, W. and Bodger, P. (2011), 'A marx generator for exploding wire experiments', In *2011 Asia-Pacific Power and Energy Engineering Conference (APPEEC)*, 25 - 28 March.

Smith, D. (2008), *The creation of long distance directional plasma discharges via the exploding wire technique : a thesis submitted in partial fulfilment of the requirements for the degree of Master of Engineering in Electrical and Computer Engineering at the University of Canterbury, Christchurch, New Zealand*.

Smith, D., Enright, W. and Bodger, P. (2007), 'A test circuit for long distance directional plasma discharge using the exploding wire technique', In *15th International Symposium on High Voltage Engineering (ISH)*, Ljubljana, Slovenia.

TAYLOR, M.J. (2002), 'Formation of plasma around wire fragments created by electrically exploded copper wire', *Journal of Physics D-Applied Physics*, Vol. 35, No. 7, pp. 700–709.

TAYLOR, M.J. (2002 - 2003), *Plasma Propellant Interactions in an Electrothermal-Chemical Gun*, PhD thesis, Royal Military College of Science, Cranfield University.

TKACHENKO, S.I., VOROB'EV, V.S. AND MALYSHENKO, S.P. (2004), 'The nucleation mechanism of wire explosion', *Journal of Physics D-Applied Physics*, Vol. 37, pp. 495 – 500.

TUCKER, T.J. AND TOTH, R.P. (1975), *A computer code for the prediction of the behavior of electrical circuits containing exploding wire elements*, report 75-0041, Sandia National Laboratory.

VAN MARUM, M. (1785), *Eerste Vervolg der Proefneemingen gedaan met Teyler's Electrizeer-Machine*.

VLASTOS, A.E. (1968), 'Restrike mechanisms of exploding wire discharges', *Journal of Applied Physics*, Vol. 39, No. 7.

WALL, D.P., ALLEN, J.E. AND MOLOKOV, S. (2003), 'The fragmentation of wires by pulsed currents: Beyond the first fracture', *Journal of Physics D-Applied Physics*, Vol. 36, pp. 2757 – 2766.

Appendix A

Unpublished: Long Distance Exploding Wire Electrical Characteristics and the Plasma Transformer

Long Distance Exploding Wire Electrical Characteristics and the Plasma Transformer

Ryan van Herel, Rowan Sinton, Wade Enright, Aniruddha Gole

***Abstract*—This letter presents findings on the electrical characteristics of long distance wire explosion. Time varying resistance models of the exploding wire are obtained using an optimisation enhanced electromagnetic transients technique. The optimisation is applied to experimental voltage and current waveforms of long wire explosion. Long distance wire explosion has been applied to create plasma coils, and a plasma-primary step-up transformer, whose operation has been identified with the help of current waveforms obtained through the optimisation.**

I. Introduction

CREATION of long wire explosion plasma is being studied at the University of Canterbury (Canterbury). The main focus of the research has been to understand the behaviour of exploding wire (EW) exceeding 1 m in length, and to catalogue the formation of plasma discharge channels. Studies of long wire explosions are also conducive to the creation of plasma windings of several turns, enabling the design of high voltage plasma-primary impulse transformers.

At the University of Canterbury High Voltage Laboratory, full plasma discharges (or EW restrikes) had been created over distances of up to 9 m. In early 2008, it was found that seed wires could be wound into coils. The ensuing EW restrike produced helical plasma discharges. Investigations were undertaken into production of high voltage impulses by an air-cored plasma primary step-up transformer, Fig. 1 [1].

In 2009, the University of Manitoba entered a collaboration to research the EW. An ElectroMagnetic Transients (EMT) optimisation routine was applied to search for the EW time varying resistance profile. The optimiser estimates the current waveform produced by the EW; current measurement was not available in the high voltage laboratory at Canterbury. In late 2009 one of the authors was at the Institute of High Voltage Engineering and System Management at the Graz University of Technology (Graz), where an opportunity transpired to measure EW current. The data collected there helped to validate the EMT program predicted EW currents.

Two experimental datasets are analysed; a set of EW voltage curves from Canterbury, and a set of voltage and current traces from experiments performed at Graz. Both circuits are capacitive discharge type; the circuit at Canterbury used a 21.4 μF bank of 20 oil filled capacitors, and at Graz, a 200 kV Haefely current impulse generator configured with a capacitance of 20 μF [2]. One particular result from each dataset is presented.

The method presented by Gole et al was used to find the resistance, $R_{ew}(t)$ of the EW for the duration of the voltage waveform [3]. The EMT program was seen as a straightforward method to determine the electrical characteristics of EW

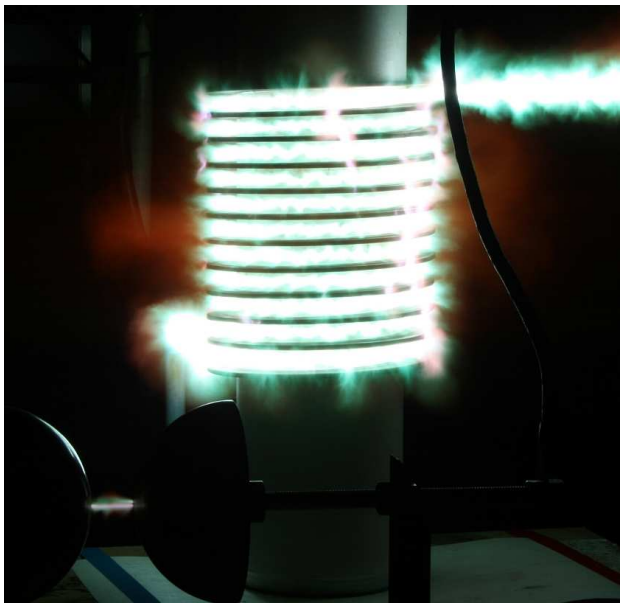

Fig. 1: A 10-turn plasma primary, 30-turn copper secondary high voltage step-up transformer at 40 kV dc. A calibrated sphere gap set to 75 kV dc can be seen flashing over twice in the foreground, measuring secondary winding voltage output.

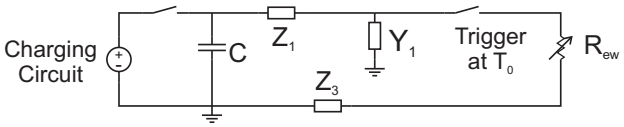

Fig. 2: Circuit used in the optimisation enabled EMT program.

experiments completed at Canterbury. Knowing the value of the capacitor bank, inductances of the delivery cables and the return cables, it was possible to draw the circuit diagram of the exploding wire in the EMT program, Fig. 2. The EMT program was used to evaluate the objective function generated by the block diagram in Fig. 3.

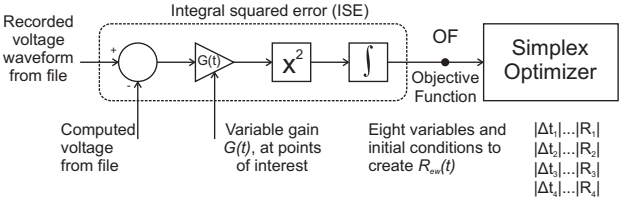

Fig. 3: Elements of the optimisation routine.

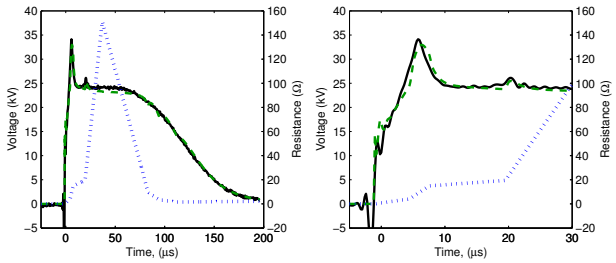

(a) Complete voltage (b) Detail of first 30 μs voltage

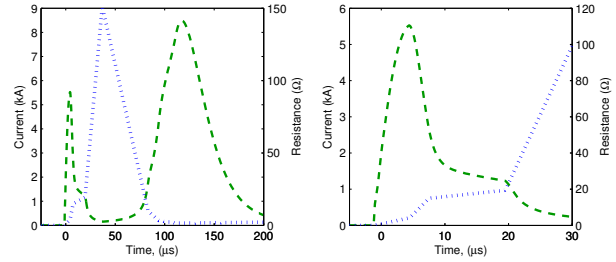

(c) Complete current (d) Detail of first 30 μs current

Fig. 4: Voltage, current and resistance curves for 3 m, 0.2 mm wire exploded at 24 kV dc. Dashed traces (green) show the simulated waveforms, solid traces show the recorded data. Dotted traces (blue) are the resistance functions, $R_{ew}(t)$.

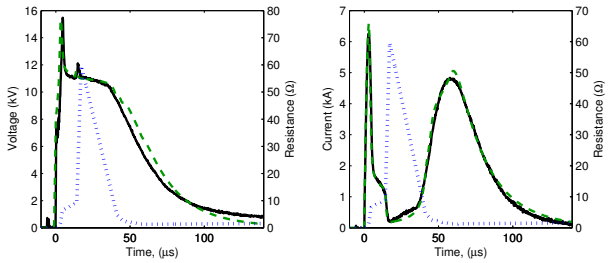

(a) Complete voltage (b) Complete current

Fig. 5: Voltage, current and resistance curves for 1.05 m, 0.2 mm wire exploded at 12.89 kV dc. Key is as per Fig. 4.

II. Results

A. Experiments at University of Canterbury, New Zealand

The model input data were voltage waveforms from EW experiments, exploded from 20 to 28 kV dc. The optimiser modelled the voltage waveforms, including the first and second voltage spikes, and also the EW restrike, Fig. 4. The optimisation provided predicted EW current and resistance waveforms. These parameters were unknown up to this point within the University of Canterbury wire explosion dataset.

In the first phase of the EW, Fig. 4b and 4d, there is an impulse of rapidly changing current. This coincides with the first voltage spike in the voltage trace. At the conclusion of this feature is a knee-point with a rapidly falling lip as the current reduces toward zero. This coincides with the second voltage spike. Beyond this, the current rises relatively slowly during what is known as the dwell period of EW. Once the dwell time is complete the restrike occurs and in the current waveform, this is marked by a large current hump.

An important result was that the rate of change of current, particularly in the first phase, indicated the means through which high voltage was being produced in the plasma transformer. The plasma transformer operation has been observed to give two flashes over the shunt-connected sphere gap on the secondary. This can be seen with a careful inspection of the sphere gap in Fig. 1. The two high-di/dt events in the characteristic of the predicted EW current, observed in Fig. 4d correspond to the high voltage flashes because of Faraday's law. The optimisation routines produce a predicted shape of current and resistance profile. The outcome of the optimisation is significant because the new plasma coil devices require large rates of change of current to produce impulse voltages.

B. Experiments at Graz University of Technology, Austria

Concurrently with modelling of the Canterbury data, EW experiments with current measurement were performed at the Graz University of Technology. The test subjects were 1.05 m, 0.2 mm diameter enamelled copper wires exploded at voltages from 8 to 17 kV dc.

The authors were interested to see current traces emerging from the optimisation of Canterbury data that resembled closely the experimental current data that was coming in from Graz at the time. The optimiser was able to model the EW voltage traces. However, the current traces, while exhibiting the correct shape, were not consistent in magnitude with the current measurements of the Graz experiments. Therefore for the Graz data the relative error in the voltage was added with the relative error in the current to produce a single overall error which was fed into the ISE step. This minimised error in both the voltage and current, accurately representing the resistance profile for the Graz exploding wire experiments. A particular Graz experimental and optimised EMT model result is presented in Fig. 5. The measured current traces exhibit many of the same features predicted by the Canterbury models.

III. Conclusion

EW experiments of 3 m and 1 m distances were performed at Canterbury and Graz respectively. Using this data, resistance models of the long EW were obtained via an optimisation enhanced EMT technique. A coarse optimisation routine of only eight points yielded a detailed template for the resistance profile of long distance EW. The EMT technique has provided valuable information about the operation of novel plasma transformer, and further experiments on long distance EW. Current traces revealed the rate of change of current in the first phase of the EW, demonstrating how high voltage is being produced in the plasma transformer.

References

[1] R. Sinton, C. Hammond, W. Enright, and P. Bodger, "Generating high voltages with a plasma coil transformer," in *Techcon Asia Pacific*, Sydney, 2009, pp. 211–219.

[2] R. Sinton, R. van Herel, W. Enright, and P. Bodger, "Investigating long-distance exploding-wire restrike," *Plasma Science, IEEE Transactions on*, vol. 38, no. 4, pp. 1015 –1018, April 2010.

[3] A. M. Gole, S. Filizadeh, R. W. Menzies, and P. L. Wilson, "Optimization enabled electromagnetic transient simulation," *IEEE Transactions on Power Delivery*, vol. 20, no. 1, pp. 512 – 518, January 2005.

Appendix B

Unpublished: Some experiments by Mr Mike Dalzell, dated 15 January 2008

15-1-08

1. Shooting plasma ring

- 22 turns of 2.125mm on grooved primary former.
- 20 turns of 0.375mm on external secondary, ends separated by spark gap.
- Test at 45 kV
- Secondary placed above primary center to hopefully promote an upwards axial force.

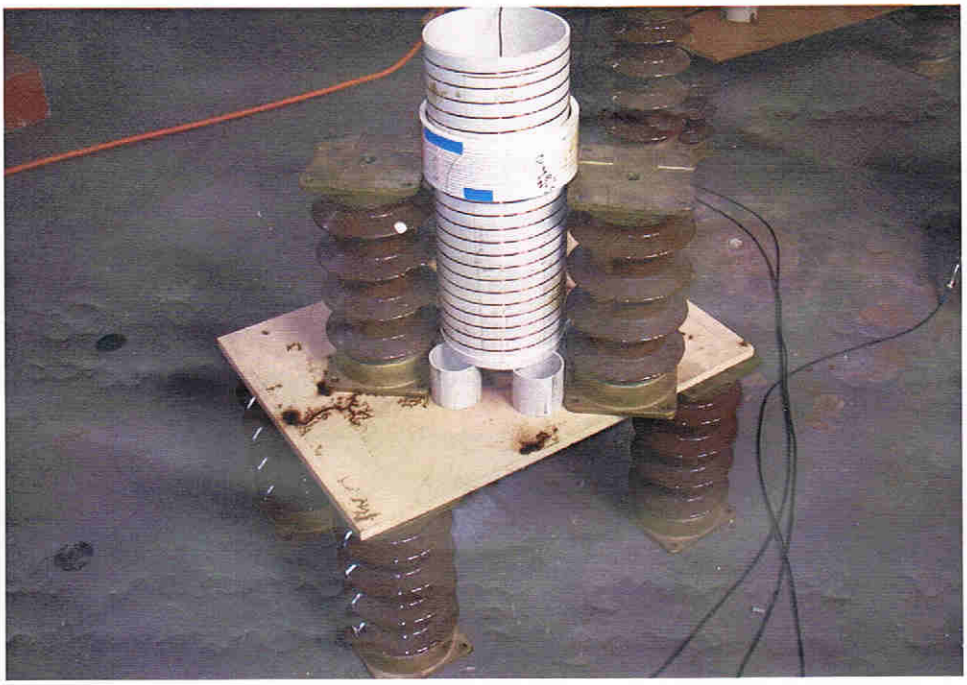

Results:

- Similar to yesterday. Wire explosion on secondary. Suspect radial forces are pushing secondary coil outwards
- Next page for post-test photo.

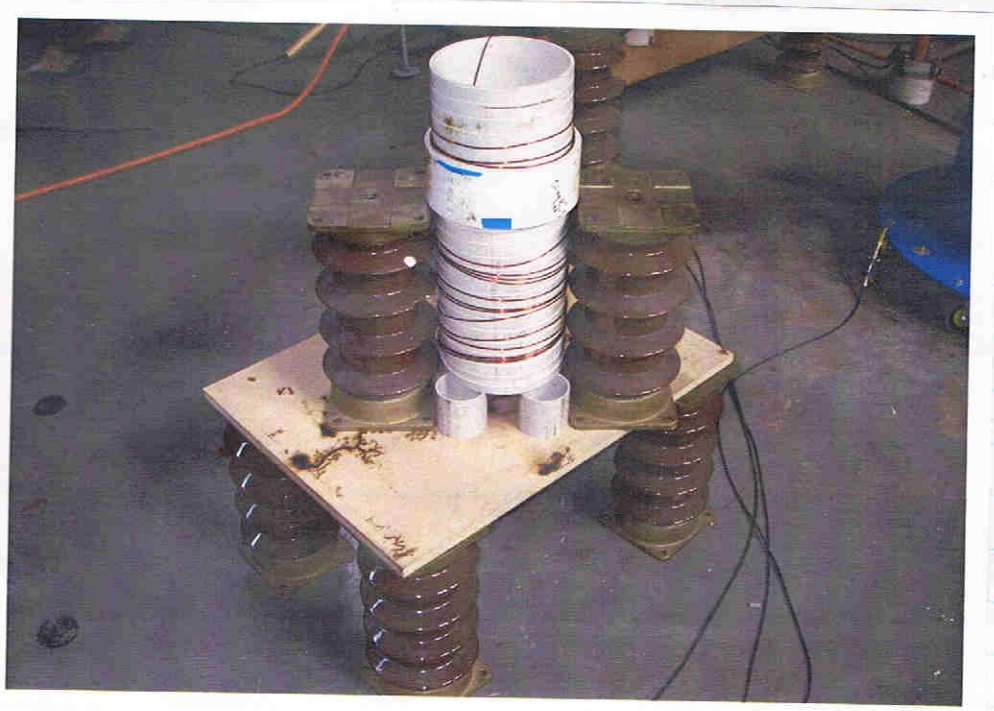

Secondary gone.

2. Shooting plasma ring

- Same set-up as test 1 but secondary ends are now bared and connected.

Results:

- Better secondary wire explosion. Beads visable indicating full plasmafication is close. Secondary still flung outwards. For shooting ring inner secondary seems preferable.

3. Shooting plasma ring - inner secondary.

- Same primary coil as test 1
- Secondary wound on former and placed inside primary. 20 turns of 0.375mm placed slightly above magnetic center of primary.

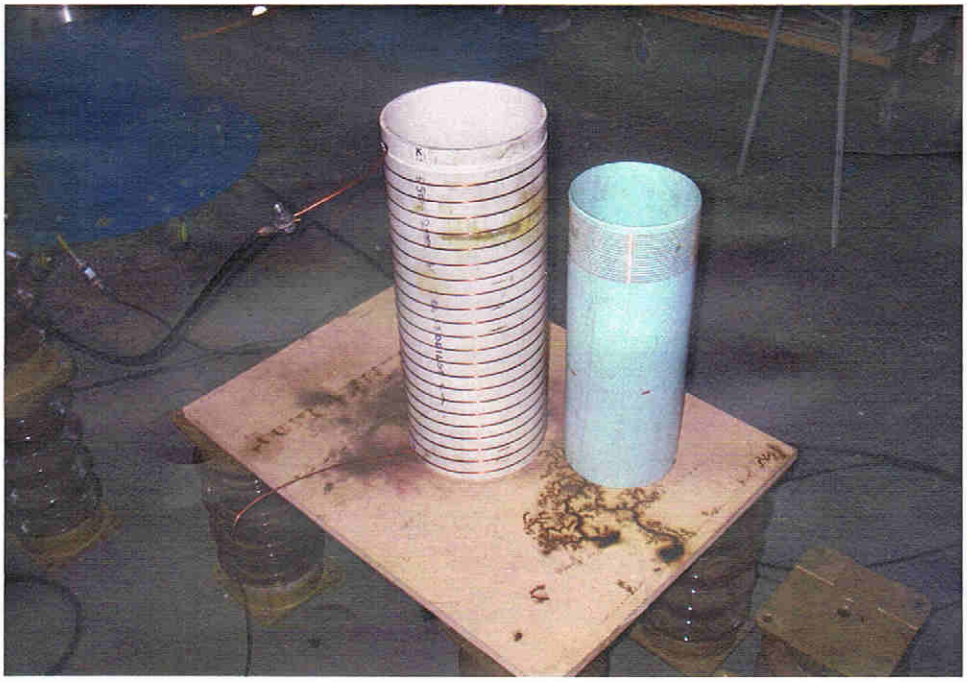

Set-up before secondary is put in primary

Results:

- Bright flash and smoke from inside of primary.
- Insulation fragments indicate wire explosion
- Birds nest of burnt wire found on floor. suspect coil is coming off former and crushing itself.